

PROPERTIES AND CYCLE PERFORMANCE OF REFRIGERANT BLENDS  
OPERATING NEAR AND ABOVE THE REFRIGERANT **CRITICAL** POINT

**Task 2: Air Conditioner System Study**

Final Report

Date Published – September 2002



Piotr A. Domanski and W. Vance Payne

NATIONAL INSTITUTE OF STANDARDS AND TECHNOLOGY  
Building and Fire Research Laboratory  
Gaithersburg, MD 20899-8631

Prepared for the  
AIR-CONDITIONING AND REFRIGERATION TECHNOLOGY INSTITUTE  
4100 N. Fairfax Drive, Suite 200, Arlington, Virginia 22203

Distribution A – Approved for public release; further dissemination unlimited.

## DISCLAIMER

This report was prepared as an account of work sponsored by the Air-conditioning and Refrigeration Technology Institute (ARTI) under its "Heating, Ventilation, ~~Air~~-Conditioning, and Refrigeration (HVAC&R) Research for the 21<sup>st</sup> Century" (21-CR) program. Neither ARTI, the financial supporters of the 21-CR program, or any agency thereof, nor any of their employees, contractors, subcontractors or employees thereof - makes any warranty, expressed or implied; assumes any legal liability or responsibility for the accuracy, completeness, any third party's use of, or the results of such use of any information, apparatus, product, or process disclosed in this report; or represents that its use would not infringe privately owned rights. Reference herein to any specific commercial product, process, or service **by** trade name, trademark, manufacturer, or otherwise, does not necessarily constitute nor imply its endorsement, recommendation, or favoring by ARTI, its sponsors, or any agency thereof or their contractors or subcontractors or NIST. The views **and** opinions of authors expressed herein do not necessarily state or reflect those of ARTI, the 21-CR program sponsors, or any agency thereof.

Funding for the 21-CR program provided by (listed in order of support magnitude):

- U.S. Department of **Energy** (DOE Cooperative Agreement No. DE-FC05-99OR22674)
- Air-conditioning & Refrigeration Institute (**ART**)
- Copper Development Association (**CDA**)
- New York State Energy Research and Development Authority (**NYSERDA**)
- Refrigeration Service Engineers Society (**RSES**)
- Heating, Refrigeration Air-conditioning Institute of Canada (HRAI)

Available to the public from

U.S. Department of Commerce  
National Technical Information Service  
5285 Port Royal Road  
Springfield, VA 22161  
(703) 487-4650

Available to U.S. Department of Energy and its contractors in paper from

U.S. Department of Energy  
Office of Scientific and Technical Information  
P.O. Box 62  
Oak Ridge, TN 37831  
(423) 576-8301

PROPERTIES AND CYCLE PERFORMANCE OF REFRIGERANT BLENDS  
OPERATING NEAR AND ABOVE THE REFRIGERANT CRITICAL POINT

Task 2: Air Conditioner System Study

Final Report

Date Published – September 2002

Piotr A, Domanski  
W. Vance Payne



Prepared for the  
AIR-CONDITIONING AND REFRIGERATION TECHNOLOGY INSTITUTE  
Under ARTI 21-CR Program Contract Number 605-500 10

### **Use of Non-SI Units in a Non-NIST Publication**

It is the policy of the National Institute of Standards and Technology to use the International System of Units (metric units) in all of its publications. However, in North America in the HVAC&R industry, certain non-SI units are so widely used instead of SI units that it is more practical and less confusing to include measurement values for customary units only in **figures** and tables describing system performance.



## EXECUTIVE SUMMARY

The main goal of this study was to investigate performance of an **R410A** air conditioner relative to an **R22** air conditioner, with specific interest in performance at high ambient temperatures at which the condenser of the **R410A** system may operate above the critical point. The study comprised experimental and modeling efforts.

Within the experimental part of the study we tested split system 3-ton **R22** and **R410A** residential air conditioners. The selected systems comprised identical evaporators and condensers, respectively, and were equipped with thermostatic expansion valves (TXVs). We tested the **R22** air conditioner in the 82.0 °F to 135.0 °F (**27.8 °C** to **57.2 °C**) outdoor temperature range. We planned the same range of ambient temperatures for the **R410A** system, however, the **R410A** compressor's safety system cut off the compressor at **135.0 °F (57.2 °C)** outdoor temperature, and the **130.0 °F (54.4 °C)** test was the highest temperature at which measurements were taken with the original **R410A** compressor. Subsequently, a custom-manufactured **R410A** compressor ~~was~~ installed in which the safety system was disabled and the electric motor was more powerful than in the original compressor. With ~~this~~ new compressor, we took data at up to **155.0 °F (68.3 °C)** ambient temperature, at which the system operated in a transcritical mode.

The **R22** and **R410A** systems operated normally during all tests, and visual observations of the **R410A** system provided no indication of vibrations or **TXV** hunting at high ambient temperatures with compressor discharge in the transcritical regime. The tests showed that capacity and energy efficiency ratio (**EER**) for both systems were nearly

linearly dependent on the ambient temperature, with the performance degradation of the R410A air conditioner being greater than that for the R22 air conditioner. The R22 and R410A systems had a similar capacity and EER at the 82.0 °F (27.8 °C) rating point, but the R22 air conditioner was a better performing system at higher temperatures. The report contains a description of the test facility, test procedures, and detailed test results.

The modeling part of this project provided a thrust for the final stage of preparing a beta version of EVAP-COND, a windows-based simulation package for predicting performance of finned-tube evaporators and condensers. Both the evaporator and condenser models can account for one-dimensional non-uniform air distributions and interaction between the air and refrigerant distributions. The visual interface helps with specifying tube-by-tube refrigerant circuitry and analyzing detailed simulation results on a tube-by-tube basis. This feature facilitates designing optimized heat exchangers. Ten refrigerant and refrigerant mixtures are available. EVAP-COND uses REFPROP6 (McLinden et al., 1998) routines for calculating refrigerant properties.

The modeling part of this study **also** included formulation of a model for a TXV-equipped air-conditioner, which ~~was~~ then **used** to simulate performance of R22, R410A, R404A, and R134a air conditioners. The model uses the EVAP-COND evaporator and condenser models, **and** simulates the compressor using a compressor map **algorithm**. The **same as** for EVAP-COND, the air conditioner model is REFPROP6-compatible and technically can include any refrigerant and refrigerant **mixture** that is covered by **REFPROP6**. We validated the system model and **performed** simulations for the four

refrigerants **for** the **82.0 °F** to **135.0 °F** (**27.8 °C** to **57.2 °C**) outdoor temperature range using the same heat exchangers that were tested with R22 and R410A systems. The simulations results are consistent with the test results obtained for **R22** and **R410A** and can be explained in terms of refrigerant thermophysical properties and their impact on performance in a system with non-optimized heat exchangers.

## **ACKNOWLEDGEMENT**

This work was sponsored by the Air-conditioning and Refrigeration Technology Institute under ARTI **21**-CR Program Contract Number 605-50010. Supplementary funding was provided by the US. Department of Energy, Contract Number DE-AI01-97EE23775, and NIST. We acknowledge the feedback and support from people associated with the sponsoring organizations, including Michael Blanford, Mark Spatz, Barbara H. Minor, Lawrence R. Grzyll, Dick Ernst, Steven Szymurski, and Esher Kweller. The two tested systems were contributed by Lennox Industries Inc. Len Van Essen provided essential advice during the unit selection process. Copeland Corporation contributed two custom-fabricated R410A compressors for transcritical tests of the R410A system along with valuable cooperation of Ken Monnier, Jim Horn, and Stan Schumann. John Wamsley provided laboratory support needed for tests in the NIST environmental chambers, and Samuel Y. Motta and Yongchan Kim assisted with their technical comments and cooperation. The authors also thank Mark O. McLinden and Keith Rice, principal investigators of the other two tasks associated with this project, for their interactions and comments.

## TABLE OF CONTENTS

<b>EXECUTIVE SUMMARY .....</b>	<b>i</b>
<b>ACKNOWLEDGMENTS .....</b>	<b>iv</b>
<b>TABLE OF CONTENTS .....</b>	<b>v</b>
<b>LIST OF TABLES .....</b>	<b>viii</b>
<b>LIST OF FIGURES .....</b>	<b>ix</b>
<b>NOMENCLATURE.....</b>	<b>xii</b>
<b>CHAPTER 1. SCOPE OF THE STUDY .....</b>	<b>1</b>
<b>CHAPTER 2.IMPACT OF ELEVATED AMBIENT TEMPERATURES ON CAPACITY AND ENERGY INPUT TO A VAPOR COMPRESSION SYSTEM _LITERATURE REVIEW .....</b>	<b>3</b>
2.1 Theoretical Background .....	3
2.2 Literature Review .....	6
2.3 Concluding Remarks .....	16
<b>CHAPTER 3. LABORATORY EXPERIMENT.....</b>	<b>17</b>
3.1 Units Selected for Testing .....	17
3.2 Experimental Set-Up .....	18
3.3 Experimental Procedure and Test Conditions .....	21
3.4 Experimental Results .....	22
3.4.1 Test Results for the R22 System .....	22
3.4.2 Test Results for the R410A System .....	26
3.4.3 R410A Oil Sampling Test Results .....	29
3.5 Comparison of Performance of <b>R22</b> and R410A Systems .....	30
3.5.1 R410A Cooling Capacity Relative to R22 .....	30

3.5.2 R410A Cooling EER Relative to R22 .....	32
<b>CHAPTER 4. MODELING .....</b>	<b>34</b>
4.1 Modeling Issues for Finned-tube Heat Exchangers .....	35
4.1.1 EVAP5 and COND5 Modeling Approach .....	35
4.1.2 Air-side Heat Transfer Correlations.....	38
4.1.3 Representation of Refrigerant Properties .....	41
4.2 Evaporator Model EVAP5 .....	43
4.2.1 Heat Transfer and Pressure Drop Correlations .....	43
4.2.2 EVAPS Validation.....	45
4.3 Condenser Model COND5 .....	54
4.3.1 Correlations Used .....	54
4.3.2 COND5 Validation.....	56
4.4 EVAP-COND Simulation Package .....	62
4.5 Modeling of Air Conditioner .....	63
4.5.1 Structure of Simulation Model .....	63
4.5.2 Model Validation with R22 and R410A Air Conditioner Test Data.....	65
4.5.3 Simulations of R22, R410A, R134a, and R404A Systems .....	70
<b>CHAPTER 5. CONCLUSIONS AND SUGGESTIONS FOR FUTURE WORK .....</b>	<b>76</b>
5.1 Experimental Work .....	76
5.2 Simulation Work .....	77
<b>APPENDIX A. SUMMARY OF TEST RESULTS FOR R22 SYSTEM .....</b>	<b>80</b>
<b>APPENDIX B. SUMMARY OF TEST RESULTS FOR R410A SYSTEM .....</b>	<b>93</b>
B.1 R410A System With Original Compressor .....	93

B.2 R410A System With Custom-Fabricated Compressor .....	104
<b>APPENDIX C. CAPACITY AND EER UNCERTAINTY .....</b>	<b>113</b>
<b>APPENDIX D. EVAP-COND INSTRUCTION PAGES.....</b>	<b>114</b>
<b>REFERENCES .....</b>	<b>133</b>

## LIST OF TABLES

Table 2.1 Capacity and COP of R22 and R410A system as function of outdoor temperature (Chin and Spatz. 1999).....	8
Table 3.1 Test conditions .....	21
Table 3.2 R410A oil sample results .....	30
Table 4.1 EVAP5 validation with R22 evaporator .....	50
Table 4.2 EVAPS validation with R410A evaporator.....	51
Table 4.3 Refrigerant parameters for outlet tubes; R22 evaporator. Test 1208a .....	54
Table 4.4 Refrigerant parameters for outlet tubes; R410A evaporator. Test b010330k ..	54
Table 4.5 COND5 validation with R22 condenser .....	59
Table 4.6 COND5 validation with R410A condenser.....	59
Table 4.7 AC model validation with R22 system data.....	67
Table 4.8 AC model validation with R410 system data.....	67
Table 4.9 Simulation results for R22, R410A, R134a, and R404A systems .....	72
Table 4.10 Selected thermodynamic parameters of studied refrigerants .....	73
Table A.1 R22 system tests .....	80
Table B.1 R410A tests with compressor #1 .....	93
Table B.2 R410A tests with compressor #2 .....	104
Table C.1 Measurement uncertainty .....	113



## LIST OF FIGURES

Figure 2.1 Impact of critical temperature on system performance .....	<b>4</b>
Figure 2.2 Refrigerant specific heat versus temperature and pressure: R410A .....	5
Figure 2.3 Refrigerant pressure drop and convection heat-transfer coefficient for supercritical flow of R410A .....	<b>5</b>
Figure 2.4 Heat transfer <del>in</del> evaporation .....	7
Figure 2.5 Comparison of capacity loss versus ambient temperature. split system A/C, 12-13 SEER .....	10
Figure 2.6 Comparison of EER loss versus ambient temperature. split system A/C, 12-13 SEER .....	10
Figure 2.7 Performance map for R410A unit with a high performance NTU (0.9) and a low condenser cfm/ton (640) .....	12
Figure 2.8 Temperature-dimensionless entropy diagram .....	13
Figure 2.9 Temperature-dimensionless enthalpy diagram .....	13
Figure 2.10 COP referenced to COP at 35°C ( <b>95°F</b> ) .....	14
Figure 2.11 COP referenced to COP of R-22 .....	14
Figure 2.12 COP for lsl-hx cycle referenced to COP for basic cycle .....	15
Figure 3.1 Condenser for R22 and R410A systems .....	17
Figure 3.2 Evaporator for R22 and R410A systems .....	18
Figure 3.3 Environmental chamber test schematic .....	<b>19</b>
Figure 3.4 High efficiency condensing unit .....	20
Figure 3.5 Indoor test section housing evaporator .....	20
Figure 3.6 R22 cooling capacity as a function of outdoor temperature .....	23
Figure 3.7 R22 reduced discharge pressure and discharge superheat <b>as</b> function of outdoor temperature .....	24
Figure 3.8 System power and R22 mass flow <b>as</b> a function of outdoor temperature .....	25

Figure 3.9 R22 cooling EER <b>as</b> a function of outdoor temperature .....	25
Figure 3.10 Cooling capacity of R410A <b>as</b> a function of outdoor temperature .....	27
Figure 3.11 R410A reduced discharge pressure and discharge superheat .....	28
Figure 3.12 R410A system power and refrigerant mass flowrate .....	28
Figure 3.13 R410A cooling EER as a function of outdoor temperature .....	29
Figure 3.14 Cooling capacity of R410A system relative <b>to</b> R22 system .....	31
Figure 3.15 Cooling EER of R410A system relative to R22 system .....	33
Figure 4.1 Representation of air distribution and refrigerant circuitry in EVAP5 and COND5 .....	36
Figure 4.2 Comparison of air-side heat transfer correlations .....	41
Figure 4.3 Design information for R22 and R410A evaporators .....	45
Figure 4.4 Refrigerant circuitry design in R22 and R410A evaporators .....	46
Figure 4.5 Tested and predicted capacities for R22 evaporator .....	52
Figure 4.6 Tested and predicted sensible heat ratios for R22 evaporator .....	52
Figure 4.7 Tested and predicted capacities for R410A evaporator .....	53
Figure 4.8 Tested and predicted sensible heat ratios for R410A evaporator .....	53
Figure 4.9 Design information for R22 and R410A condensers .....	56
Figure 4.10 Refrigerant circuitry design in R22 and R410A condensers .....	57
Figure 4.11 Tested and predicted capacities for R22 condenser .....	60
Figure 4.12 Tested and predicted pressure drops for R22 condenser .....	60
Figure 4.13 Tested and predicted capacities for R410A condenser .....	61
Figure 4.14 Tested and predicted pressure drops for R410A condenser .....	61
Figure 4.15 Component schematic of a tested <b>air</b> conditioner .....	<b>64</b>

Figure 4.16 Tested and predicted capacities of <b>R22</b> air conditioner .....	68
Figure 4.17 Tested and predicted EERs of R22 air conditioner.....	<b>68</b>
Figure 4.18 Tested and predicted capacities of R410A air conditioner.....	69
Figure 4.19 Tested and predicted EERs of R410A air conditioner .....	69
Figure 4.20 Tested and predicted refrigerant mass <b>flow</b> rates for R410A air conditioner .....	70
Figure 4.21 Simulated capacities of R22, R410A, R134a, and R404A air conditioners.....	73
Figure 4.22 Simulated EERs for R22, R410A, R134a, and R404A air conditioners .....	74
Figure 4.23 Simulated capacities of R410A, R134a, and R404A air conditioners relative to capacity of R22 air conditioner .....	74
Figure 4.24 Simulated EERs of R410A, R134a, and R404A air conditioners relative to EER of R22 air conditioner .....	75

## NOMENCLATURE

$A_f$	= finned surface area ( $\text{ft}^2$ )
$A_{pm}$	= pipe mean surface area ( $\text{ft}^2$ )
$A_{po}$	= pipe outside surface area ( $\text{ft}^2$ )
COP	= coefficient of performance
Cond	= condenser
$C_p$	= specific heat at constant pressure for air ( $\text{Btu}/(\text{lb}\cdot^\circ\text{F})$ )
DP	= pressure drop (inches of water gage)
EER	= energy efficiency ratio ( $\text{Btu}/\text{Wh}$ )
Evap	= evaporator
$h_i$	= inside-tube heat-transfer coefficient ( $\text{Btu}/(\text{ft}^2\cdot\text{h}\cdot^\circ\text{F})$ )
$h_l$	= heat-transfer coefficient for condensate (frost) layer ( $\text{Btu}/(\text{ft}^2\cdot\text{h}\cdot^\circ\text{F})$ )
$h_{pf}$	= heat-transfer coefficient for tube/fin contact ( $\text{Btu}/(\text{ft}^2\cdot\text{h}\cdot^\circ\text{F})$ )
$h_c$	= air-side heat transfer coefficient ( $\text{Btu}/(\text{ft}^2\cdot\text{h}\cdot^\circ\text{F})$ )
K	= material thermal conductivity ( $\text{Btu}/(\text{ft}\cdot\text{h}\cdot^\circ\text{F})$ )
$\dot{m}_a$	= air mass flow rate ( $\text{lb}/\text{h}$ )
NTU	= number of transfer units (non-dimensional)
P	= pressure (psi)
$P_{crit}$	= critical pressure (psia)
Q	= capacity ( $\text{Btu}/\text{h}$ )
$\dot{m}_{ref}$	= refrigerant <del>mass</del> flow rate ( $\text{lb}/\text{h}$ )
SEER	= seasonal energy efficiency ratio ( $\text{Btu}/\text{Wh}$ )
s	= entropy ( $\text{Btu}/(\text{lb}\cdot^\circ\text{F})$ )
T	= temperature ( $^\circ\text{F}$ )
$T_{crit}$	= critical temperature ( $^\circ\text{F}$ )
$T_{sat}$	= saturation temperature ( $^\circ\text{F}$ )
$T_{sup}$	= superheat ( $^\circ\text{F}$ )
TXV	= thermostatic expansion valve
UA	= heat-transfer conductance ( $\text{Btu}/(\text{h}\cdot^\circ\text{F})$ )
$X_p$	= thickness of the tube wall (ft)

$$a = i_{fgw}(\omega_a - \omega_w)/(C_{pa}(T_a - T_w))$$

$$E = \text{heat-transfer effectiveness (fraction)}$$

$$\phi = \text{fin efficiency (fraction)}$$

$$\omega_{ai} = \text{humidity ratio of air at tube inlet (lb}_w/\text{lb}_{a,dry})$$

$$\omega_{ao} = \text{humidity ratio of air at tube outlet (lb}_w/\text{lb}_{a,dry})$$

$$\omega_{fm} = \text{humidity ratio of saturated air at mean temperature of condensate wetting the fin (lb}_w/\text{lb}_{a,dry})$$

$$\omega_w = \text{humidity ratio of saturated air at temperature of condensate wetting the tube (lb}_w/\text{lb}_{a,dry})$$

Subscripts

$$a = \text{air}$$

$$o = \text{outside}$$

$$P = \text{pipe}$$

$$\text{sat} = \text{saturated}$$

$$\text{vol} = \text{volumetric}$$

$$w = \text{water}$$



## **1. SCOPE OF THE STUDY**

In September 1999, the Working Fluids Subcommittee of ~~the~~ ARTI-21CR program identified R410A performance at high temperatures to be a very high research priority. Consequently, a research project was arranged covering broad research needs related to application of R410A in unitary equipment. The three distinct tasks were formulated and assigned to three research teams ~~as~~ follows:

### **Task 1. Refrigerant Property Measurements and Modeling**

Principal Investigator: Dr. Mark O. McLinden

Physical and Chemical Properties Division

National Institute of Standard and Technology

Project Number: ARTI-21CR/605-50010-01-Pt. 1

This task encompassed selected property measurements for R125 and R410A. These new data and additional literature data would provide a basis for further improvement of REFPROP's robustness and predictions for R410A.

### **Task 2. Air Conditioner and System Study**

Principal Investigator: Dr. Piotr. A. Domanski

Building Environment Division

National Institute of Standards and Technology

Project Number: ARTI-21CR/605-50010-01-Pt. 2

This task consisted of experimental and modeling parts. The experimental part included laboratory tests of R22 and R410A units at a wide range of ambient temperatures. The specific interest in high ambient temperatures was due to the low critical temperature of R410A, which may results in transcritical operation of the R410A system on extremely

hot summer days. The tests were to allow performance comparison of **R22** and R410A systems and to observe operation of the R410A system while working in the transcritical cycle regime.

The modeling **part** of Task **2** included (1) development of REFPROP6-based models for finned-tube evaporators and condensers, EVAPS and COND5, (2) implementation of these simulation models into a user-friendly EVAP-COND simulation package, and (3) simulations of R22, R410A, R134a, and R404A systems at typical and elevated ambient temperatures for performance comparison using a reactivated NIST heat pump simulation model.

Task 3. Modeling, Validation, and Analysis of Sub- and Transcritical Performance of

R410A Under Extreme Air Conditioning Conditions

Principal Investigator: Dr. C. Keith Rice

*Oak Ridge National Laboratory*

Project Number: **ARTI-21CR/605-50015-01**

Task 3 stipulated detailed validating/calibrating of the DOE/ORNL Heat Pump Model against the test data obtained at NIST under Task 2.

This document covers the work carried out under Task 2. Task 1 and Task 3 are covered by separate reports.



## **2. IMPACT OF ELEVATED AMBIENT TEMPERATURES ON CAPACITY AND ENERGY INPUT TO A VAPOR COMPRESSION SYSTEM – LITERATURE REVIEW\***

### **2.1 Theoretical Background**

Operation of a system at elevated ambient temperatures inherently results in a lower coefficient of performance (COP). This conclusion comes directly from examining the Carnot cycle. The COP relation,  $COP = T_{\text{evap}} / (T_{\text{cond}} - T_{\text{evap}})$  indicates that the COP decreases when the condenser temperature increases at a constant evaporation temperature. This theoretical indication derived from the reversible cycle is valid for all refrigerants. For refrigerants operating in the vapor compression cycle, the COP degradation is greater than that for the Carnot cycle and varies among fluids.

The two most influential fundamental thermodynamic properties affecting refrigerant performance in the vapor compression cycle are refrigerant's critical temperature and molar heat capacity. (e.g., McLinden, 1987, Domanski, 1999). For a given application, a fluid with a lower critical temperature will tend to have a higher volumetric capacity ( $Q_{\text{vol}}$ ) and a lower coefficient of performance (COP). The difference between COPs is related to different levels of irreversibility because of the superheated vapor horn and the throttling process, as shown conceptually in Figure 2.1. The levels of irreversibility vary with operating temperatures because the slopes of the saturated liquid and vapor lines change, particularly when approaching the critical point.

---

\* Authored by S.Y. Motta and P.A. Domanski, this section was submitted to ARTI as a letter report in August 2000.

Refrigerants with a low critical temperature have a high pressure, a low drop of saturation temperature for a given pressure drop, and a low condenser-to-evaporator pressure ratio. These properties offer some advantages, which can be exploited in a real system for the betterment of its performance. Some researchers reported that a low pressure ratio promotes an improved compressor isentropic efficiency (e.g., Rieberer and Halozan, 1998). The low drop of refrigerant saturation temperature for a given pressure drop ( $dT/dP|_{\text{sat}}$ ) allows designing heat exchangers with a high refrigerant mass flux, which promotes an improved refrigerant-side heat transfer coefficient.

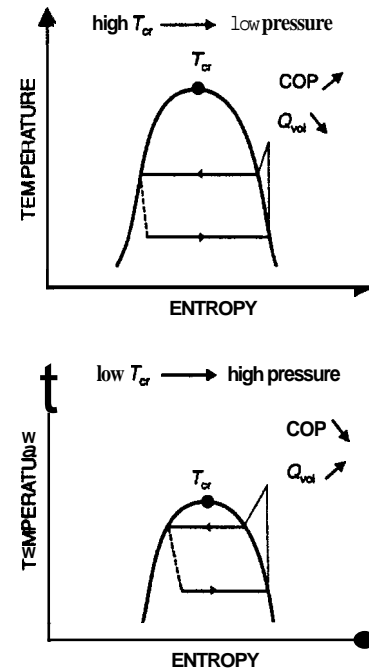


Figure 2.1 Impact of critical temperature on system performance

The condenser temperature increases at elevated ambient temperatures, which causes changes in refrigerant transport properties. These changes do not override the thermodynamic consideration, but they should be noted to foster complete understanding of the phenomena involved. The changes of liquid viscosity, conductivity, and heat capacity are smooth and favorable while approaching the critical temperature (viscosity decreases, conductivity and heat capacity increase). In the supercritical region, density has a smooth transition above the critical point, but specific heat has a pronounced peak, as Figure 2.2 shows for R410A (Bullock, 1999). This trend in the neighborhood of the critical point is typical for all fluids as has been recently presented for carbon dioxide in several studies (e.g., Olson, 1999 who showed that conductivity and viscosity have a

smooth transition as well). Because of the abrupt change in specific heat (Figure 2.2), the heat transfer coefficient at constant pressure (Figure 2.3) has a peak while approaching the critical temperature.

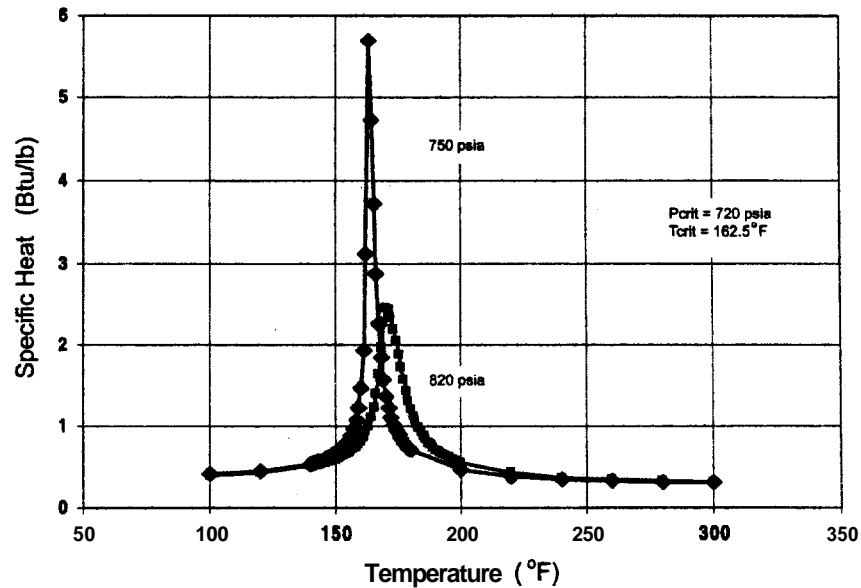


Figure 2.2 Refrigerant specific heat versus temperature and pressure: **R410A** (Bullock,1999)

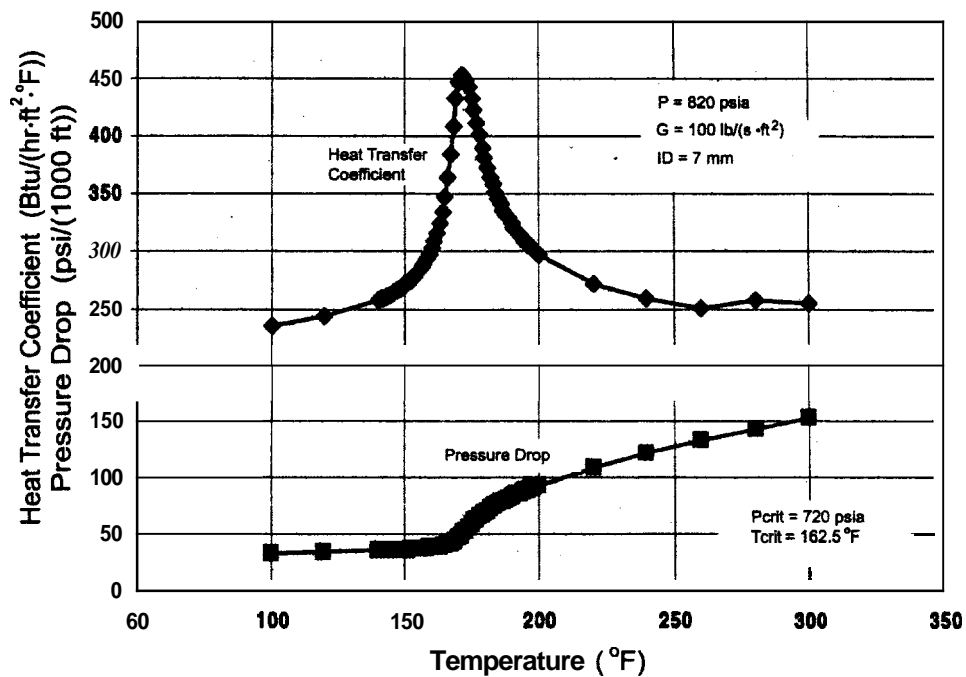


Figure 2.3 Refrigerant pressure drop and convection heat-transfer coefficient for supercritical flow of **R410A** (Bullock, 1999)

## 2.2 Literature Review

We were able to locate only a few publications concerned with air conditioner operation at elevated temperatures. They **are** reported here along with two seminar presentations made during the ASHRAE summer meeting in 1999. LeRoy et al. (1997) investigated capacity and power demands of R22 unitary systems under extreme operating conditions. The main goal of the study was to validate performance predictions of three public-domain heat pump simulation models. The authors used data of ten systems from tests at the 95.0 °F (35.0 °C) rating point and at higher outdoor temperatures. Three of these systems were tested at 115.0 °F (46.1 °C) and another three at 125.0 °F (51.7 °C) with the same indoor conditions of 80.0 °F (26.7 °C) dry-bulb and 67.0 °F (19.4 °C) wet-bulb temperature. The reported decrease in capacity at 115.0 °F (**46.1 °C**) was in the 14 % to 19 % range while **the** decrease in the energy efficiency ratio (EER) was in the 24 % to 41 % range. At 120.0 °F (48.9 °C), the capacity and EER decreases were within the 11 % to 20 % range and 34 % to 39 % range, respectively. These data indicate that performance degradation at high ambient temperature varies significantly from one system to another.

**Chin** and Spatz (1999) explored some of the advantages and disadvantages of R410A use in air conditioning systems. They used compressor performance data and a heat pump simulation model to compare R22 and R410A. In this study, they also performed heat exchanger optimization to exploit the favorable thermophysical properties of R410A. The authors reviewed experimental heat transfer and pressure drop data for R22 and R410A in evaporation and condensation processes. Figure 2.4 helps to explain the authors' findings. As a reference, they used the R22 pressure drop and saturation

temperature drop at a mass flux of **147158 lb/(h·ft<sup>2</sup>) (200 kg/(s·m<sup>2</sup>))**. For these conditions, **R410A** requires a ~~mass~~ flux of **206022 lb/(h·ft<sup>2</sup>) (280 kg/(s·m<sup>2</sup>))** to match the **R22** pressure drop **and** a mass flux of **250170 lb/(h·ft<sup>2</sup>) (340 kg/(s·m<sup>2</sup>))** to match the **R22** drop in saturation temperature. If the **R410A** mass flux is selected to match the **R22** drop in saturation temperature, **R410A** will have a **55 %** higher heat transfer coefficient than **R22**.

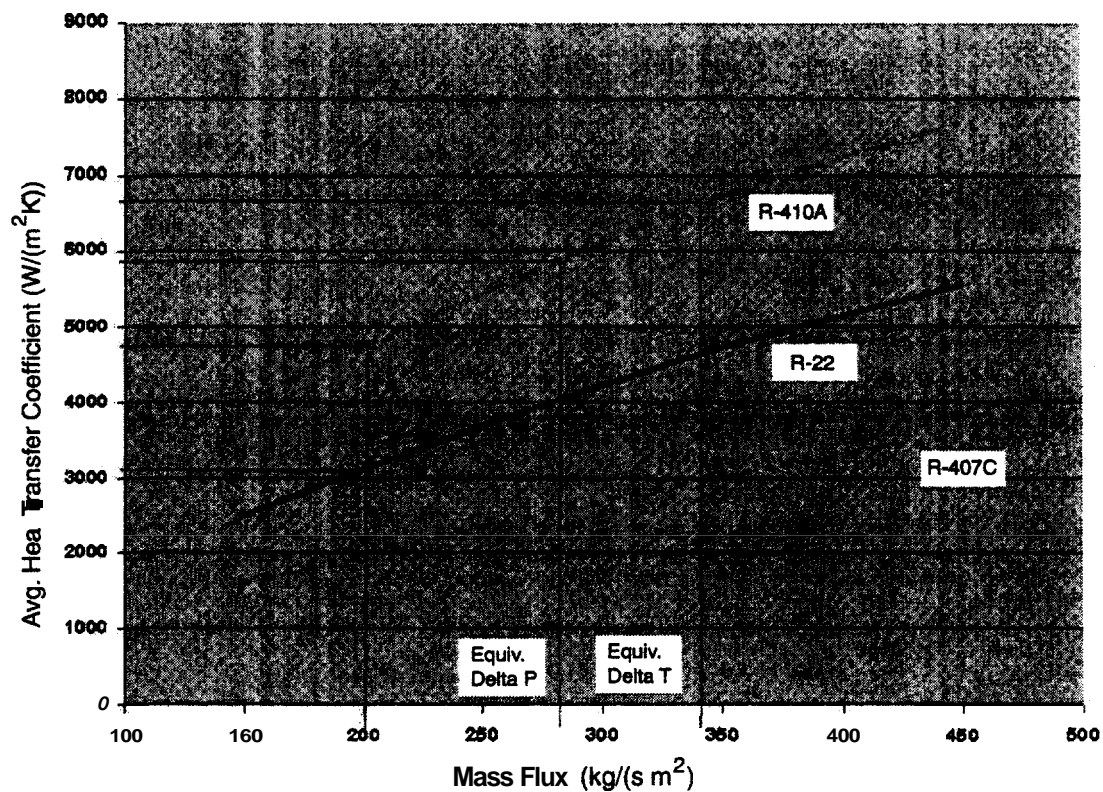


Figure 2.4 Heat transfer – evaporation (Spatz, 2000)

Table 2.1 Capacity and COP of R22 and R410A systems as function of outdoor temperature (Chin and Spatz, 1999)

Ambient Air Temperature		28 °C (82 °F)	35 °C (95 °F)	46 °C (115 °F)	52 °C (125 °F)	57 °C (135 °F)
Capacity (kW)	R22	12.84	11.98	10.63	9.95	9.32
	R410A	13.01	11.92	10.20	9.32	8.50
	Rel* (%)	1.3%	-0.5%	-4.0%	-6.3%	-8.8%
COP	R22	3.79	3.11	2.26	1.92	1.64
	R410A	3.99	3.19	2.19	1.79	1.47
	Rel* (%)	5.3%	2.4%	-3.4%	-6.9%	-10.7%

After the evaporator and condenser were optimized, Chin and Spatz performed for R22 and R410A simulations system. Table 2.1 shows their capacity and COP results. The authors concluded that the superior performance of the R410A compressor and optimized heat exchangers compensated for the lower thermodynamic efficiency of R410A relative to R22 at low and moderate condensing temperatures. However, the R410A optimized-system experienced a loss in COP relative to the R22 system at condensing temperatures exceeding 116.6 °F (47.0 °C).

Meurer et al. (1999) compared the performances of R22 and R410A working at elevated condensing temperatures up to 140.0 °F (60.0 °C) in a breadboard apparatus. The components of the system were an open reciprocating compressor, a water-cooled condenser, a methanol-heated evaporator, a thermostatic expansion valve, and a liquid-line accumulator. The authors reported the R410A compressor having higher isentropic

(+14 %) and volumetric (+22 %) efficiencies than **R22**. For a typical evaporation temperature of **48.2 °F (9.0 °C)**, the COP of **R410A** was higher by **16 %** at a condensing temperature of **80.6 °F (27.0 °C)**, but it was lower by **1 %** at a **134.6 °F (57.0 °C)** condensing temperature. The authors stated that a lower compressor speed accounted for part of the benefits measured with **R410A**, but the use of equal rotational speed would negatively affect the **R410A** compressor and system performance.

Wells et al. (1999) compared the performance of **R410A** and **R22** in split and window-type air conditioners. Their study included theoretical simulations, laboratory testing of split systems, laboratory testing of window units with several hardware modifications, and simulations using the ORNL heat pump model. Figures 2.5 and 2.6 show the capacity and **EER** trends obtained from the **R22** and **R410A** split system tests referenced to the respective values at a **95.0 °F (35.0 °C)** ambient temperature. At an ambient temperature of **125.0 °F (51.7 °C)**, the capacity and **EER** ratios of **R410A** fell **12 %** below that of **R22**. Similar results (within the data scatter) were obtained for the window units. Increased subcooling benefited performance at high ambient temperatures. The study also concluded that using a TXV versus a short tube restrictor or capillary tube results in less performance loss.

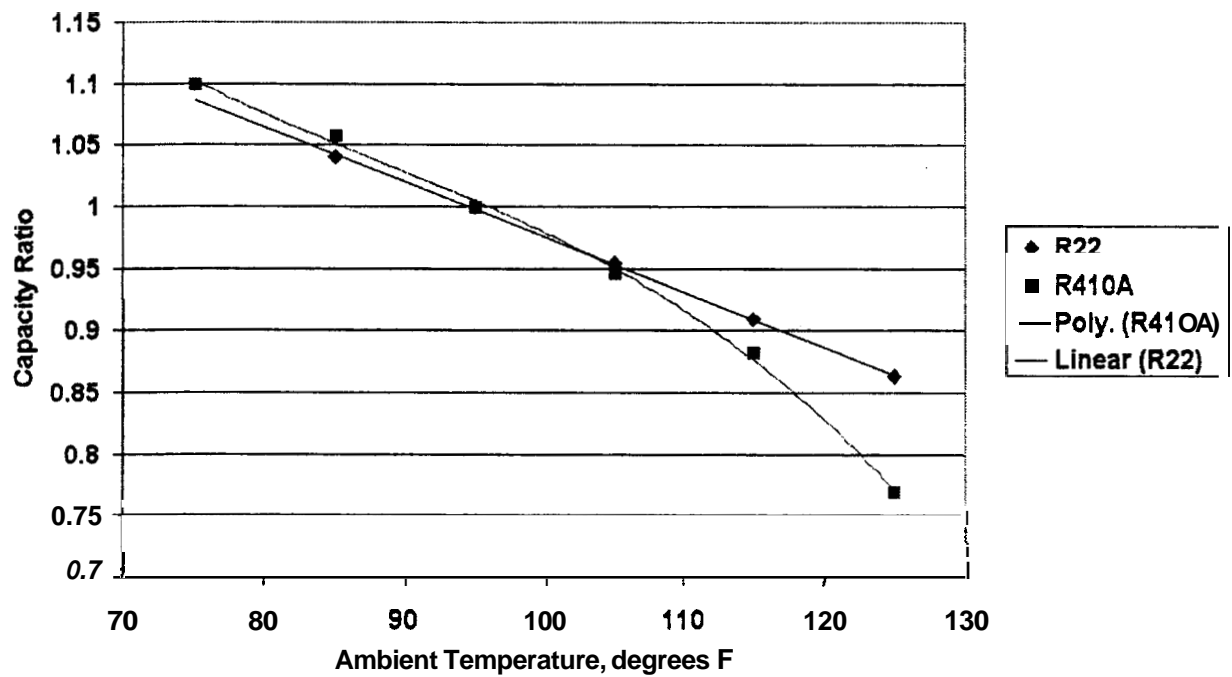


Figure 2.5 Comparison of capacity **loss** versus ambient temperature, split system A/C, 12-13 **SEER** (Wells et al., 1999)

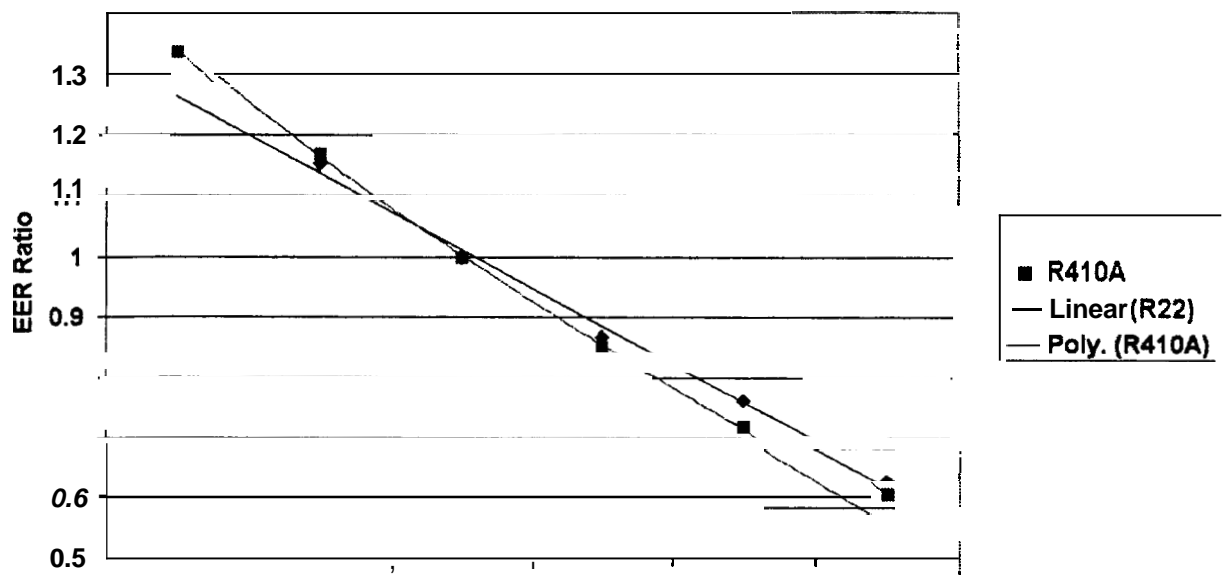


Figure 2.6 Comparison of EER loss versus ambient temperature, split system A/C, 12-13 SEER (Wells et al., 1999)



Bullock (1999) investigated the performance of **HVAC** systems working with two low-critical temperature refrigerants: R404A and R410A. The study included theoretical analysis of **the** refrigerant properties, simulations of the basic thermodynamic cycle, and simulations of three split systems: two using R410A and one using R404A. The main difference between the systems studied was the condenser and blower size. In Bullock's A/C simulation model, the compressor, expansion device, and condenser/gas cooler models were modified to accommodate transcritical system operation.

Figure 2.7 presents simulation results for one of the systems studied by Bullock (1999). The vertical arrow indicates the outdoor temperature at which the condenser pressure exceeded that of the critical point. The simulations show that the capacity degradation and compressor power increase become more significant with an increase of outdoor temperature when the condenser pressure is above the critical point. Based on simulation results from the three systems, Bullock offered the following key conclusions: a typical unitary system will cross over to transcritical operation at about 135.0 °F to 140.0 °F (57.2 °C to 60.0 °C). At the ambient temperature when the critical point is reached, the cooling capacity will be about 60 % to 70 % of the capacity at the 95.0 °F (35.0 °C) rating point, and the compressor power will be about 110 % to 160 % of the power at the 95.0 °F (35.0 °C) rating point (depends greatly on the compressor type). The system performance at high ambient temperatures can be improved by providing an oversized condensing unit.

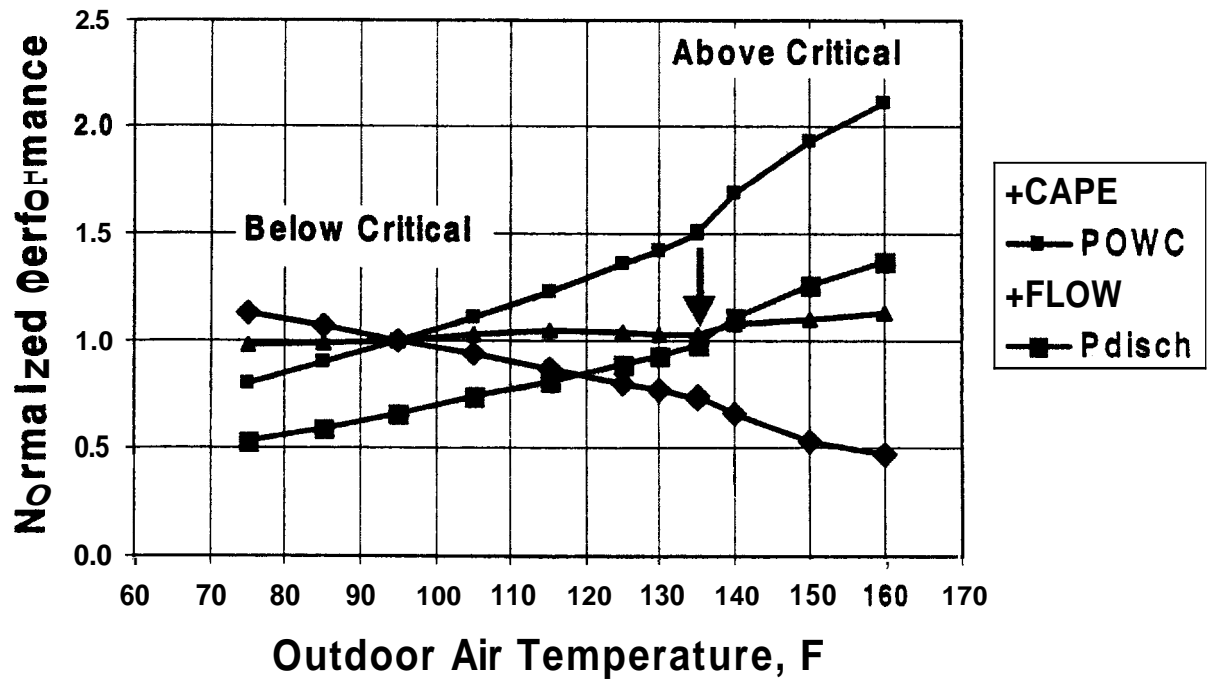


Figure 2.7 Performance map for R410A unit with a high performance NTU(0.9) and a low condenser cfm/ton, (640). **CAPE** = capacity of evaporator; **POWC** = power of compressor; **FLOW** = refrigerant flow rate; **Pdisch** = compressor discharge pressure (all normalized to their values at 95.0 °F (35.0 °C), except for the compressor discharge pressure, which is related to the critical pressure); (Bullock, 1999)

Yana Motta and Domanski (2000) performed a simulation study to evaluate capacity and COP of an air conditioner working with R22, R134a, R290, R410A, and R407C. Figures 2.8 and 2.9 present two-phase domes of the studied refrigerants with the horizontal axes using non-dimensional entropy,  $s^*$ , and enthalpy,  $h^*$ , respectively (where  $s^* = (s - s_1^0) / (s_v^0 - s_1^0)$ ,  $h^* = (h - h_1^0) / (h_v^0 - h_1^0)$ ,  $s$ ,  $h$  = entropy and enthalpy,  $s_v^0$ ,  $h_v^0$  = entropy and enthalpy of saturated vapor at 0 °C (32 °F), and  $s_1^0$ ,  $h_1^0$  = entropy and enthalpy of saturated liquid at 0 °C (32 °F)). These figures are suitable for qualitative analyses of the impact of the shape of the two-phase dome on the COP because the width of the two-phase dome is

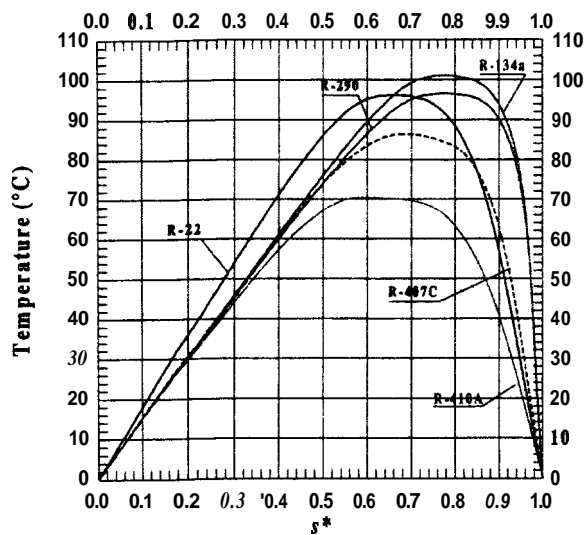


Figure 2.8 Temperature-dimensionless entropy diagram (Yana Motta and Domanski, 2000).

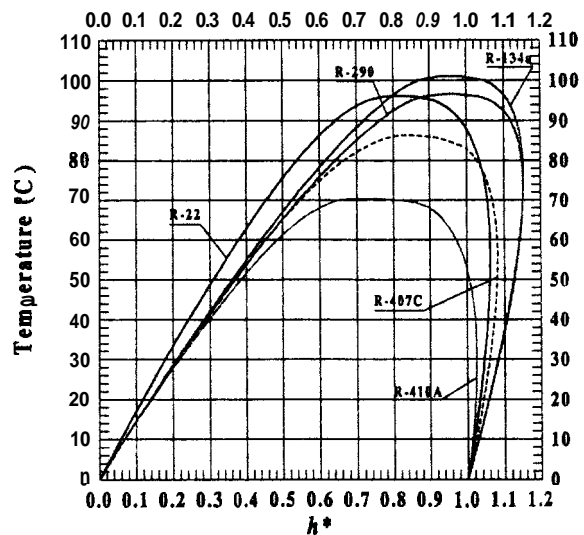


Figure 2.9 Temperature-dimensionless enthalpy diagram (Yana Motta and Domanski, 2000).

normalized. If we envision vapor-compression cycles with their corresponding Carnot cycles drawn for each refrigerant with the same condensing and evaporating temperatures, we can conclude that the superheated-vapor horn irreversibilities (Figure 2.8) and throttling-induced capacity losses (Figure 2.9) will be greater for **R410A** than for **R22** due to **R410A**'s smaller two-phase dome.

Yana Motta and Domanski simulated performance of different refrigerants using the **UA** version of NIST's semi-theoretical vapor-compression model **CYCLE-11** (Domanski and McLinden, 1992). All system components were the same for the five fluids, except the compressor for which the swept volume was adjusted to obtain the same capacity at the **95.0 °F (35.0 °C)** rating point for each fluid. A reference scheme was used to account for different transport properties and their impact on heat transfer coefficient and pressure drop for the different refrigerants.

Figure 2.10 shows changes of COP for each refrigerant for different outdoor temperatures. The COP values are normalized by the COP at 95 °F (35 °C) for each fluid. R410A **has** the highest degradation in COP and R134a has the lowest. The lines representing performance of R410A (the lowest-critical-temperature fluid) and R134a (the highest-critical-temperature fluid) bracket the performance of the remaining refrigerants. The change of COP for R22, R290, and R407C is **very** similar, because their critical temperatures are within 18.0 °F (10.0 °C) of each other.

Figure 2.11 presents the COP of the four alternatives normalized by the COP of the R22 system. R134a, the fluid with the highest critical temperature, improves its performance in relation to R22, and it has a higher COP **than** R22 at outdoor temperatures greater than 95 °F (35 °C). On the other hand, the COP of R410A drops dramatically at increasing outdoor temperature. Regarding the fluids with critical temperatures similar to R22 (R407C and R290), the small COP differences are caused by the different shapes of the two-phase domes of these fluids rather than their different critical temperatures.

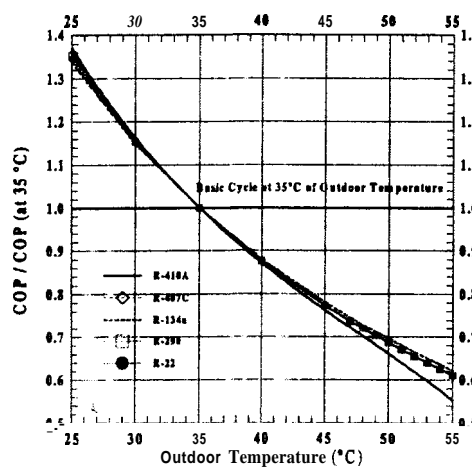


Figure 2.10 COP referenced to COP at 95 °F (35 °C) (Yana Motta and Domanski, 2000).

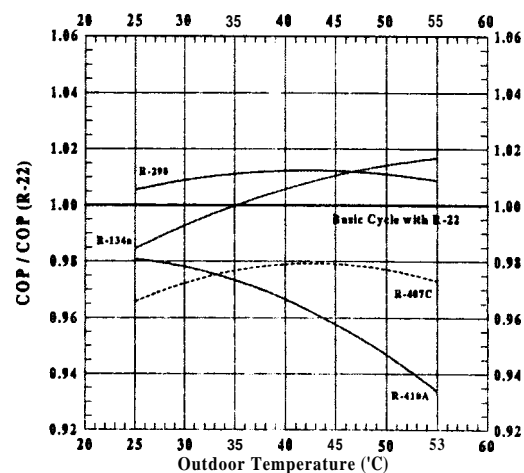


Figure 2.11 COP referenced to COP of R22 system (Yana Motta and Domanski, 2000).

Yana Motta and Domanski also evaluated the impact of using a liquid-line/suction-line heat exchanger (llsl-hx). As Figure 2.12 shows, the use of llsl-hx provided COP improvement for all fluids. Refrigerants having high molar capacity benefited more ~~with~~ the llsl-hx application. The benefit ~~of~~ llsl-hx for R410A increased slightly at high ambient temperatures due to a change in the slope of the saturated liquid line while approaching the critical point; however, the overall impact of approaching the critical point was not significant. At an outdoor temperature of 131.0 °F (55.0 °C), the COP increase due to the llsl-hx ~~was~~ **1.9%** higher for R410A than that for R22.

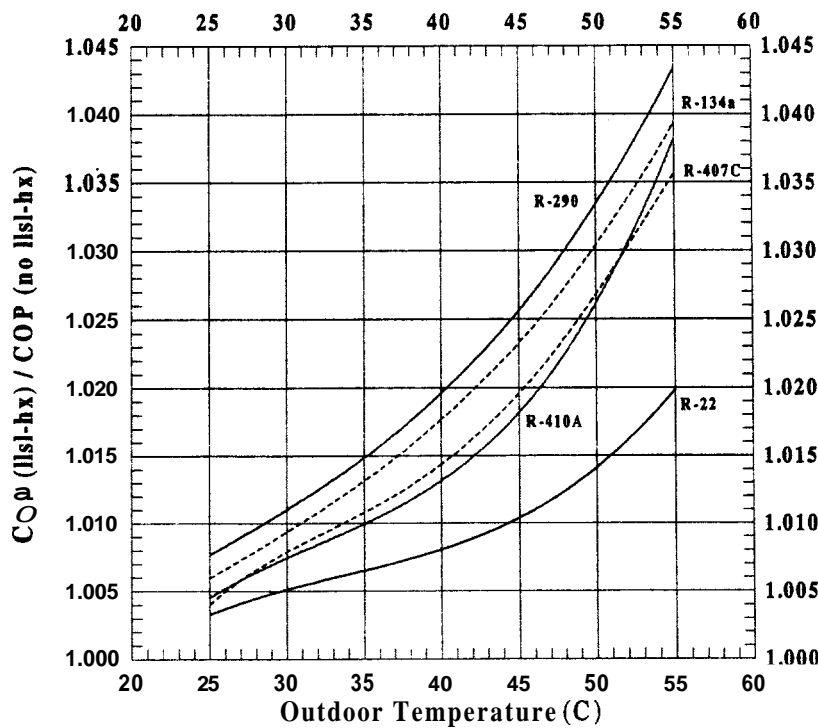


Figure 2.12 COP for llsl-hx cycle referenced to COP for basic cycle (Yana Motta and Domanski, 2000).

## 2.3 Concluding Remarks

1. Operation of a vapor compression system at elevated ambient temperatures inherently results in a lower COP. For refrigerants operating in the vapor compression cycle, the COP degradation is greater than that for the Carnot cycle and varies between fluids. The refrigerant-related factors that most influence the degradation are the critical temperature and the shape of the two-phase dome.
2. Degradation of capacity and **COP** at high outdoor temperatures can vary significantly between systems. The system design (size of the condenser, refrigerant charge, refrigerant expansion device) influences performance degradation.
3. All experimental and simulation studies reported a loss of performance for R410A systems at elevated ambient temperatures by approximately 10 % **as** compared to R22.
4. Simulation results indicate that the use of lsl-hx provides slightly better improvement of COP for R410A than for R22. At an outdoor temperature of 131.0°F (55.0 °C), the COP increase for R410A was 1.9 % higher than for R22.
5. The thermodynamic loop of a typical unitary R410A A/C will cross above the critical point at an outdoor temperature of approximately 135.0°F (57.2 °C).

## CHAPTER 3. LABORATORY EXPERIMENT

### 3.1 Units Selected for Testing

The systems consisted of 3-ton nominal cooling capacity units with scroll compressors, finned tube condensers, and finned tube evaporators. Manufacturer data listed the **R22** system with a **SEER** of **12.5** and the **R410A** system with a **SEER** of **13**. Both the **R22** system and the **R410A** system had identical evaporator and condenser coils. Only the thermostatic expansion valve and liquid line filter differed between the two system's piping arrangements. Figure 3.1 below shows the circuiting of the condenser finned tube coil. The condenser is **28 in x 80.5 in (71.1 cm x 204.5 cm)** finned length, **22 fins/in (9 fins/cm)**.

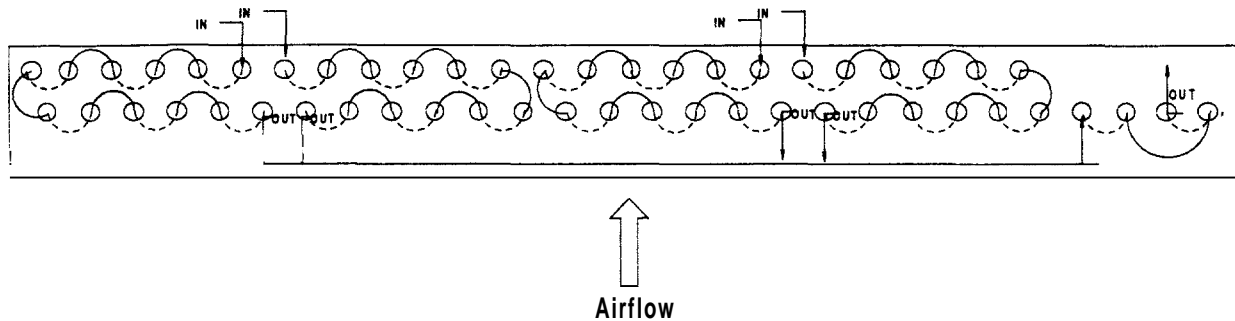


Figure 3.1 Condenser for **R22** and **R410A** systems

The evaporator for both systems was a vertical slab coil designed for installation with airflow from the left or right. Figure 3.2 shows the circuiting of the evaporator used by both systems. For all of the tests, the airflow rate through the evaporator was set at **1200.0scfm (34.0 m<sup>3</sup>/min)**. The evaporator is **22.0 in x 26.0 in (55.9 cm x 66.0 cm)** finned length with **12 fins/in**. The evaporator and condenser have a fin thickness of **0.0045 in (0.1143 mm)**.

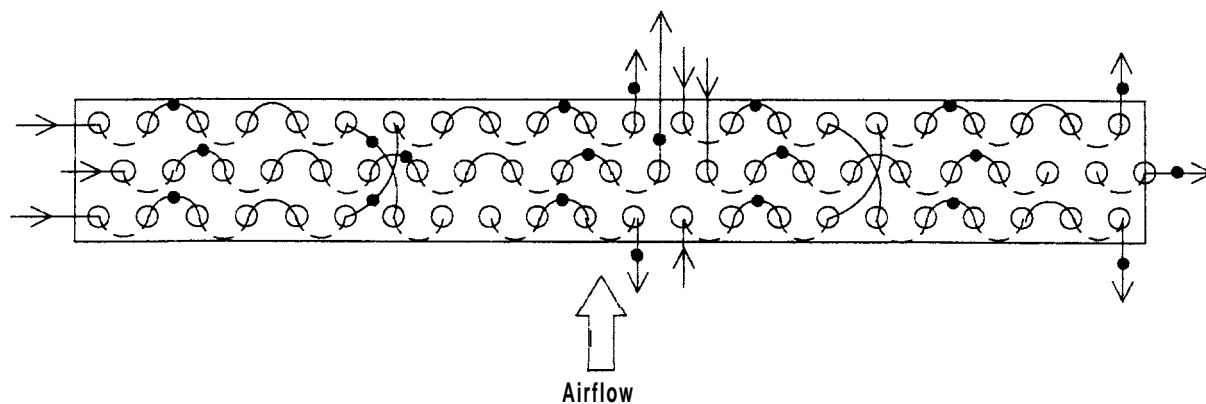


Figure 3.2 Evaporator for **R22** and **R410A** systems

### 3.2 Experimental Set-Up

Figure 3.3 shows the arrangement of the system in the environmental chambers. The airflow chamber contained a **7.0 inch (17.8 cm)** diameter **ASME** nozzle and was constructed according to **ANSI/ASHRAE 51-1985** and **ANSI/ASHRAE Standard 37-1988**. The air conditioning systems consisted of a condensing unit in the outdoor chamber (Figure 3.4) and a finned tube coil evaporator in the indoor test section (Figure 3.5). Air was pulled through the evaporator by a centrifugal fan at the outlet of the nozzle chamber ductwork. Dew-point temperature was measured at the inlet of the evaporator ductwork and in the ductwork after the evaporator once the air passed through several mixers. Twenty-five node thermocouple grids and thermopiles measured the air temperatures and temperature change, respectively. The thermocouple grids were used to ensure that the *air* was well mixed before and after the evaporator. Barometric pressure, evaporator air pressure drop, nozzle pressure drop, and nozzle temperature were used along with the dew-point measurements to establish the thermodynamic state of the air. The air enthalpy method was used at the primary measurement of air-side capacity. The



refrigerant enthalpy method was used as the secondary measurement of capacity. These two measurements always agreed within 3.5 %.

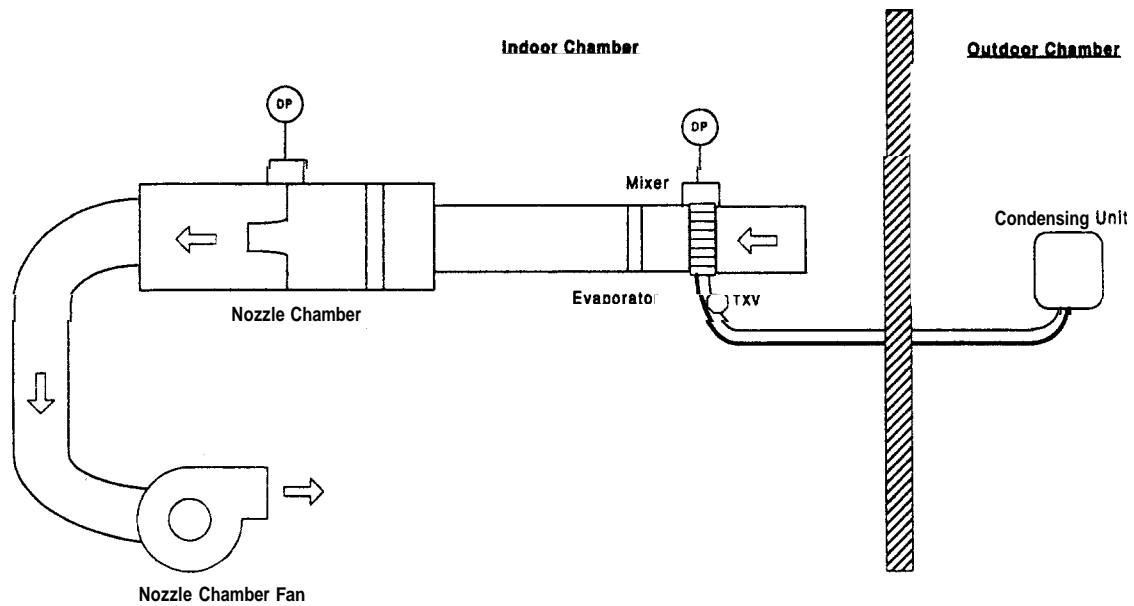
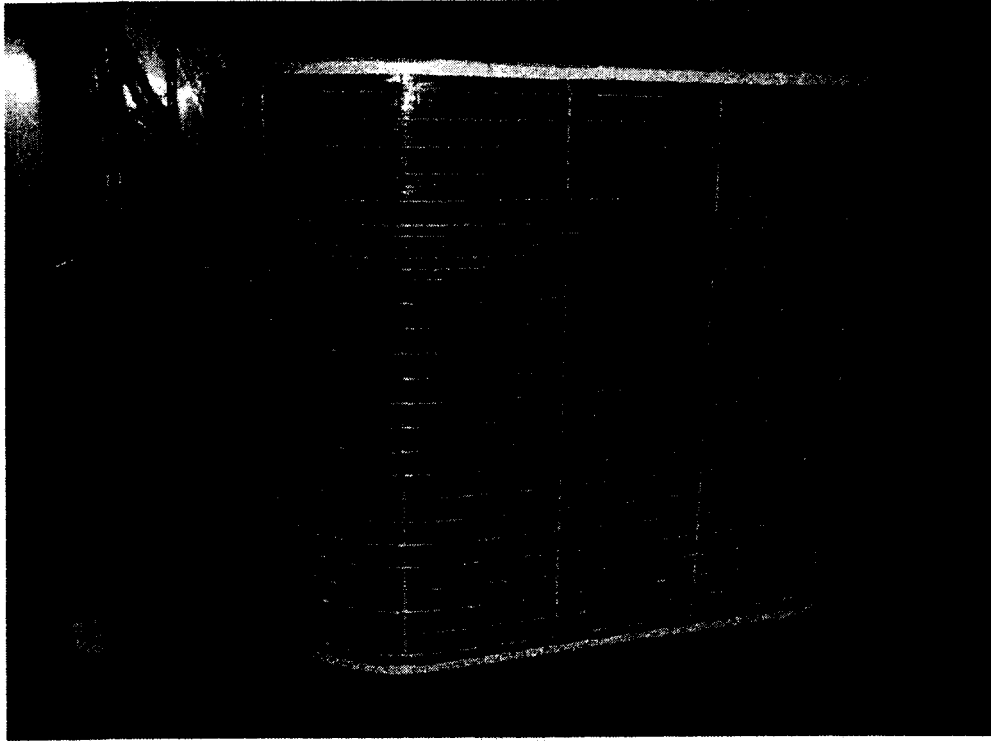
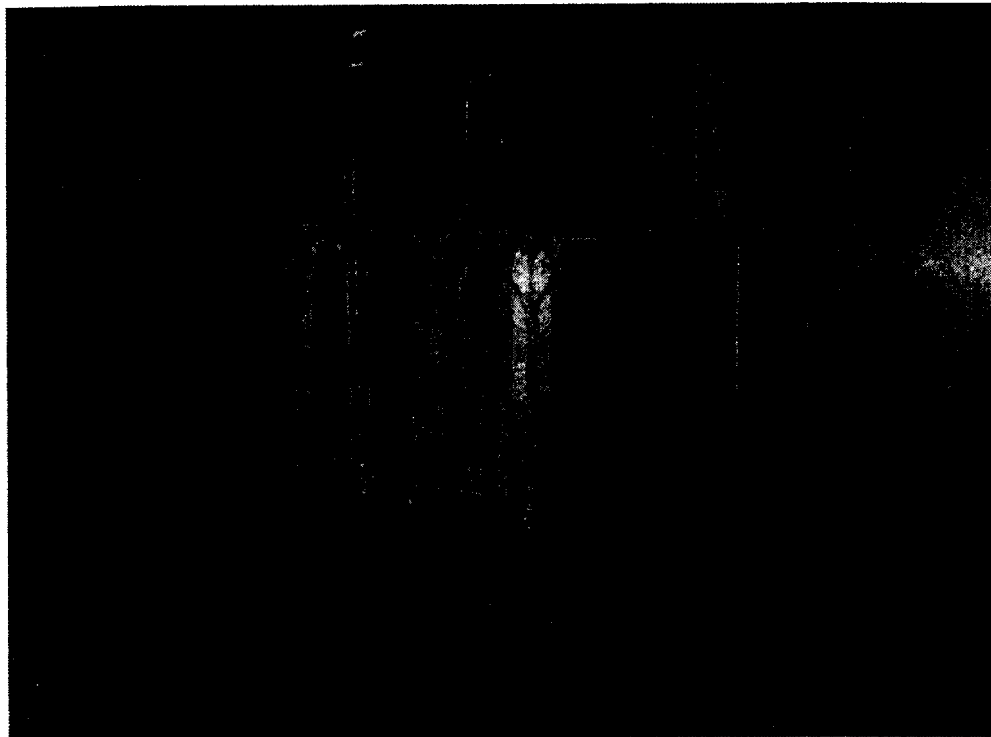


Figure 3.3 Environmental chamber test schematic



**Figure 3.4 High efficiency condensing unit**



**Figure 3.5 Indoor test section housing evaporator**

### 3.3 Experimental Procedure and Test Conditions

The two **units** were tested at the same indoor conditions of 80.0 °F (26.7°C) dry-bulb and 67.0 °F (19.4°C) wet-bulb temperature according to **ASHRAE Standard 37-1988**. The outdoor **conditions** varied according to the table **below**.

Location	Cooling	
	Setpoint (°F)	Tolerance (°F)
Indoor Dry-bulb Temperature	80.0	±0.5
Indoor Dew-point Temperature	60.4	±0.5
Outdoor Chamber Temperature	82.0' 95.0 <sup>2</sup> 115.0 <sup>2</sup> 125.0' 130.0 <sup>2</sup> 135.0 <sup>3</sup> 140.0 <sup>4</sup> 150.0 <sup>4</sup> 152.0 <sup>4</sup> 155.0 <sup>4</sup>	±0.5
Evaporator Airflow, scfm	1200	

- 1) **R22 and R410A Compressor #1**
- 2) **R22 and both R410A Compressors**
- 3) **Only R22**
- 4) **Only R410A Compressor #2**

Indoor and outdoor conditions remained stable for one hour before data were taken. A steady flow of condensate from the evaporator was present for all tests. Before any

testing began, the system charge was set according to manufacturer's recommendations. The charge for both units was set by measuring the difference between the liquid line temperature exiting the condensing unit and the outdoor air temperature (95.0 °F (35.0 °C)). This temperature difference ~~was~~ decreased by adding refrigerant or increased by removing refrigerant. For the R22 system **this** temperature difference was set at 5.0 °F (2.8 °C). For the R410A system **this** temperature difference was set at **6.0 °F** (3.3 °C).

Experimental uncertainty was calculated using a propagation of uncertainty technique considering uncertainty in all the parameters associated with the capacity and EER (Payne and Domanski, 2001). Appendix D summarizes the propagation of errors approach that was used to determine the uncertainty in capacity and EER. The 95 % (two sigma) uncertainty in capacity and EER **varied** from 2.9 % to 3.5% **and** 3.5 % to 5.4 %, respectively.

### 3.4 Experimental Results

#### 3.4.1 Test Results for the R22 System

The R22 system performed without any difficulty over the full range of outdoor temperatures. The sensible heat ratio remained at  $0.8 \pm 0.05$  for all tests. Figure 3.6 shows the cooling capacity **as** a function of the outdoor temperature. Capacity ranged from 40201 Btu/h (11781 **W**) to 29711 Btu/h (8707 **W**) over the range of outdoor temperatures. This was a decrease of 26.1 % from the high value at 82.0 **°F** (27.8 °C) to the low value at 135.0 **°F** (57.2 °C).

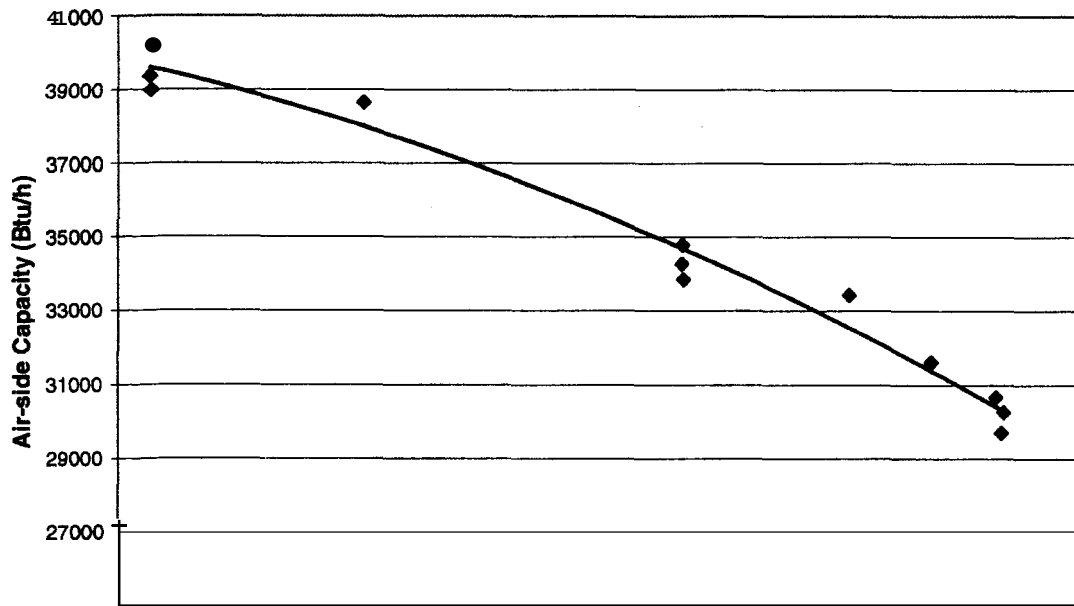


Figure 3.6 **R22** cooling capacity as a function of outdoor temperature

The compressor performance was characterized by power measurements and refrigerant conditions at its inlet and exit. Figure 3.7 shows the reduced discharge pressure and discharge superheat for the tests shown in Figure 3.6. Reduced pressure ranged from 0.30 to **0.56** with the discharge superheat ranging from 44.0 °F to **83.0 °F** (24.4 °C to 46.1 °C) ( $P_{crit} = 723.7$  psia (4989.7 kPa),  $T_{crit.} = 205.06$  °F (96.14 °C)). The discharge pressure and discharge superheat increased by **84.4%** and **83.3 %**, respectively, from their values at **82.0 °F** (27.8 °C).

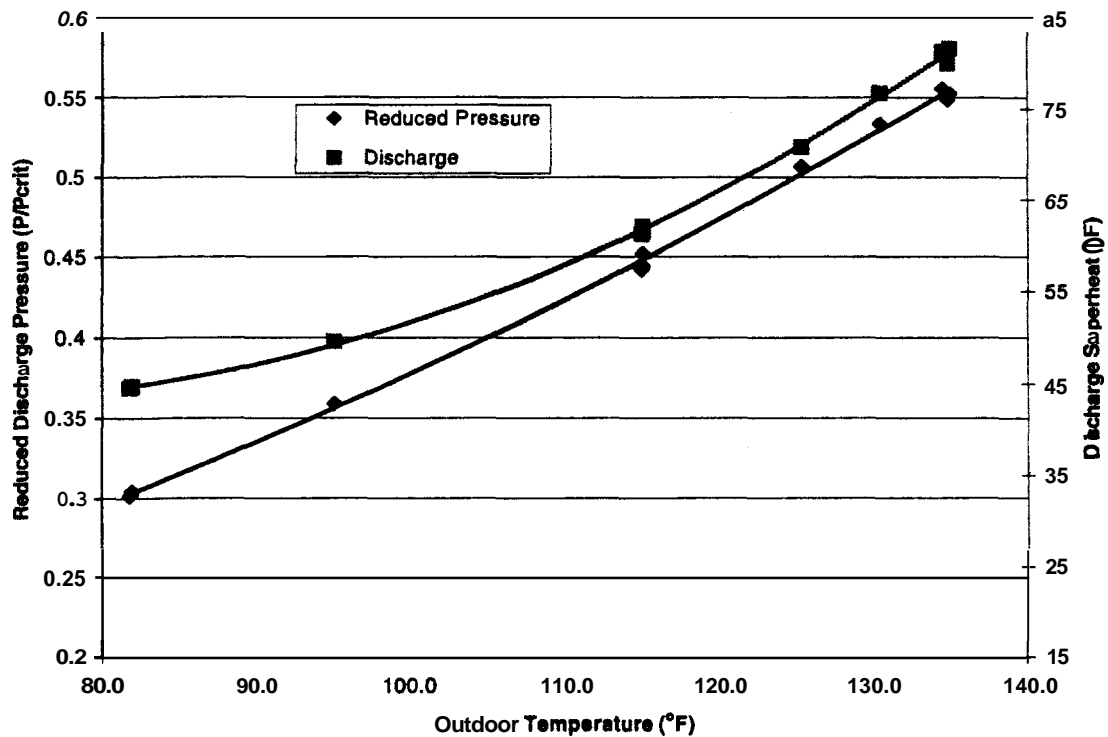


Figure 3.7 R22 reduced discharge pressure and discharge superheat as function of outdoor temperature

System power and refrigerant ~~mass~~ flowrate are shown in Figure 3.8. Power increased from 2080 W to 4140 W as the mass flowrate decreased from 8.93 lb/min (4.05 kg/min) to 8.54 lb/min (3.87 kg/min). This produced an increase of 87.9% in system power with a 4.7 % decrease in refrigerant ~~mass~~ flowrate.

R22 cooling ~~EER~~ decreased as the outdoor temperature increased (Figure 3.9). As the outdoor temperature increased from 82 °F to 135 °F (27.8 °C to 57.2 °C), the EER (COP) decreased by 60.3 % as it dropped from 18.3 Btu/Wh (5.36) to 7.3 Btu/Wh (2.14).

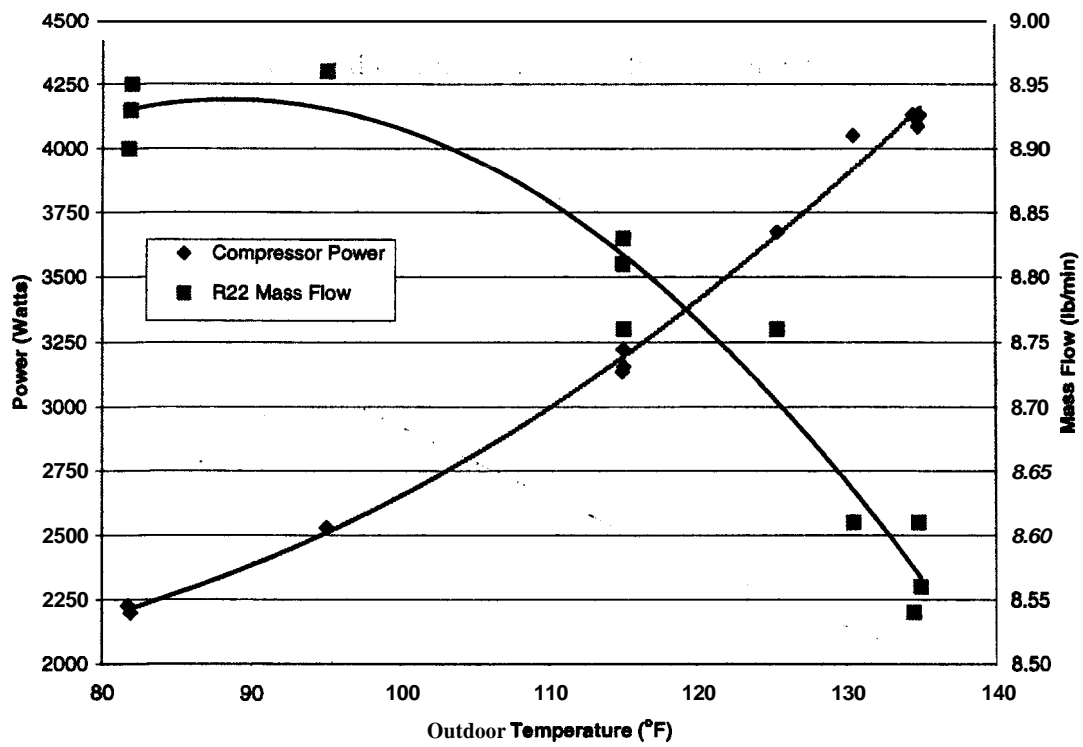
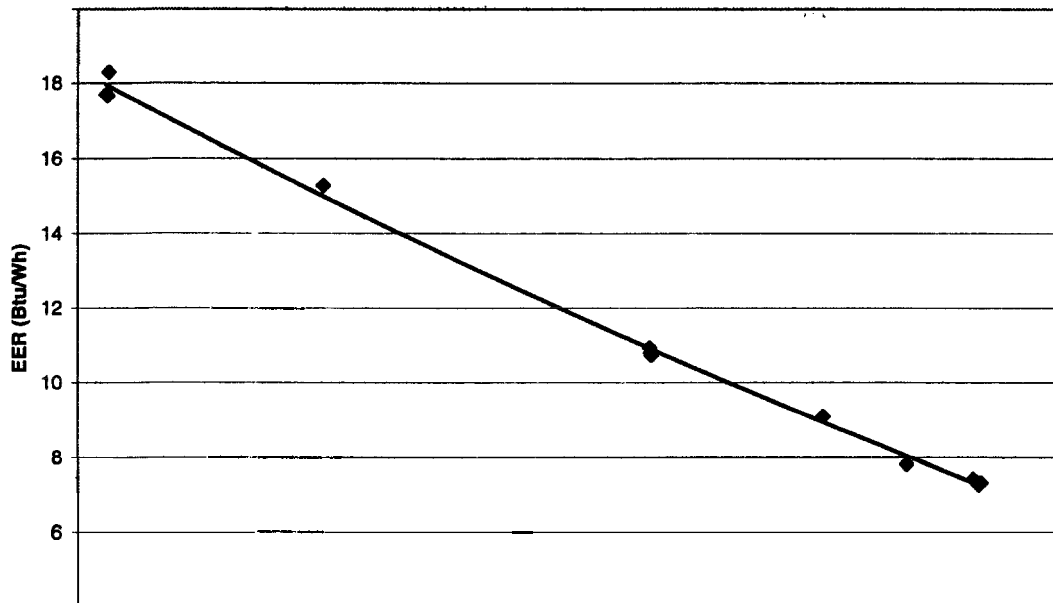


Figure 3.8 System power and R22 mass flow as a function of outdoor temperature



### 3.4.2 Test Results for the R410A System

We performed **R410A** system tests using two compressors designated here as compressor #1 and compressor #2. Compressor #1 was the original compressor supplied with the system. The internal safeties for **this** compressor prevented the system from operating continuously at outdoor temperatures above **130.0 °F (54.4 °C)**. Another compressor that had all internal safeties removed was used to test the system at higher outdoor temperatures. Compressor #2 allowed testing to proceed **up** to **155.0 °F (68.3 °C)**. Compressor #2 had a more powerful electric motor than compressor #1.

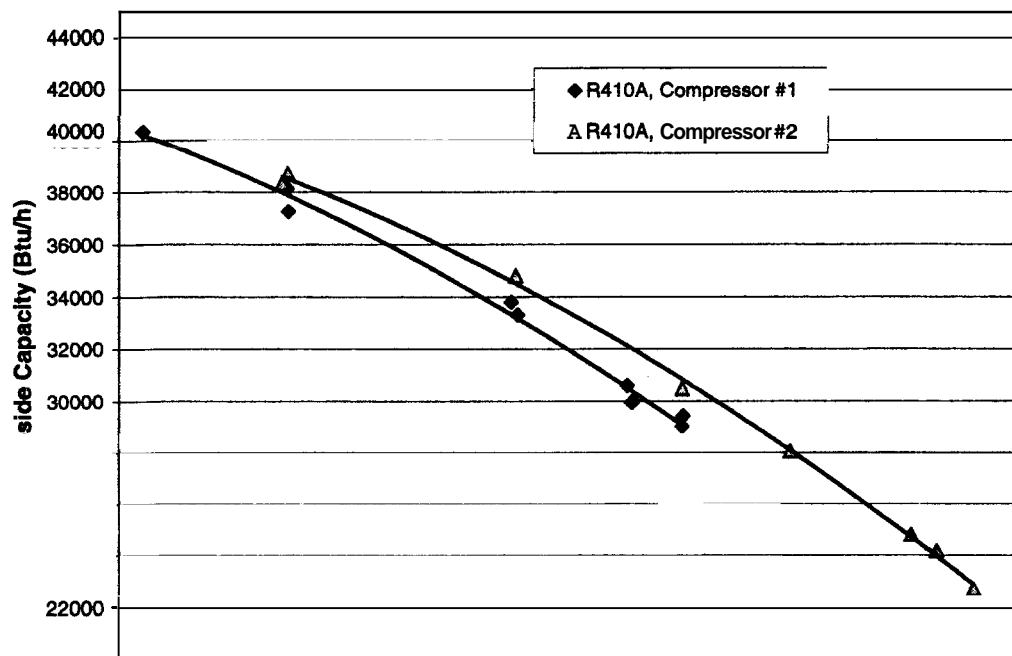
The cooling capacity of the **R410A** system is show in Figure **3.10**. Air-side capacity decreased in a nearly linear manner **as** the outdoor temperature was increased from **82.0 °F** to **155.0 °F (27.8 °C to 68.3 °C)**. Over this temperature range, air-side capacity decreased from **40345 Btu/h (11824 W)** to **22699 Btu/h (6652 W)**; a decrease of **43.7 %**.

Figure **3.11** shows the compressor reduced discharge pressure and discharge superheat over the range of outdoor temperatures. The discharge pressure was above the critical pressure of **691.8 psia (4769.8 kPa)** during three **of** the high ambient tests. Discharge superheat increased **as** the outdoor temperature increased and the refrigerant mass flowrate decreased. Compressor discharge superheat ranged from **22.0 °F (12.2 °C)** at the lowest outdoor temperature to **97.0 °F (53.9 °C)** at the highest outdoor temperature (for the tests above the critical temperature and pressure, superheat is calculated with respect to the critical temperature of **158.3 °F (70.2 °C)**,  $T_{sup} = T - T_{crit}$ ).



R410A system power and refrigerant mass flowrate are shown in Figure 3.12. The power increased from 2201 W to 6287 W as the mass flowrate decreased from 8.95 lb/min to 8.26 lb/min. This was an increase of 185 % in system power with a 7.7 % decrease in refrigerant mass flowrate.

R410A cooling EER decreased as the outdoor temperature increased (Figure 3.13). As the outdoor temperature increased from 82.0 °F to 155.0 °F (27.8 °C to 68.3 °C), the EER (COP) decreased by 80.3 % as it dropped from 18.3 Btu/Wh (5.36) to 3.6 Btu/Wh (1.06).



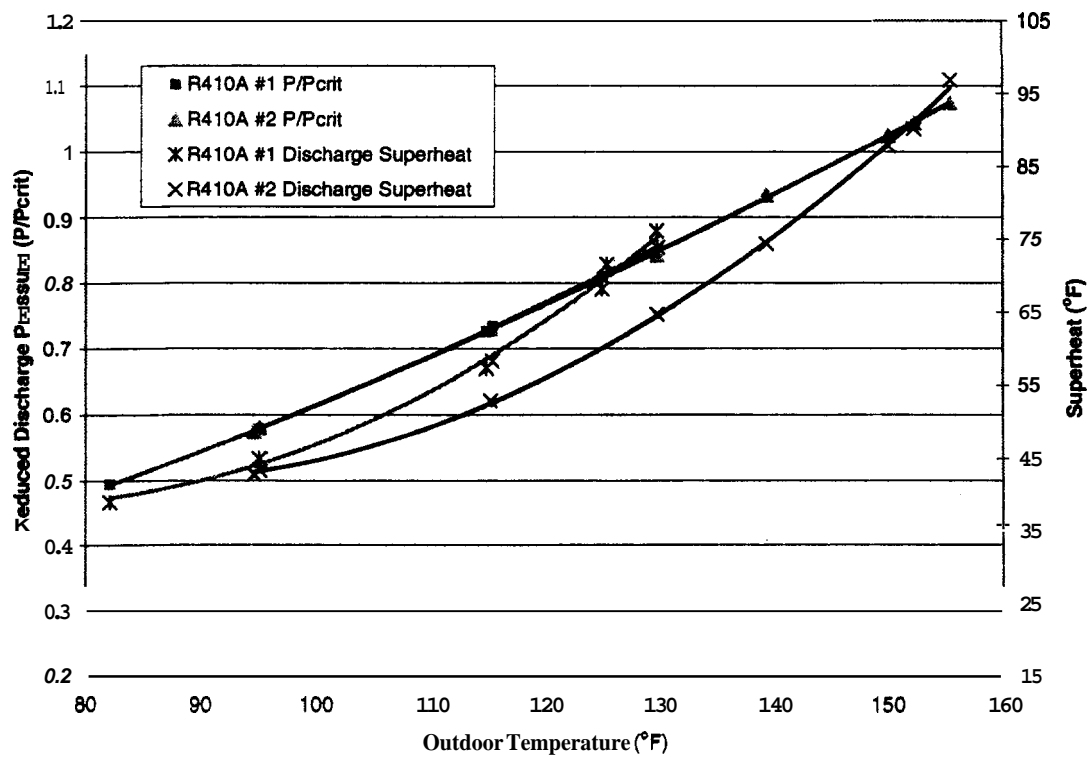


Figure 3.11 R410A reduced discharge pressure and discharge superheat

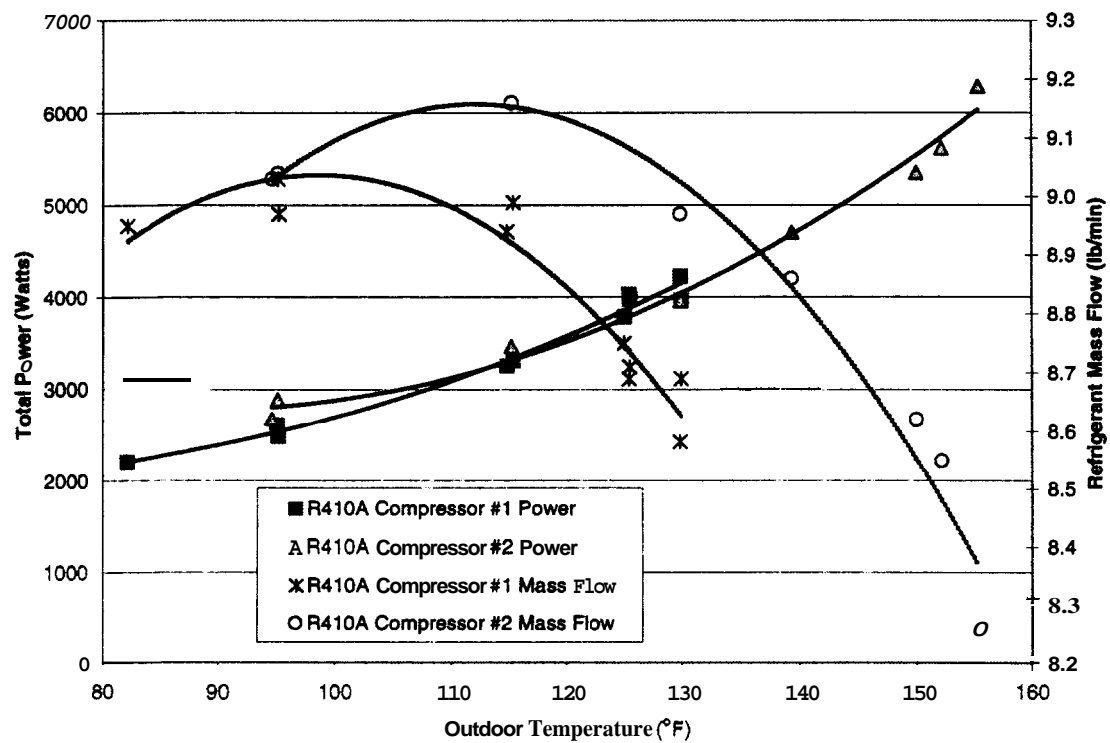


Figure 3.12 R410A system power and refrigerant mass flowrate

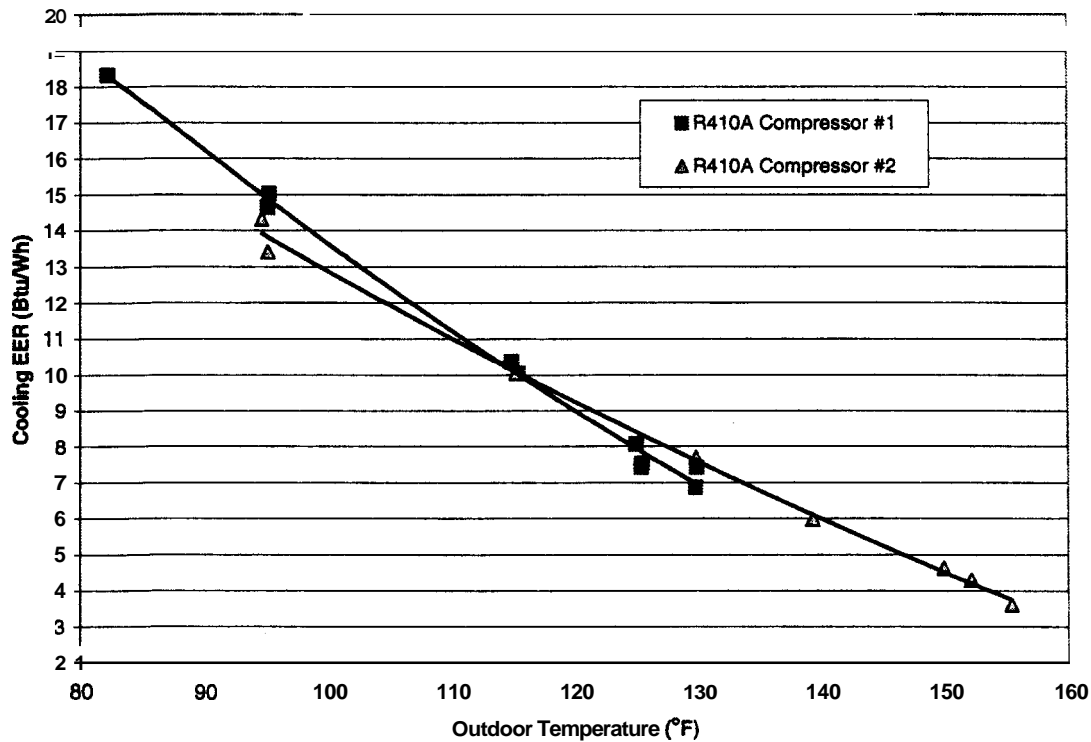


Figure 3.13 R410A cooling EER as a function of outdoor temperature

### 3.4.3 R410A Oil Sampling Test Results

POE oil (RL32S) was sampled from the R410A system at outdoor temperatures of 95.0 °F (35.0 °C) and 125.0 °F (51.7 °C). The sample cylinder was connected to the liquid line by a length of 1/8 inch (3.2 mm) copper tubing. The evacuated cylinder was submerged in an ice bath while a needle valve allowed a slow flow of liquid into the cylinder. Approximately 3 ounces (85 grams) of refrigerant and oil were sampled. The refrigerant was evacuated from the cylinder over a one-hour period. The cylinder was weighed before and after the sample was taken and after the refrigerant had been removed. The mass fraction of oil was defined as the mass of oil in the sample divided by the mass of refrigerant. The masses were recorded with an uncertainty at the 95 %

level of  $\pm 0.000071$  ounces ( $\pm 0.002$  grams). Table 3.2 lists the temperatures and sample masses for the R410A tests on compressor #1.

Table 3.2 R410A oil sample results

Outdoor Temperature (°F)	Mass of Oil (gram)	Mass of Refrigerant (gram)	(Mass of Oil) / (Mass of Refrigerant)
95	0.456	86.438	0.53 %
95	0.352	89.041	0.40 %
95	0.258	91.437	0.28 %
125	0.164	88.988	0.18 %
125	0.218	91.705	0.24 %

### 3.5 Comparison of Performance of R22 and R410A Systems

#### 3.5.1 R410A Cooling Capacity Relative to R22

Cooling capacity comparisons were made between the R22 system and the R410A system with its different compressors by fitting a curve to the R22 cooling capacity as a function of outdoor temperature. All of the R22 cooling data points were fit to a polynomial function given below by equation 3.1:

$$Q(\text{Btu/h}) = 42196.9 - 4.8705 \times 10^{-3} \cdot T(^{\circ}\text{F})^3 \quad (3.1a)$$

$$Q(\text{kW}) = 11.877 - 1.638 \times 10^{-5} \cdot T(^{\circ}\text{C})^3 \quad (3.1b)$$

The cubic polynomial above fit the R22 capacity data with a Pearson correlation coefficient ( $R^2$ ) of 0.978 and a fit standard error of 591.06 Btu/h (173.22 W) over the temperature range of 82.0 °F to 130.0 °F (27.8 °C to 54.4 °C). Using equation 3.1, the

R410A cooling capacity ~~was~~ divided by the R22 cooling capacity calculated at the appropriate outdoor temperature to calculate the cooling capacity ratio.

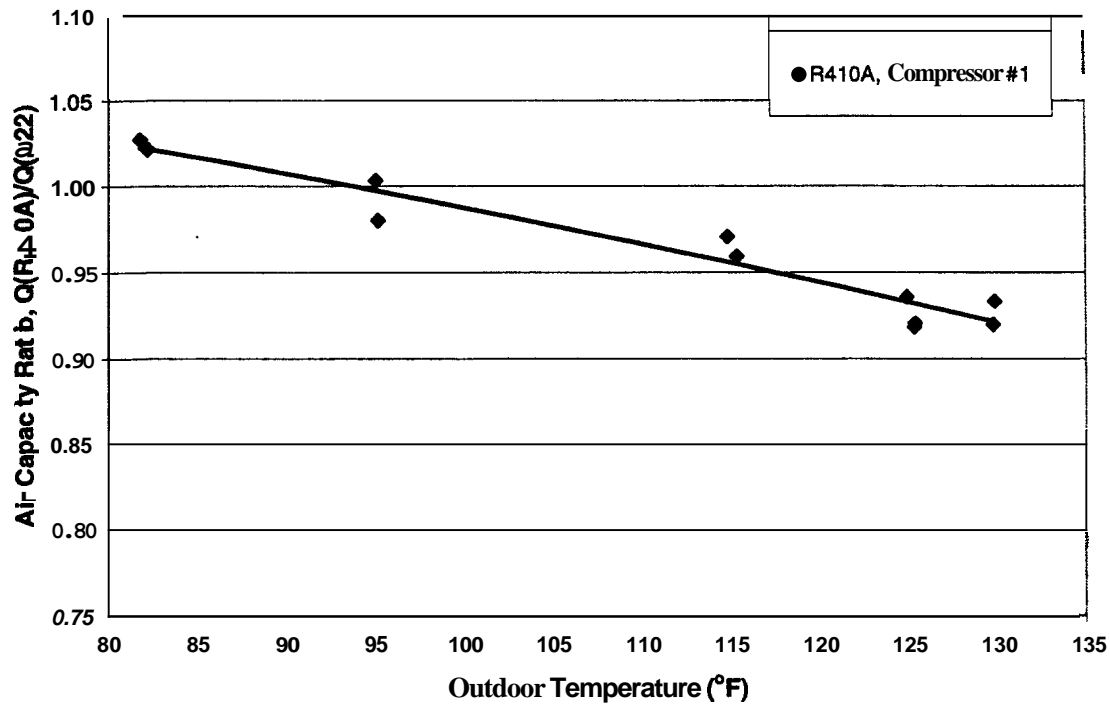


Figure 3.14 Cooling capacity of R410A system relative to R22 system

The capacities of the R22 system and R410A system were equal at the 35.0 °C (95.0 °F) outdoor temperature. At the 82.0 °F (27.8 °C) rating point, the R410A system capacity ~~was~~ approximately 2 % greater than that of the R22 system. As the outdoor temperature increased, the capacity of the R410A system decreased more rapidly than the R22 system capacity, and at the 130.0 °F (54.4 °C) test point ~~was~~ 9 % below the R22 value.

### 3.5.2 R410A Cooling EER Relative to R22

Cooling EER for the R22 system was fit to a polynomial function of the outdoor temperature using statistical analysis software. Cooling EER (COP) as a function of outdoor temperature was fit to the polynomial shown below:

$$\text{EER(Btu/Wh)} = 36.692 - 0.3611 \cdot T(^{\circ}\text{F})^{0.8981} \quad (3.2a)$$

$$\text{COP} = 9.459 - 0.3323 \cdot T(^{\circ}\text{C})^{0.7654} \quad (3.2b)$$

The power law function fit R22 EER (COP) as a function of outdoor temperature with a Pearson correlation coefficient ( $R^2$ ) of 0.998 and a fit standard error of 0.2749 Btu/Wh (0.081) over the outdoor temperature range of 82.0 °F to 130.0 °F (27.8 °C to 54.4 °C). Just as in the cooling capacity case, R410A EER (COP) was divided by the calculated R22 EER (COP) at the given outdoor temperature to produce a relative value.

The efficiency trend was similar to the trend for capacity; however, the performance degradation of R410A was more pronounced, as shown in Figure 3.15. At the 27.8 °C (82.0 °F) rating point, the EER (COP) of the R410A system was a few percent higher than that for the R22 system. At the 95.0 °F (35.0 °C) rating point, at which the capacities were equal, the R410A EER (COP) was approximately 4 % below the R22 EER (COP). At the highest ambient temperature of 130.0 °F (54.4 °C), the R410A EER (COP) was about 15 % lower than the EER (COP) of the R22 system. In addition to typical measurement uncertainties, we attribute the scatter shown in the EER (COP) ratios for a given outdoor temperature to day-to-day variations of voltage at the testing

facility. However, these voltage variations were always within the range allowed by the **ARI 210/240 (1994)**.

No rapid **drop** in capacity and **EER** occurred for the **R410A** system as the outdoor temperature increased to **155.0 °F (68.3 °C)**. This is similar to the split-system testing performed by Wells et al. **1999**. They showed a 10 % lower capacity of the **R410A** system than the **R22** system at **125.0 °F (51.7 °C)**. The literature has shown that capacity and EER **are** very sensitive to the expansion device and the size of the heat exchangers (Farzad and O'Neal **1991**, Gates et al. **1967**). This work has shown that a **TXV** in combination with sustained subcooling can mitigate some of the performance degradation seen at high ambient temperatures.

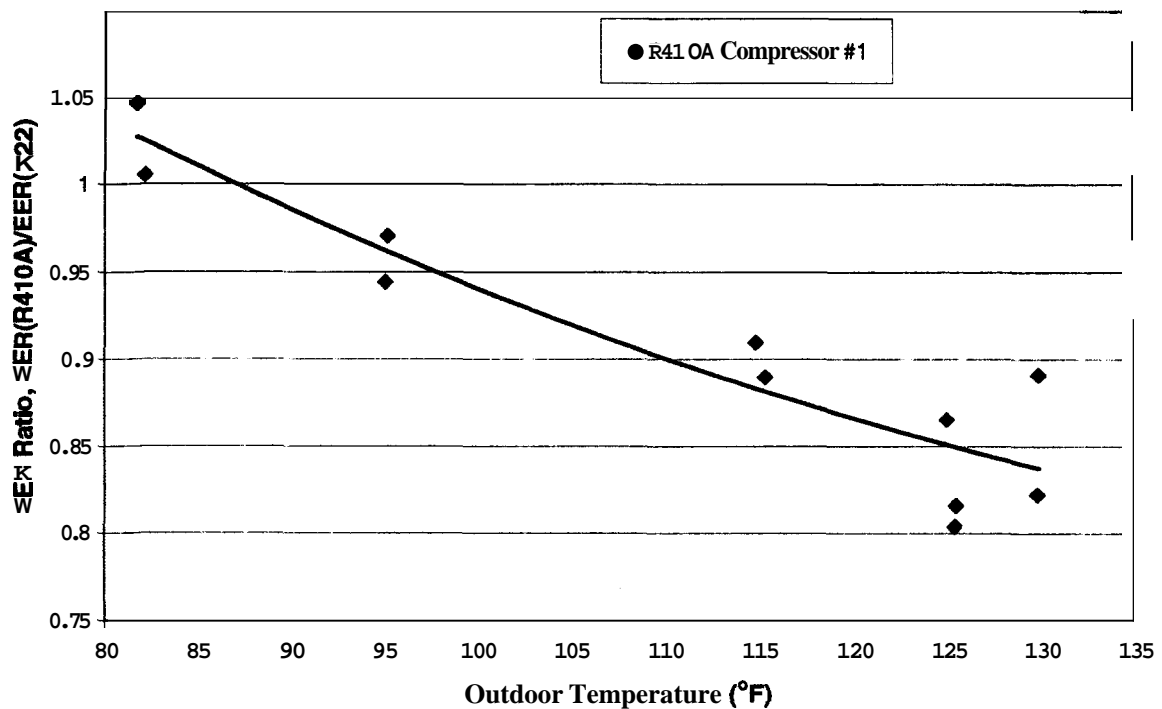


Figure 3.15 Cooling EER of **R410A** system relative to R22 system

## 4. MODELING

Laboratory tests conducted for this project provided performance information on **R22** and **R410A** systems and their components, including the evaporators and condensers. The two systems employed the evaporators and condensers of identical design, respectively. Hence, these data constitute a rare material for validation of simulation models working with different fluids.

Development of evaporator and condenser models is the dominant effort in building up a model of a vapor-compression air conditioner. This is because we can readily simulate compressor's performance using compressor maps available from the compressor manufacturer, and the expansion valve is an easy to model isenthalpic device. In fact, with the tube-by-tube representation of a finned-tube heat exchanger applied in the NIST heat pump model, ninety percent of the code is used for evaporator and condenser modeling. For this reason and considering the difficulty associated with designing optimized heat exchangers, our task included development and validation of the evaporator and condenser models, EVAPS and CONDS, and packaging them with a visual interface in one software package called EVAP-COND.

It is not in the scope of this report to provide a comprehensive description of the evaporator and condenser models but rather to provide practical information on how the models were formulated, what their features are, and how they can be **used**. This information is provided in sections **4.1** through **4.4**. The remaining sections discuss implementation of **EVAPS** and **CONDS** into a simulation model of an air conditioner, it's



validation, and comparative simulations of R22, R410A, R134a, and R404A air conditioners.

#### 4.1 Modeling Issues for Finned-tube Heat Exchangers

##### 4.1.1 EVAP5 and **CONDS** Modeling Approach

Finned-tube air-to-refrigerant heat exchangers constitute the predominant heat exchanger type used in air conditioning. They are manufactured with a variety of refrigerant circuitry designs. Simulation models that account for refrigerant circuit architecture are better equipped for accurately predicting the heat exchanger performance. This is because the refrigerant path through the heat exchanger can have a significant effect on heat exchanger performance. The models presented here, EVAP5 and CONDS, originated in the tube-by-tube simulation model formulated by Chi (1979). Over the years, several significant new features were implemented, which included the capability to account for air maldistribution and its interaction with refrigerant distribution, extension of the models to zeotropic mixtures, extension to new refrigerant property representations, new simulation correlations, etc. (Domanski and Didion (1983), Domanski (1991), Lee and Domanski (1997), Domanski (1999b)).

Figure 4.1 presents the refrigerant circuitry and air velocity representation used by EVAP5 and CONDS. Due to the tube-by-tube modeling approach, the programs recognize each tube as a separate entity for which it calculates heat transfer. These calculations are based on inlet refrigerant and air parameters, properties, and mass flow rates. The simulation begins with the inlet refrigerant tubes and proceeds to successive

tubes along the refrigerant path. At the outset of the simulation, the air temperature is only known for the tubes in the first row and has to be estimated for the remaining tubes. A successful **run** requires several passes (iterations) through the refrigerant circuitry, each time updating inlet air and refrigerant parameters for each tube.

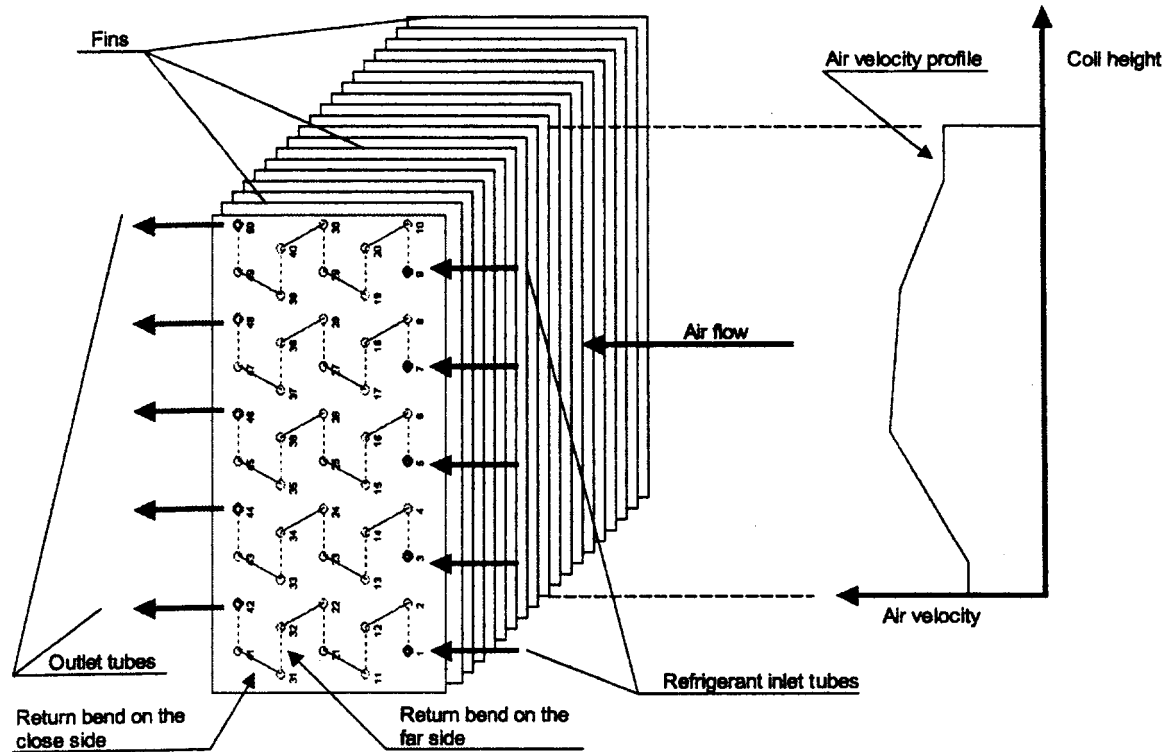


Figure 4.1 Representation of air distribution and refrigerant circuitry in **EVAPS** and **CONDS**

Heat transfer calculations start by calculating the heat-transfer effectiveness,  $E$ , by one of the applicable relations (Kays and London, 1984). With the air temperature changing due to heat transfer, the selection of the appropriate relation for  $E$  depends on whether the refrigerant undergoes a temperature change during heat transfer. Once  $E$  is determined, heat transfer from air to refrigerant is obtained using eq. (4.1).

$$\dot{Q}_r = \dot{m}_a C_{pa} (T_{ai} - T_{ri}) \epsilon \quad (4.1)$$

The overall heat-transfer coefficient,  $U$ , is calculated by eq. (4.2), which sums up the individual heat-transfer resistances between the refrigerant and the air.

$$U = \left[ \frac{A_o}{h_i A_{pi}} + \frac{A_o X_p}{A_{pm} K_p} + \frac{1}{h_l} + \frac{A_o}{A_{po} h_{pf}} + \frac{1}{h_o (1 + \alpha) \left( 1 - \frac{A_f}{A_o} (1 - \phi) \right)} \right]^{-1} \quad (4.2)$$

The first term of eq. (4.2) represents the refrigerant-side convective resistance. The second term is the conduction heat-transfer resistance through the tube wall, and the third term accounts for the conduction resistance through the water layer on the fin and tube. The fourth term represents the contact resistance between the outside tube surface and the fin collar. The fifth term is the convective resistance on the air-side where the multiplier  $(1 + \alpha)$  in the denominator accounts for the latent heat transfer on the outside surface. For a dry tube  $\alpha = 0.0$  and  $1/h_l = 0.0$ . Once the heat transfer rate from the air to the refrigerant is calculated, the tube wall and fin surface temperatures can be calculated directly using heat-transfer resistances. Then, the humidity ratios for the saturated air at the wall and fin temperatures are calculated, and mass transfer from the moist air to the tube and fin surfaces is determined. For more detailed information on heat transfer calculations refer to Domanski (1991).

Simulating refrigerant distribution is an important part of simulating performance of heat exchangers, particularly for cases with non-uniform air distribution. In a heat exchanger with multiple circuits, refrigerant distributes itself in appropriate proportions so that the refrigerant pressure drop from inlet to outlet is the same for all circuits. This observation is essential for calculating a fraction of the total refrigerant mass flow rate flowing through a particular circuit. At the outset of this ARTI project, the evaporator model used a scheme for predicting refrigerant distribution that was based on the Pierre evaporation-pressure-drop correlation (Domanski, 1991), while the condenser model did not have this capability at all. Under the current project, we developed a new scheme for simulating refrigerant distribution between different circuitry branches by treating the problem as a nonlinear system of equations and solving it using the Newton-Raphson method. The new scheme can be applied to the evaporator, refrigerant distributor/evaporator system, and condenser regardless of the correlation used to calculate refrigerant pressure drop in a given heat exchanger. The Pierre-based method has been retained in EVAPS and CONDS to simulate refrigerant distribution for the first two iteration loops. At the outset of simulation, the initial refrigerant distribution is estimated based on the number of tubes in a given circuit and the circuit's layout (circuit split points and their locations).

#### 4.1.2. Air-side Heat Transfer Correlations

A significant, often the major, part of heat transfer resistance between the air and refrigerant is on the air side of the heat exchanger. For this reason we reviewed literature on the latest air-side heat transfer correlations at the beginning of this project.

Figure 4.2 compares predictions of different correlations available in the literature. We calculated these predictions for typical designs for fins of different categories for a three-depth-row heat exchanger. The figure does not include a slit-wavy fin - the type used in the tested R22 and R410A systems - since we could not locate a slit-wavy fin correlation in the literature. The layout of different lines on the figure may serve as an explanation why predicting performance of a finned-tube heat exchanger equipped with an enhanced fin may be difficult. For wavy fins, the correlation by Wang et al. (1999a) and Kim et al. (1997) are in a close agreement, while the correlation by Webb (1990) calculates heat transfer coefficients up to 50 % lower than the two first methods. At one point, the Webb correlation provides the wavy fin heat transfer coefficient to be lower than that for flat fins, which is not a realistic prediction.

For slit (lanced) fins, the correlations by Nakamura and Xu (1983) and Wang et al. (2001) are apart by as much as 40 %, depending on air velocity. This spread may be indicative of the general fact that some correlations do not predict well outside the geometries for which they were developed. A measurement uncertainty in one or both experiments may also be a contributing factor to the 40 % discrepancy. Regarding the louver fin, the correlation by Wang et al. (1999b) shows a step change caused by using two different algorithms depending on the Reynolds number. Two separate algorithms are also causing a step change in predictions by the Webb correlation for flat fins.

The analysis of relative predictions of air-side heat transfer coefficient for different surfaces prompted us to replace the existing correlations in EVAPS and CONDS with

correlations published by Wang and his co-workers for all type of fins, i.e., flat, slit, wavy and louver fins. In our judgment, this will ensure a higher degree of prediction consistency when comparing performance of heat exchangers with different fin designs since it can be expected that a prediction consistency for the air-side heat transfer coefficient will be maintained by correlations developed by the same author. We may note one reservation with this choice; we expect a slit (lanced) fin to perform better in relation to a wavy fin than it is reflected by the slit and wavy Correlations authored by Wang (Wang et al., 2001, and Wang et al., 1999a). We could expect rather the values calculated by the Nakayama and Xu correlation would be in general more representative for most practical air velocities. However, we were disturbed by the fact that the Nakayama and Xu (1983) predictions do not degrade more at ~~air~~ velocities below 4 ft/s (the trend exhibited by the other correlations), and for this reason we opted for the ~~Wang~~ correlation for slit fins. Hence, the Wang correlation for slit fins (Wang et al., 2001) was selected not for its absolute predictions, but rather for the shape of the prediction line, which can be adjusted to proper absolute values with a correction multiplier.

All air-side heat transfer correlations authored by Wang include the tube-to-collar heat transfer resistance. Hence, his correlations do not have the ambiguity of the previously used flat-fin correlation by Gray and Webb (1986) developed using data on 16 heat exchangers, 10 of which had no fin-to-collar heat transfer resistance due to a metallurgical bond. For this reason, when incorporating the correlations by Wang et al. we removed the algorithm for calculating the tube-collar junction resistance, which up to this point was calculated by the correlation by Sheffield et al. (1988).

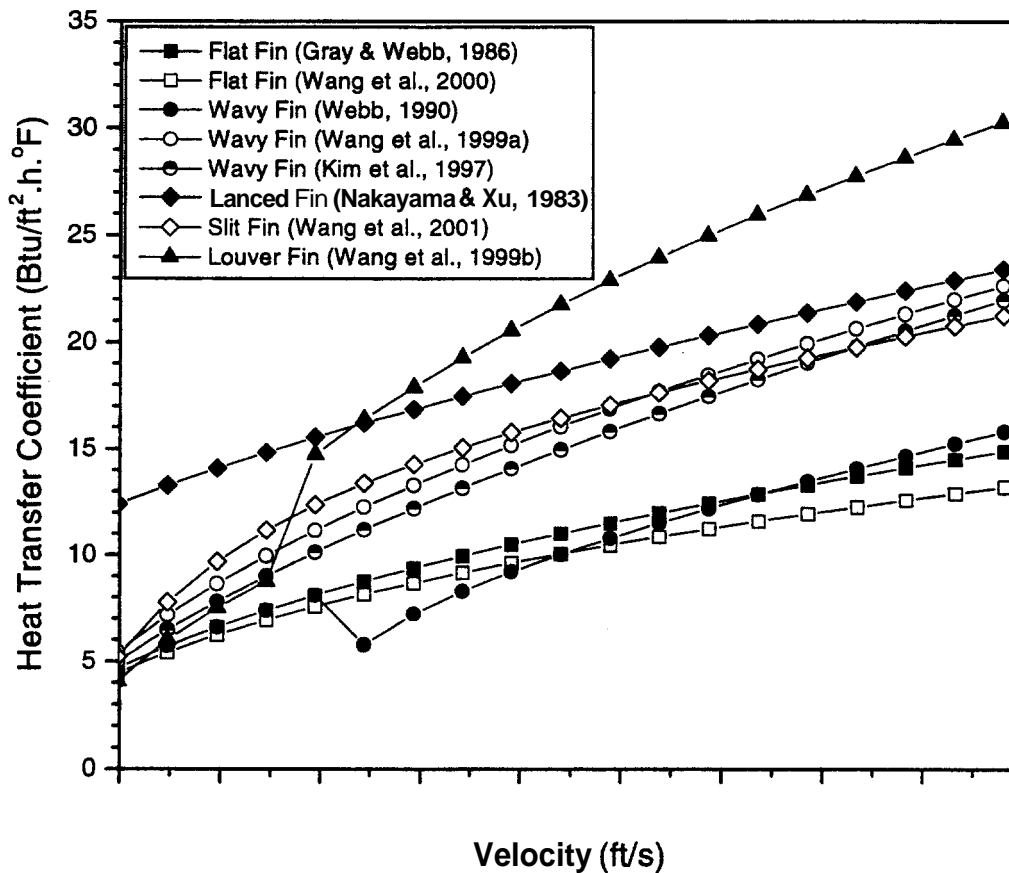


Figure 4.2 Comparison of air-side heat transfer correlations

#### 4.1.3 Representation of Refrigerant Properties

The following upgrades were made to EVAP5 and CONDS under this project:

- Upgrade of **EVAPS** and **CONDS** to REFPROP6

We upgraded EVAPS and **CONDS** from REFPROPS (Gallagher et al., 1996) to REFPROP6 (McLinden et al., 1998) routines. Since these refrigerant property packages employ different equations of state, we used a system of bridging routines to make the conversion.

- Development of Pressure-Enthalpy Based Property Look-up Tables

EVAPS and CONDS simulations are computationally intensive, and using a refrigerant property look-up tables is a practical necessity if simulation runs are expected to last less than 60 seconds. This is particularly true in case of REFPROP6, for which property calculations **are** several times more CPU demanding than for REFPROPS. The pressure-quality-based look-up tables used so far with R22 were not adequate for this study since the R410A air conditioner may enter the transcritical operating regime at extremely high ambient temperatures. A new pressure-enthalpy based system of look-up tables was developed to facilitate simulation above the critical point of refrigerant. This look-up scheme includes eight different property routines that retrieve the desired state or transport property depending on the available properties identifying the refrigerant's thermodynamic state. The look-up scheme is applicable to single component refrigerants and refrigerant mixtures.

- Development of an Error Evasive Scheme for Refrigerant Property Calculations

Although REFPROP6 provides improved representation of thermodynamic properties over REFPROPS, it occasionally crashes, particularly when calculating properties of refrigerant mixtures. Such occasional crashes may be acceptable in manually set-up property calculations with REFPROP's user's interface. However, they are unacceptable in heat exchanger and system simulations due to the high number of calls to property routines, which eventually may cause every simulation run to crash. To be able to use REFPROP6 routines, we developed an error evasive scheme that attempts to calculate properties even if REFPROP flash



calculations do not converge, e.g., if PHFLSH crashes, a routine that uses TPRHO is invoked to attempt to iteratively match TPRHO's h value with the known (target) h value. If both REFPROP **flash** calculations do not converge, then the data in the refrigerant look-up table is flagged and look-up table routines iterate this point using refrigerant properties in the neighboring nodes of the table. If the critical pressure falls between the lower and upper pressure limits of the table, an additional set of data are generated for the critical pressure and the entire enthalpy grid (this is done to improve the accuracy of the iterations near the critical pressure).

## 4.2 Evaporator Model EVAP5

### 4.2.1 Heat Transfer and Pressure Drop Correlations

EVAPS uses the following correlations for calculating heat transfer and pressure drop.

#### Air Side

- heat-transfer coefficient for flat fins: Wang et al. (2000)
- heat-transfer coefficient for wavy fins: Wang et al. (1999a)
- heat-transfer coefficient for slit fins: Wang et al. (2001)
- heat-transfer coefficient for louver fins: Wang et al. (1999b)
- fin efficiency: Schmidt method, described in McQuiston et al. (1982)

## Refrigerant Side

- single-phase heat-transfer coefficient, smooth tube: McAdams, described in **ASHRAE** (2001)
- evaporation heat-transfer coefficient up to 80% quality, smooth tube: Jung and Didion (1989)
- evaporation heat-transfer coefficient up to 80% quality, rifled tube: Jung and Didion (1989) correlation with a 1.9 enhancement multiplier suggested by Schlager et al. (1989)
- mist flow, smooth and rifled tubes: linear interpolation between heat transfer coefficient values for 80 % and 100 % quality
- single-phase pressure drop, smooth ~~tube~~: Petukhov (1970)
- two-phase pressure drop, smooth tube, lubricant-free refrigerant: Pierre (1964)
- two-phase pressure drop, rifled tube: Pierre (1964) correlation for smooth tube with a 1.4 multiplier suggested by Schlager et al. (1989)

We incorporated the correlation that accounts for a **0.5** % content of lubricant in the refrigerant.

- single-phase pressure drop, return bend, smooth tube: White, described in Schlichting (1968)
- two-phase pressure drop, return bend, **smooth** tube: Chisholm, described in Bergles et al. (1981)

The length of a return bend depends on the relative locations of the tubes connected by the bend. **This** length was accounted for in pressure drop calculations.

#### 4.2.2 EVAP5 Validation

We used evaporator test data obtained during **R22** and **R410A** system tests to validate the evaporator model. For all tests, the indoor air dry-bulb temperature ~~was~~ 80.0 °F (26.7 °C) and the wet-bulb temperature was 67.0 °F (19.4 °C). The evaporator saturation temperature varied from 45.0 °F to 59.0 °F (7.2 °C to 15.0 °C) due to the wide range of outdoor temperature for which the **R22** and **R410A** systems were tested (82.0 °F to 135.0 °F (27.8 °C to 57.2 °C)). This resulted in different refrigerant inlet qualities, which ranged from **0.25** to 0.30.

The screenshot displays the 'Coil Design Data' window, which is organized into several sections for inputting design parameters. The top section is titled 'R22 and R410A evaporator'. Below this, there are two main columns of input fields. The left column contains five fields for refrigerant properties, all set to '22' or '0'. The right column contains two fields for refrigerant properties, set to '1' and '0.0035'. Below these, there are two sections for coil design parameters. The left section contains six fields for coil design parameters, with values ranging from 0.36 to 223. The right section contains two fields for coil design parameters, with values 'Wavy' and '128'. At the bottom, there are two buttons labeled 'OK' and 'Cancel'.

Parameter	Value
Refrigerant	22
Refrigerant	22
Refrigerant	22
Refrigerant	0
Refrigerant	0
Refrigerant	1
Refrigerant	0.0035
Refrigerant	0.083
Refrigerant	Wavy
Refrigerant	128
Refrigerant	0.36
Refrigerant	0.392
Refrigerant	1
Refrigerant	0.866
Refrigerant	Riffled
Refrigerant	223

Figure 4.3 Design information for **R22** and **R410A** evaporators

The R22 and R410A evaporators were identical heat exchangers. Copying from respective windows of the EVAP-COND interface, Figure 4.3 shows evaporator key design parameters, and Figure 4.4 shows a side-view schematic with the refrigerant circuit. The circles symbolize the tubes, the solid lines symbolize the returning bends on the near side, and the broken lines denote the returning bends on the far side. The refrigerant circuit had six branches. The refrigerant entered the evaporator via tubes 1, 13, 23, 35, 45, 57, and left via tubes 12, 22, 34, 44, 56, and 66. The tube crossing over tube 28 and tube 38 is a result of graphical simplifications in the EVAP-COND interface. In fact, tube 6 feeds tube 51, tube 28 feeds tube 29, and tube 50 feeds tube 7.

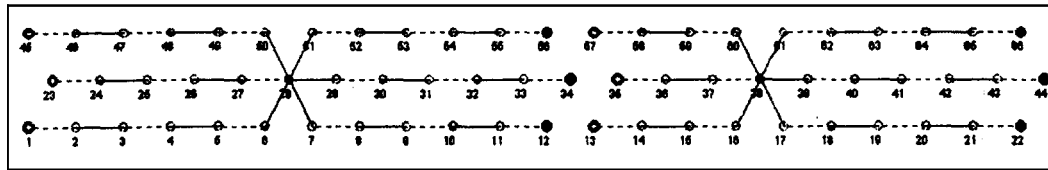


Figure 4.4 Refrigerant circuitry design in R22 and **R410A** evaporators

The evaporators were equipped with fins of a wavy/slit design. Since a correlation for a wavy/slit fin is not available in literature, we selected a wavy fin in our simulations and used a correction multiplier of 2.0 to compensate for the enhancement provided by the slits. This value approximate the average of the enhancements for a slit fin over a flat surface as calculated by Wang et al. (2001) and Nakayama and Xu (1983) for the air velocity range from 4 ft/s to 5 ft/s (1.22 m/s to 1.52 m/s). If the Nakayama and Xu correlation was selected for our simulations, the same value of the air-side heat transfer coefficient would be obtained by applying a correction multiplier of 0.30 to represent the

enhancement due to the wavy design. As we note that this correction is lacking analytical rigor, we also have to recognize that not providing any correction is not proper as well.

For our validations, we selected five **R22** test points and seven **R410A** data points. The **R22** data points were obtained during system tests at **82.0 °F (27.8 °C)**, **95.0 °F (35.0 °C)**, **115.0 °F (46.1 °C)**, **125.0 °F (51.7 °C)**, and **135.0 °F (57.2 °C)** ambient temperatures. The **R410A** data points came from the **82.0 °F (27.8 °C)**, **95.0 °F (35.0 °C)**, **115.0 °F (46.1 °C)**, **125.0 °F (51.7 °C)**, and **130.0 °F (54.4 °C)** tests using the original compressor, and the **150.0 °F (65.6 °C)** and **155.0 °F (68.3 °C)** tests using the custom-fabricated compressor. The inlet operating parameters included the air dry-bulb temperature, relative humidity, air volumetric flow rate, refrigerant inlet quality (based on refrigerant thermodynamic state at the TXV inlet), and refrigerant saturation temperature and superheat at the evaporator outlet. The program iterated inlet pressure and refrigerant mass flow rate to obtain the target conditions at the evaporator outlet.

Tables **4.1** shows the refrigerant input parameters and simulation results for the **R22** evaporator, while Figures **4.5** and **4.6** graphically present evaporator total capacities and sensible heat ratios. For **R22**, the inlet quality ranged from **0.15** to **0.34**, and the saturation temperature for different tests was between **48.7 °F (9.3 °C)** and **53.9 °F (12.2 °C)**. These variations resulted in a capacity difference between different tests being as much as **30 %**. **EVAP5** underpredicted all measured capacities with three underpredictions being within the **3.7 %** and **4.7 %** range and two significantly larger

underpredictions of **7.4 %** and **11.4 %**. **EVAPS** overpredicted the sensible heat ratio by **6.1 %** to **10.7 %**. -

Table **4.2** shows the refrigerant input parameters and simulation results for the **R410A** evaporator, while Figures **4.7** and **4.8** graphically present evaporator total capacities and sensible heat ratios. For the seven **R410A** tests, the evaporator saturation temperature was between **50.5 °F (10.3 °C)** and **59.1 °F (15.1 °C)**, and the inlet quality ranged from **2.0 %** to **4.7 %**. This range ~~was~~ greater for **R410A** than for **R22**. In general, a higher inlet quality for **R410A** than that for **R22** was a result of a lower **R410A** critical temperature. The highest value of inlet quality came from the test at the **155.0 °F (68.3 °C)** ambient temperature, to which the **R22** system was not subjected. As a result of different operating conditions, evaporator capacities differed by ~~as~~ much as **46 %**. Table **4.2** shows that **EVAPS** predictions were more consistent with **R410A** than with **R22**. For tests with evaporator saturation temperatures up to **55.0 °F (12.8 °C)** (practical operation range), **EVAPS** underpredictions were approximately **4.5 % ± 1.3 %**. At higher saturation temperatures, evaporator total capacities were within **2.7 %** of the tested value. As was the case with **R22** predictions, the model overpredicted the sensible heat ratio for all tests by a similar percentage.

**EVAPS** provides detail information on performance of individual tubes. Predictions of refrigerant superheat (or quality and temperature) for evaporator exit tubes are indicative of the correctness of this information. Tables **4.3** and **4.4** show exit temperatures, qualities, and refrigerant distribution for **R22** and **R410A** evaporators. The tube number

identifiers used are consistent with Figure 4.4. The level of agreement in outlet temperatures between the tested and simulated values is better for the **R22** evaporator than for ~~the~~ **R410A** evaporator due to the higher overall superheat set in the **R22** evaporator. (In an extreme case with an undercharged system, the refrigerant exit temperature approaches the *air* temperature). Considering the difficulty of predicting individual superheats, the simulated values can be considered **as** acceptable.

A common aspect of **R22** and **R410A** predictions is the underprediction of refrigerant superheat in tube **44**. In EVAPS, this underprediction is caused by a lower air mass flow rate seen by tube **44** because this tube is located next to the side of the heat exchanger. It appears that in a real heat exchanger, heat transfer via fins between neighboring tubes provides a compensating effect. This heat transfer has been neglected in EVAPS and should be studied for proper implementation into the next version of the model.

The observed capacity underpredictions for **R22** and **R410A** evaporator were reasonably consistent, and improved prediction accuracy could be obtained by tuning the evaporator model farther. While accurate simulation of the evaporator is important, we should note that inaccurate predictions of evaporator capacity are “scaled down” when the evaporator model is incorporated into a model of an *air* conditioner. According to a simplified algorithm (Domanski, 1990), a 10 % lower evaporator capacity will result in a 3.6 % lower cooling capacity of the system. This is due to the fact that the system will rebalance itself at different saturation temperatures in the evaporator and condenser when inaccurate heat exchanger predictions are generated.

Table 4.1 EVAP5 validation with R22 evaporator

Test number	Refrigerant input data			Test results			Simulation results			Difference*	
	Inlet quality (fraction)	Outlet Tsat (°F)	Outlet Tsup (°F)	Total capacity (Btu/h)	Sensible capacity (Btu/h)	Sensible heat ratio (fraction)	Total capacity (Btu/h)	Sensible capacity (Btu/h)	Sensible heat ratio (fraction)	Total capacity (%)	Sensible heat ratio (%)
1208a	0.15	48.7	13.7	39364	28892	0.73	37925	29533	0.78	-3.7	6.1
10105	0.20	50.0	11.5	38640	28306	0.73	35777	28414	0.79	-7.4	8.4
010108a	0.22	51.6	10.3	34782	26784	0.77	33154	27557	0.83	-4.7	7.9
010110a	0.31	52.7	9.8	33420	25659	0.77	29617	25250	0.85	-11.4	10.7
1212a	0.34	53.9	11.6	30270	24808	0.82	28899	25510	0.88	-4.5	7.7

\*100% (simulated value – tested value)/tested value



Table 4.2 EVAP5 validation with R410A evaporator

Test number	Refrigerant input data			Test results			Simulation results			Difference *	
	Inlet quality (fraction)	Outlet Tsat (°F)	Outlet Tsup (°F)	Total capacity (Btu/h)	Sensible capacity (Btu/h)	Sensible heat ratio (fraction)	Total capacity (Btu/h)	Sensible capacity (Btu/h)	Sensible heat ratio (fraction)	Total capacity (%)	Sensible heat ratio (%)
b010330k	0.20	50.5	4.5	40345	29412	0.73	39072	29933	0.77	-3.2	5.1
b010328a	0.25	52.1	3.8	38144	27998	0.73	36509	28772	0.79	-4.3	7.4
b010331x	0.29	54.4	3.5	33305	26677	0.80	31396	27433	0.87	-5.7	9.1
010403a	0.33	55.2	3.9	30586	25356	0.83	29262	26340	0.90	-4.3	8.6
b010425x	0.35	56.0	4.2	29414	24884	0.85	28611	25660	0.90	-2.7	6.0
C010719a	0.44	58.1	5.7	24801	22519	0.91	24894	23748	0.95	0.4	5.1
C010723d	0.47	59.1	5.3	22645	22590	1.00	22916	22916	1.00	1.2	0.2

\* 100% (simulated value – tested value)/tested value

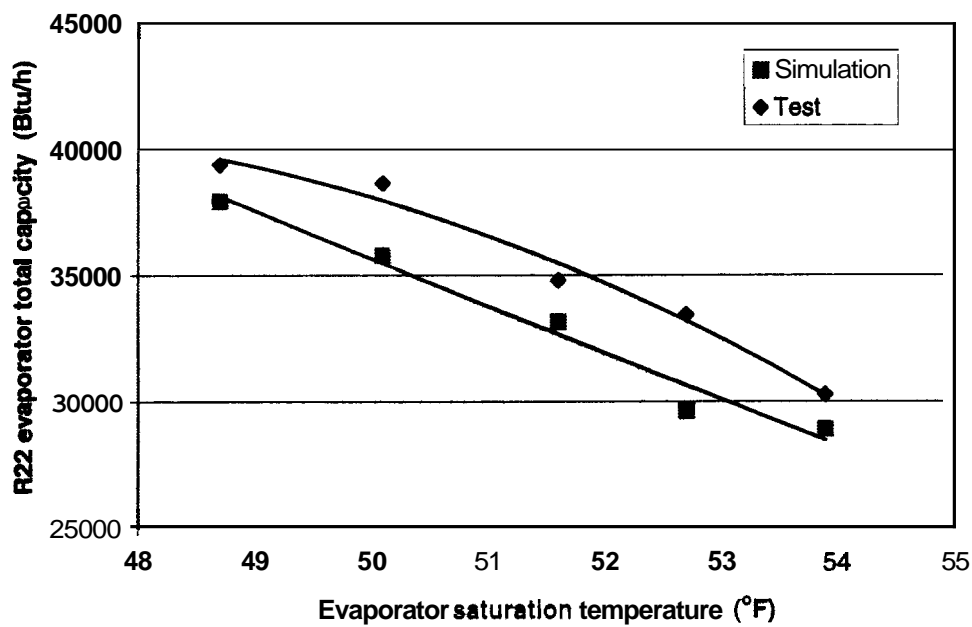


Figure 4.5 Tested and predicted capacities for **R22** evaporator

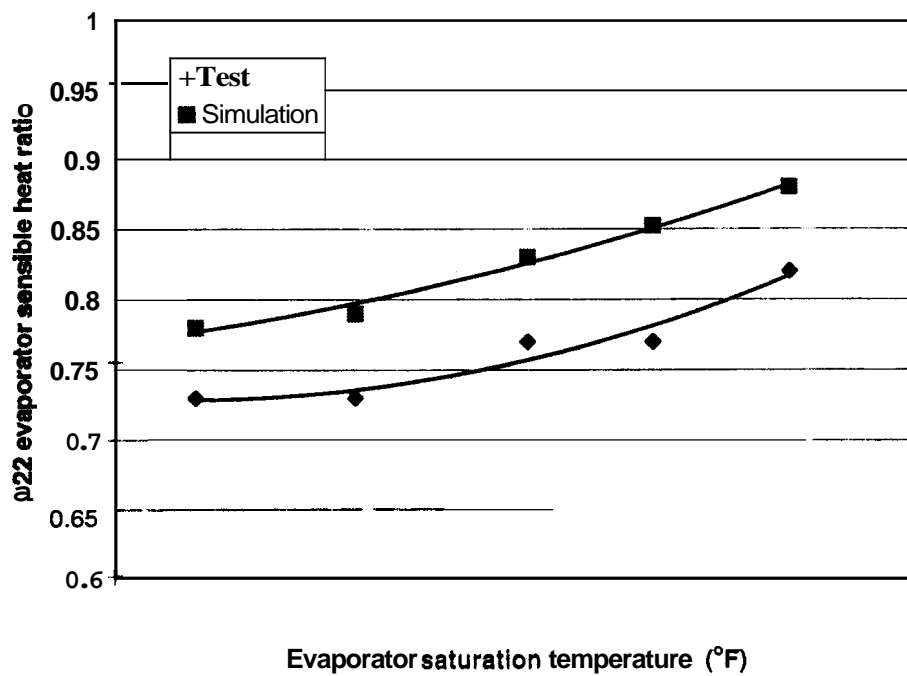


Figure 4.6 Tested and predicted sensible heat ratios for **R22** evaporator

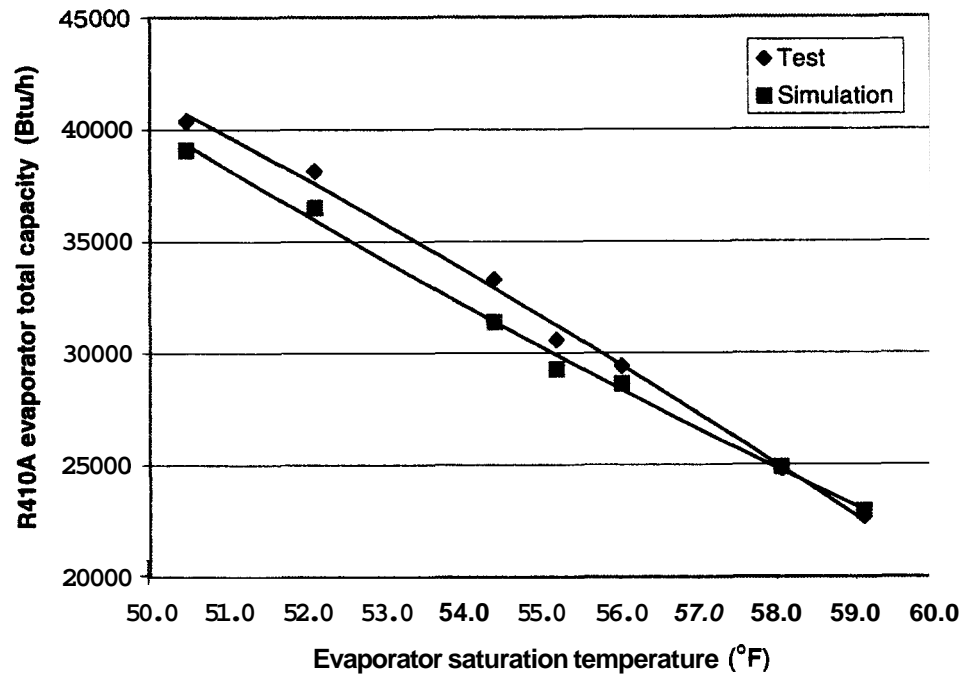


Figure 4.7 Tested and predicted capacities for R410A evaporator

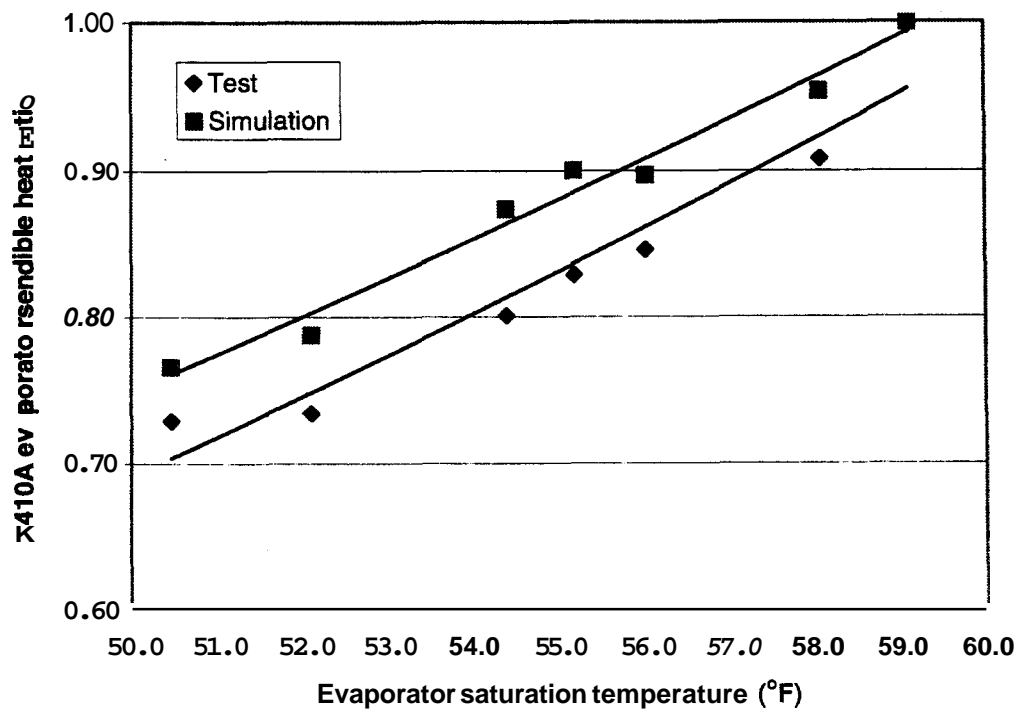


Figure 4.8 Tested and predicted sensible heat ratios for R410A evaporator

Tube Number	Test	Simulation		
	Outlet temperature (°F)	Outlet temperature (°F)	Outlet quality (fraction)	Refrigerant distribution (fraction)
12	63.3	74.5	1.00	0.167
22	63.5	71.0	1.00	0.168
34	62.5	63.1	1.00	0.166
44	58.5	51.3	1.00	0.169
56	60.6	63.2	1.00	0.163
66	55.6	53.6	1.00	0.166

Tube Number	Test	Simulation		
	Outlet temperature (°F)	Outlet temperature (°F)	Outlet quality (fraction)	Refrigerant distribution (fraction)
12	70.2	70.7	1.00	0.167
22	64.9	65.6	1.00	0.168
34	71.3	55.8	1.00	0.166
44	72.8	50.5	0.94	0.169
56	69.8	60.4	1.00	0.163
66	70.4	50.5	0.98	0.167

#### 4.3 Condenser Model COND5

##### 4.3.1 Heat Transfer and Pressure Drop Correlations.

**COND5** uses the following correlations for calculating heat transfer **and** pressure drop.

##### Air Side

- heat-transfer coefficient for flat fins: Wang et al. (2000)
- heat-transfer coefficient for wavy fins: Wang et al. (1999a)

- heat-transfer coefficient for slit fins: Wang et al. (2001)
- heat-transfer coefficient for louver fins: Wang et al. (1999b)
- fin efficiency: Schmidt method, described in McQuiston et al., (1982)

## Refrigerant Side

- single-phase heat-transfer coefficient, smooth tube: McAdams, described in ASHRAE (2001)
- condensation heat-transfer coefficient, smooth tube: Shah (1979)
- condensation heat-transfer coefficient, rifled tube: Shah (1979) correlation with a 1.9 enhancement multiplier suggested by Schlager et al. (1989)
- single-phase pressure drop, smooth tube: Petukhov (1970)
- two-phase pressure drop, smooth tube: Lockhart and Martinelli (1949)
- two-phase pressure drop, rifled tube: Lockhart and Martinelli (1949) correlation for smooth tube with a 1.4 multiplier suggested by Schlager et al. (1989)

We incorporated the correlation that accounts for a 0.5 % content of lubricant in the refrigerant.

- single-phase pressure drop, return bend, smooth tube: White, described in Schlichting (1968)
- two-phase pressure drop, return bend, smooth tube: Chisholm, described in Bergles et al. (1981)

The length of a return bend depends on the relative locations of the tubes connected by the bend. This length **was** accounted for in pressure drop calculations.

#### 4.3.2 CONDS Validation

To validate the condenser model, we applied condenser test data obtained during the same **R22** and **R410A** system tests we used for EVAPS validation. The **R22** and **R410A** condensers were identical heat exchangers. Copying from respective windows of the EVAP-COND interface, Figure 4.9 shows condenser key design parameters, and Figure 4.10 shows a side-view schematic with the refrigerant circuit. As for the evaporator, the circles symbolize the tubes, the solid lines symbolize the returning bends on the near side, and the broken lines denote the returning bends on the far side. The refrigerant circuit had four branches merging into tube 25. The refrigerant entered the condenser via tubes 32, 33, 44,

The screenshot displays the 'Coil Design Data' window, which is divided into several sections for inputting design parameters. The title bar reads 'Coil Design Data'. The main content area includes the following fields and values:

- Refrigerant:** A dropdown menu showing 'R22 and R410A condenser'.
- Tube ID:** A list of tube IDs: 26, 26, 0, 0, 0.
- Tube Length (ft):** A list of values: 60.5118, 0.303937, 0.327953, 1, 0.625.
- Tube Material:** A dropdown menu showing 'Smooth'.
- Tube Schedule:** A dropdown menu showing '223.034'.
- Coil Type:** A dropdown menu showing '1'.
- Coil Material:** A dropdown menu showing '0.0045'.
- Coil Thickness:** A dropdown menu showing '0.0454528'.
- Coil Schedule:** A dropdown menu showing 'Lanced'.
- Coil ID:** A dropdown menu showing '128.02'.
- Coil Material:** A dropdown menu showing 'Smooth'.
- Coil Thickness:** A dropdown menu showing '223.034'.

Figure 4.9 Design information for **R22** and **R410A** condensers



Figure 4.10 Refrigerant circuitry design in **R22** and **R410A** condensers

and **45**, and left via tube **52**. The refrigerant circuit shown in Figure 4.10 (and simulated by **COND5**) is a modified version of the circuit implemented in the tested condensers. The difference is in the final tubes in that the actual condenser had tubes **51** and **52** placed in the first depth row extending the condenser to the right side of tube **26**, and tube spaces in the second depth row were empty. (Figure 3.1 shows the actual refrigerant circuitry.) The current version of **COND5** cannot handle "non-existing" tubes so this circuitry simplification was necessary. Considering the large size (for cooling capacity) of this condenser and its low refrigerant/air approach temperature, we believe that our simplification of circuitry does not compromise **COND5** simulation to a significant degree.

The **R22** data points were obtained during system tests at **82.0 °F (27.8 °C)**, **95.0 °F (35.0 °C)**, **115.0 °F (46.1 °C)**, **125.0 °F (51.7 °C)**, and **135.0 °F (57.2 °C)** ambient temperatures. The **R410A** data points came from the **82.0 °F (27.8 °C)**, **95.0 °F (35.0 °C)**, **115.0 °F (46.1 °C)**, **125.0 °F (51.7 °C)**, and **130.0 °F (54.4 °C)** tests using the original compressor and the **150.0 °F (65.6 °C)** and **155.0 °F (68.3 °C)** tests using the custom-fabricated compressor. The condensers wavy fins were tightly spaced (**22 fins per inch (9 fins/cm)**). Simulation input parameters included the air dry-bulb temperature, relative humidity, air volumetric flow rate, and refrigerant inlet temperature and pressure.

Table **4.5** shows the input parameters and simulation results for the **R22** condenser, while Figures **4.11** and **4.12** graphically present the condenser capacities and pressure drops at different ambient temperatures. We selected the ambient air temperature as the abscissa because it provides a common reference scale for **R22** and **R410A** test points. **COND5** predicted condenser capacities well, within **1.6 %** of the measured values; however, underpredicted refrigerant pressure drops by **32.3 %** to **55.7 %**.

Table **4.6** shows the refrigerant input parameters and simulation results for the **R410A** condenser, while Figures **4.13** and **4.14** depict the condenser capacities and pressure drops. **COND5** overpredicted capacities for all tests. The largest overprediction was **3.6 %**. Pressure drop predictions were acceptable for the normal operating range (**82.0 °F (27.8 °C)** to **95.0 °F (35.0 °C)** ambient temperature). At higher temperatures, these underpredictions increased to above 50 % when the condenser operated close and above the **R410A** critical pressure.

While the reported capacity predictions were satisfactory, we have to note that these tests do not conclusively validate the condenser model because of the low approach temperature between the air and refrigerant during the condenser tests (maximum **6.9 °F (3.8 °C)**). Since the tested condensers operated near a temperature pinch, additional tests with larger approach temperatures condensers would provide needed data to **fully** validate **COND5**.



Table 4.5 COND5 validation with R410A condenser

Test number	Air dry-bulb temperature (°F)	Refrigerant input data						Test results		Simulation results		Difference *	
		Condenser inlet		Condenser outlet		rmass (lb/h)	Capacity (Btu/h)	Pressure drop (psi)	Capacity (Btu/h)	Pressure drop (psi)	Capacity (%)	Pressure drop (%)	
		Temperature (°F)	Pressure (psia)	Temperature (°F)	Pressure (psia)								
1208a	81.7	150.0	217.3	88.6	197.5	534.0	46351	19.8	46953	13.4	1.3	-32.3	
10105	95.1	168.4	259.1	100.0	240.5	537.6	45911	18.6	46618	12.4	1.5	-33.3	
010108a	115.1	199.8	326.4	119.6	307.4	529.8	44185	19.0	44434	9.8	0.6	-48.4	
010110a	125.4	218.6	365.9	129.9	346.9	525.6	43520	19.0	44204	9.8	1.6	-48.4	
1212a	135.0	237.2	399.0	141.7	378.7	513.6	41961	20.3	42380	9.0	1.0	-55.7	

\*100% (simulated value – tested value)/tested value

Table 4.6 COND5 validation with R410A condenser

Test number	Air dry-bulb temperature (°F)	Refrigerant input data						Test results		Simulation results		Difference*	
		Condenser inlet		Condenser outlet		rmass (lb/h)	Capacity (Btu/h)	Pressure drop (psi)	Capacity (Btu/h)	Pressure drop (psi)	Capacity (%)	Pressure drop (%)	
		Temperature (°F)	Pressure (psia)	Temperature (°F)	Pressure (psia)								
b010330k	82.1	141.4	341.6	89.5	329.1	537.0	47525	12.5	48861	11.4	2.8	-8.4	
b010328a	95.0	159.2	399.8	100.7	388.8	541.8	46703	11.1	47743	10.7	2.2	-3.2	
b010331x	115.4	190.9	507.1	122.3	497.0	539.4	43961	10.2	45538	8.4	3.6	-17.2	
b010403a	125.0	208.8	559.1	130.2	549.6	525.0	42683	9.4	43841	7.6	2.7	-19.8	
b010425x	129.9	218.6	587.4	134.7	578.0	521.4	42233	9.4	43313	7.2	2.6	-23.4	
c010719a	150.0	248.6	709.1	152.3	699.4	517.2	39618	9.7	40170	4.4	1.4	-54.4	
c010723d	155.4	261.6	742.8	156.9	733.5	495.6	37913	9.3	38039	4.5	0.3	-51.1	

100% (simulated value – tested value)/tested value

\*100% (simulated value – tested value)/tested value

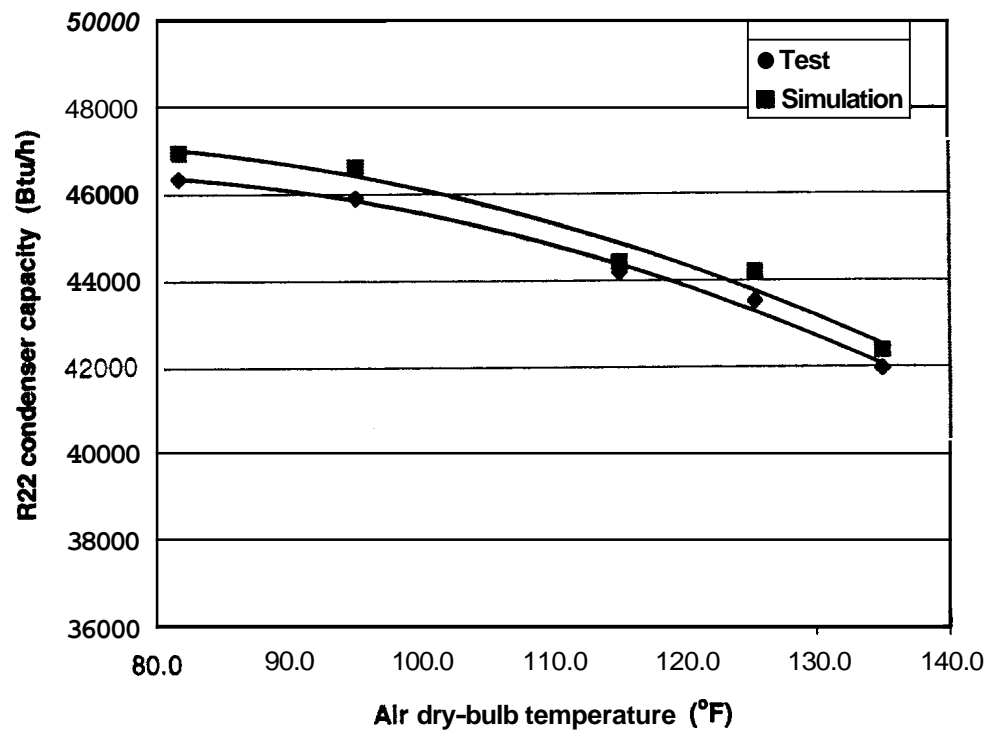


Figure 4.11 Tested and predicted capacities for R22 condenser

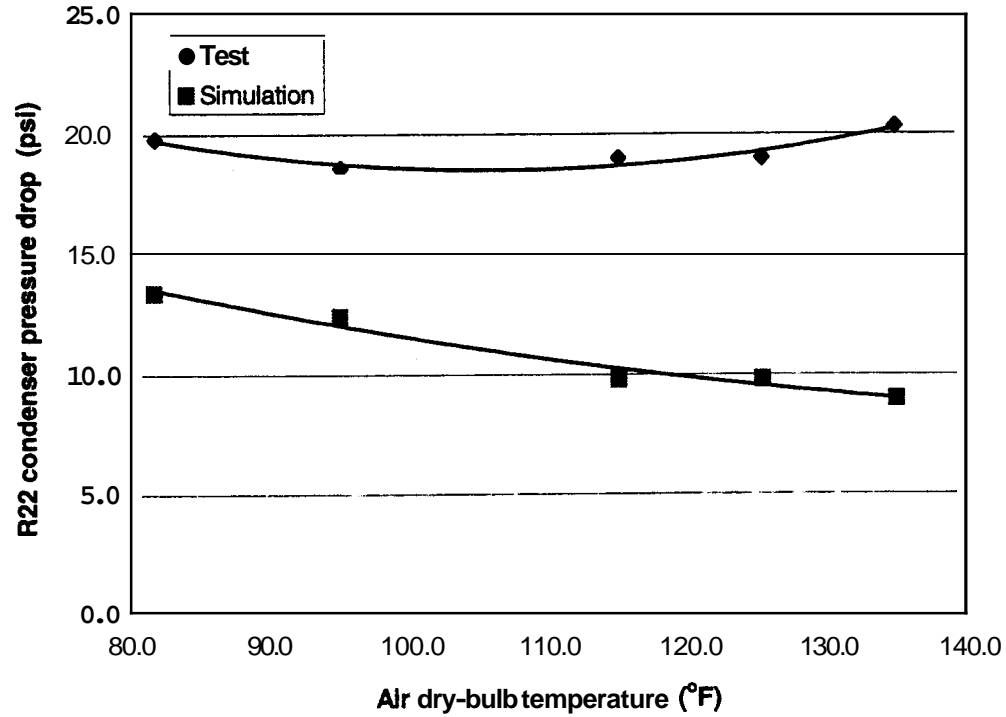


Figure 4.12 Tested and predicted pressure drops for R22 condenser

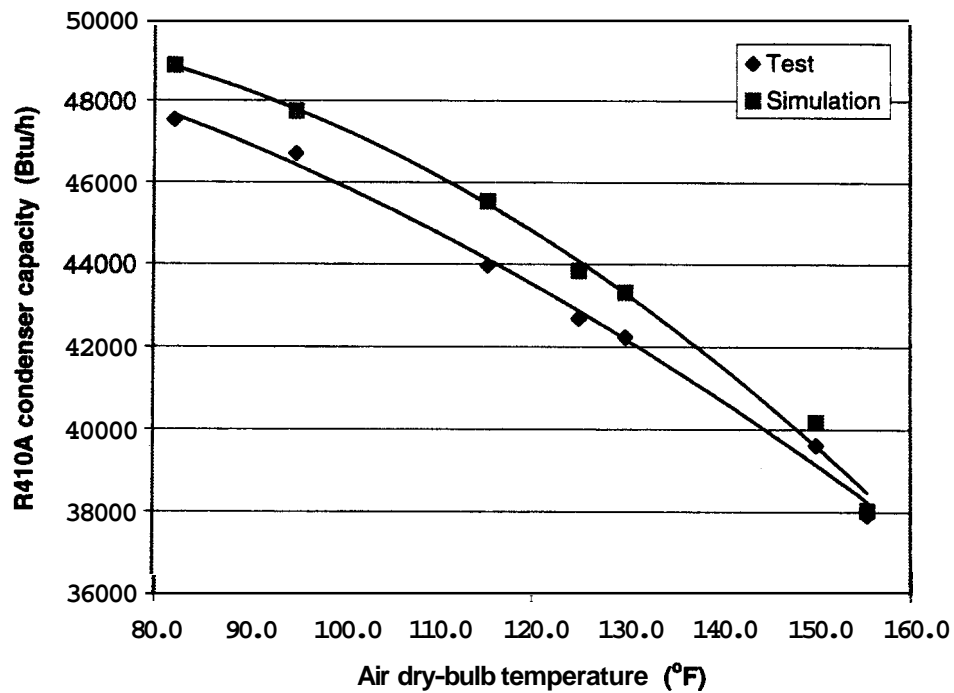


Figure 4.13 Tested and predicted capacities for R410A condenser

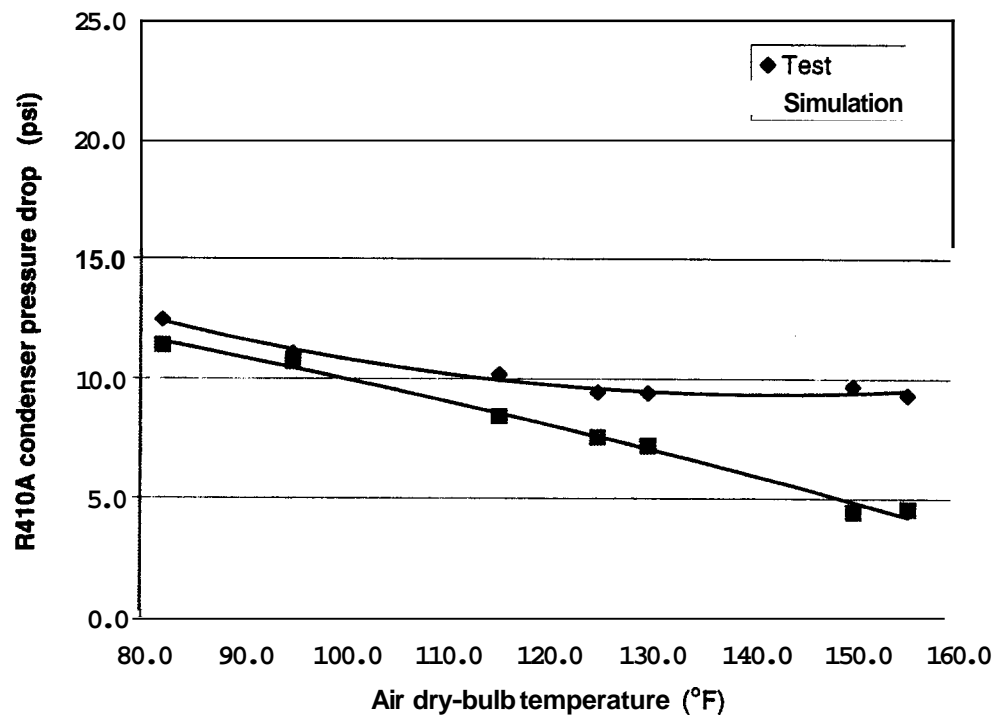


Figure 4.14 Tested and predicted pressure drops for R410A condenser

#### 4.4 EVAP-COND Simulation Package

This project built on the ongoing effort at NIST to develop a simulation package for finned-tube evaporators and condensers called EVAP-COND. The beta version of EVAP-COND package is attached to this report. Version 1 of EVAP-COND is scheduled to be available for free download from <http://www.bfrl.nist.gov/863/refrig.html> in November 2002.

At the outset of this project, the first version of the graphical user interface (**GUI**) was already developed and linked with the evaporator model, EVAPS, allowing evaporator simulations using two options for input data. The effort exerted under this project led to new capabilities for EVAP-COND. Some of the new features go beyond the scope of the current project and were implemented due to supplemental support from NIST and DOE. The major upgrades of EVAP-COND are:

- Implementation of a refrigerant selection option and implementation of ten refrigerants (ammonia, propane, carbon dioxide, R134a, R22, **R32**, R407C, R404A, R507A, R410A).
- Implementation of corrections parameters for air-side heat transfer coefficient, refrigerant heat transfer Coefficient, and refrigerant pressure drop.
  - Implementation of REFPROP6-based refrigerant properties
  - Implementation of six new input data options for simulation of the evaporator. (Total of eight options are available.) The new options include simulation of the evaporator in conjunction with the refrigerant distributor for improved simulation of refrigerant distribution. A nominal pressure drop in the distributor lines is assumed.
- Incorporation of the condenser simulation model CONDS, which simulation capabilities include:

- subcritical and supercritical operation
- non-uniform **air** distribution
- refrigerant distribution

The scope of this project did not include development of a User's Manual. To facilitate the use of EVAP-COND, we prepared visual instruction pages in lieu of the manual. These pages are presented in Appendix D.

## 4.5 Modeling of Air Conditioner

### 4.5.1 Structure of Simulation Model

We formulated a simulation model of a vapor-compression air conditioner equipped with a TXV **as** the expansion device to simulate the systems tested under this project. The model consists of the following models of system components: evaporator, suction line, compressor, discharge line, and condenser (see Figure 4.15). The liquid line is not modeled; the practical significance of this simplification is that heat transfer between the ambient and liquid line is not accounted for. Physical modeling of the TXV is substituted with the assumption of a constant refrigerant superheat at the evaporator outlet and a constant refrigerant subcooling at the condenser outlet. Our test data show that the later assumption is less rigorous than the assumption of a constant superheat, however, it appears to facilitate accurate performance predictions better than using other simulation constraints (e.g. refrigerant mass inventory). For the two **R410A** simulations that involved transcritical operation at the ambient temperatures of 150.0°F (65.6 °C) and **155.0°F** (68.3 °C) we used a constraint of specified approach temperature in place of a constant subcooling at the condenser outlet.

The condenser and evaporator models are those incorporated in the EVAP-COND package. The compressor is represented by a compressor map routine implementing a ten-term correlation described in **ARI Standard 540** (*ARI 1999*). A correction is provided for a different than tested vapor superheat at the compressor inlet. The suction and discharge line model accounts for refrigerant pressure drop and heat transfer between the refrigerant and ambient. Most of the support routines have their origin in the NIST **HPSIM** simulation model (Domanski and Didion, **1983**). They were either applied directly or modified. All refrigerant properties are calculated using **REFPROP6** (McLinden et al., **1998**) refrigerant property look-up tables. Having tested the program with **REFPROPS** (Gallagher et al., **1996**) and **REFPROP6**, we saw no practical differences in predictions with **R22** and visible differences with **R410A**. The formulated air conditioner model consists of **109** routines (**93** subroutines and **16** functions) with **90%** of them supporting simulations of the evaporator and condenser. The total count of subroutines **does** not include neither the **REFPROP6** code nor the visual interface routines.

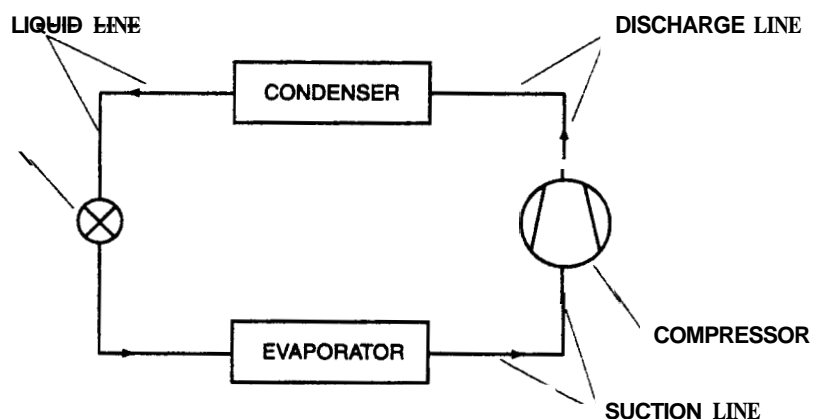


Figure **4.15** Component schematic of a tested air conditioner

#### 4.5.2 Model Validation with **R22** and **R410A** Air Conditioner Test Data

We validated the **AC** model with the five **R22** and seven **R410A** system test data we used for **EVAP5** and **COND5** validations. For **R22**, these test points were obtained at outdoor temperatures of **82.0 °F (27.8 °C)**, **95.0 °F (35.0 °C)**, **115.0 °F (46.1 °C)**, **125.0 °F (51.7 °C)**, and **135.0 °F (57.2 °C)**. For **R410A**, the points taken at **82.0 °F (27.8 °C)**, **95.0 °F (35.0 °C)**, **115.0 °F (46.1 °C)**, **125.0 °F (51.7 °C)**, and **130.0 °F (54.4 °C)** were obtained with the original compressor, while the tests at **150.0 °F (65.6 °C)** and **155.0 °F (68.3 °C)** were obtained using a custom-fabricated compressor of similar characteristics but a different electric motor. We included the **150.0 °F (65.6 °C)** and **155.0 °F (68.3 °C)** conditions with the understanding that these tests cannot be accepted as rigorous validation points.

When performing simulations at different operating conditions, we used as input the same evaporator superheat and condenser subcooling as it was measured during the **95.0 °F (35.0 °C)** outdoor temperature test. This approach validates the adequacy of the assumption of constant superheat and subcooling for modeling TXV-equipped systems. All simulation runs were performed without making any adjustments to the simulation model beyond the adjustment for the evaporator air-side heat transfer coefficient discussed in chapter **4.2.2**.

Tables **4.7** presents selected validation results for the **R22** system. Figures **4.16** and **4.17** graphically present capacities and **EERs** at different operating conditions. The model predicted capacities within 1.9 % for all tests except the test at **135.0 °F (57.2 °C)**, where the simulated and tested capacities differed by 6.3 %. **EER** at the **135.0 °F (57.2 °C)** test point also has the largest prediction error of 7.8 %. Other **EERs** are predicted within 5.1 %. We may note that assuming a constant evaporator superheat and condenser subcooling is not

responsible for the highest prediction error at the 135.0 °F (57.2 °C) outdoor temperature; a simulation run performed with the tested values of superheat and subcooling yielded a capacity that was within 100 Btu/h and EER that was within 0.1 of the simulated values reported in Table 4.7.

Table 4.8 presents validation results for the R410A system, and Figures 4.18 and 4.19 compare tested and simulated capacities and EERs, respectively. While predictions are very good for the low-end ambient temperatures (115.0 °F (46.1 °C) and lower), their accuracy tends to deteriorate when the ambient temperature is above 115.0 °F (46.1 °C), as this also was the case with the R22 system. We can connect this trend with improper predictions of refrigerant mass flow rate. Figure 4.19 displays this disparity for the R410A system; a similar disparity took place for the R22 system as well. Since validations of EVAP5 and CONDS did not show significant disparity between simulation and test results, detailed examination of the compressor performance and its representation in our system model is merited in the future. At this point it can be speculated that the increase in refrigerant mass flow simulated by compressor map correlations was in response to a higher suction pressure (and higher density of the suction vapor), which dominated the effect of the lower compressor volumetric efficiency at an increased compressor pressure ratio. The difference between compressor map correlations and a real system is that compressor map tests were performed at 90.0 °F (32.2 °C), while during system tests the compressor was exposed to the ambient temperature. At high ambient temperatures heat transfer from the compressor to the ambient was inhibited, which may have resulted in significant internal heat transfer and large refrigerant superheat at the suction valve and led to a decrease in refrigerant mass flow rate as compared to compressor map predictions.



Table 4.7 AC model validation with R22 system data

Test number	Outdoor dry-bulb temperature (°F)	Test results					Simulation results					Difference			
		Capacity (Btu/h)	Work (W)	EER (Btu/h. W)	m <sub>mass</sub> (lb/h)	Evap. outlet pressure (psi)	Cond. inlet pressure (psi)	Capacity (Btu/h)	Work (W)	EER Btu/h. W)	m <sub>mass</sub> (lb/h)	Evap. outlet pressure (psi)	Cond. inlet pressure (psi)	Capacity (%)	EER (%)
1208a	81.7	39364	2225	17.7	534.0	96.6	217.3	39729	2283	17.4	525.0	93.1	213.0	0.9	-1.6
10105	95.1	38640	2529	15.3	537.6	98.8	259.1	37905	2614	14.5	528.0	94.6	251.7	-1.9	-5.1
010108a	115.0	34782	3221	10.8	529.8	101.4	326.4	35026	3100	11.3	534.0	97.2	318.4	0.7	4.6
010110a	125.4	33421	3673	9.1	525.6	103.4	365.9	33532	3645	9.2	538.2	99.4	357.5	0.3	1.1
1212a	135.0	30270	4130	7.3	513.6	105.4	399.0	32169	4072	7.9	541.2	101.1	397.8	6.3	7.8

\* 100% (simulated value – tested value)/tested value

Table 4.8 AC model validation with R410 system data  
(shaded area indicates tests with a custom-fabricated compressor)

Test number	Outdoor dry-bulb temperature (°F)	Test results					Simulation results					Difference*			
		Capacity (Btu/h)	Work (W)	EER (Btu/h.W)	rmass (lb/h)	Evap. outlet pressure (psi)	Cond. inlet pressure (psi)	Capacity (Btu/h)	Work (W)	EER (Btu/h.W)	rmass (lb/h)	Evap. outlet pressure (psi)	Cond. inlet pressure (psi)	Capacity (%)	EER (%)
b010330k	82.1	40345	2201	18.3	537.0	158.1	341.6	40008	2260	17.7	519.6	153.3	331.8	-0.8	-3.4
b010328a	95.0	38144	2604	14.6	541.8	162.4	399.8	37955	2618	14.5	528.0	157.2	389.0	-0.5	-1.0
b010331x	115.4	33305	3315	10.0	539.4	168.6	507.1	34168	3317	10.3	538.8	162.5	494.0	2.6	2.5
b010403a	125.0	30586	3789	8.1	525.0	170.7	559.1	32260	3708	8.7	543.0	164.7	550.0	5.5	7.8
b010425x	129.9	29414	3963	7.4	521.4	173.0	587.4	31462	3933	8.0	549.0	166.9	581.0	7.0	7.8
c010719a	150.0	24801	5357	4.6	517.2	179.3	709.1	26806	4964	5.4	587.4	171.8	696.1	8.1	16.6
c010723d	155.4	22699	6288	3.6	495.6	182.2	742.8	25253	5261	4.8	610.2	175.7	727.7	11.3	33.3

\* 100% (simulated value – tested value)/tested value

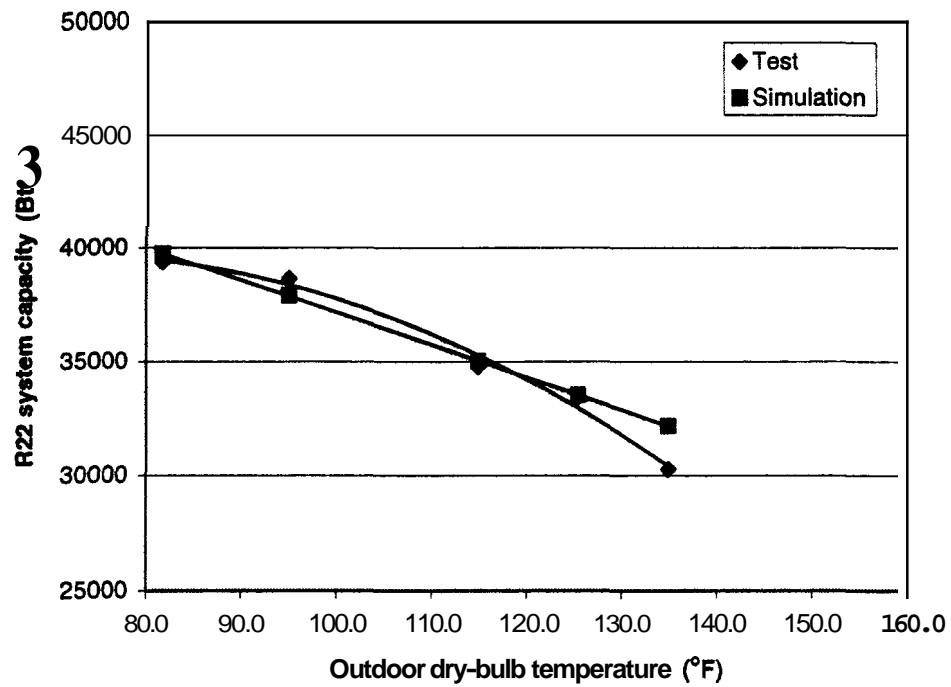


Figure 4.16 Tested and predicted capacities of R22 air conditioner

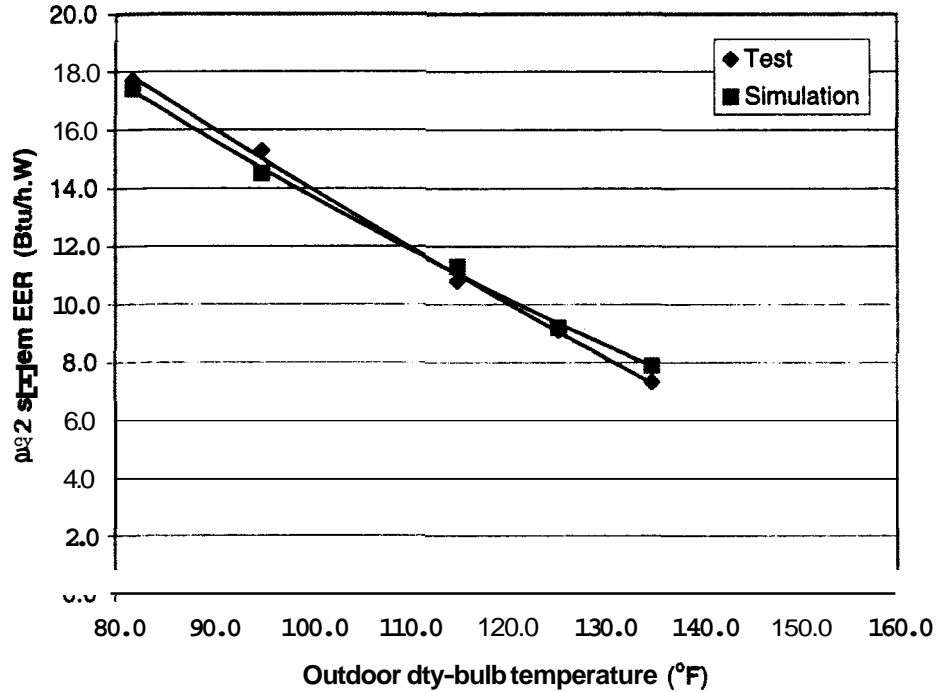


Figure 4.17 Tested and predicted EERs of R22 air conditioner

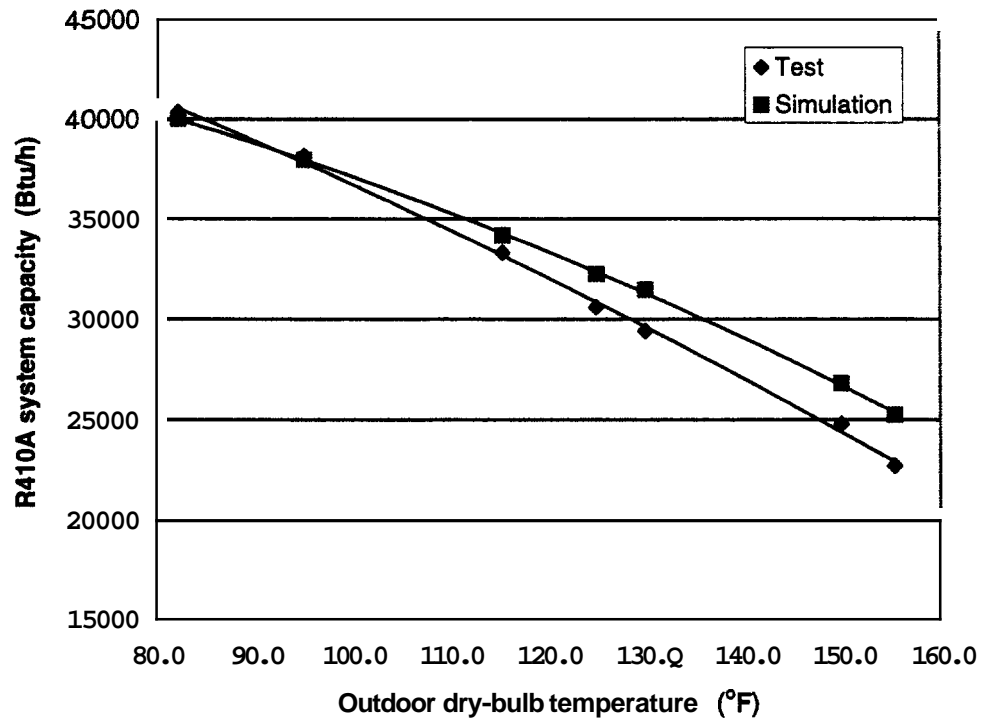


Figure 4.18 Tested and predicted capacities of R410A air conditioner

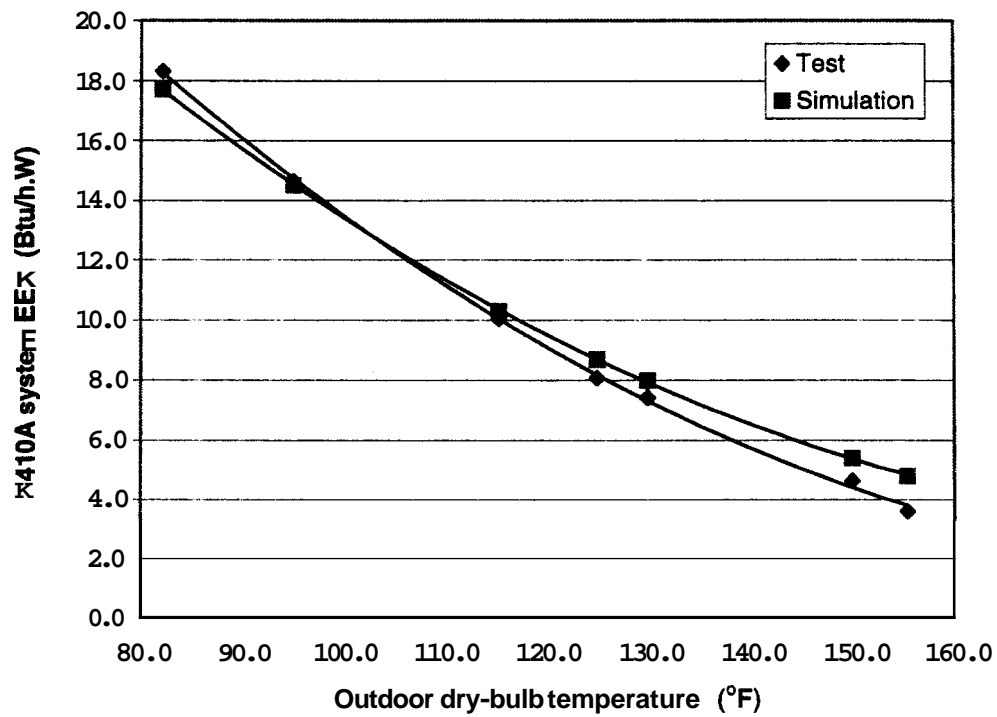


Figure 4.19 Tested and predicted EERs of R410A air conditioner

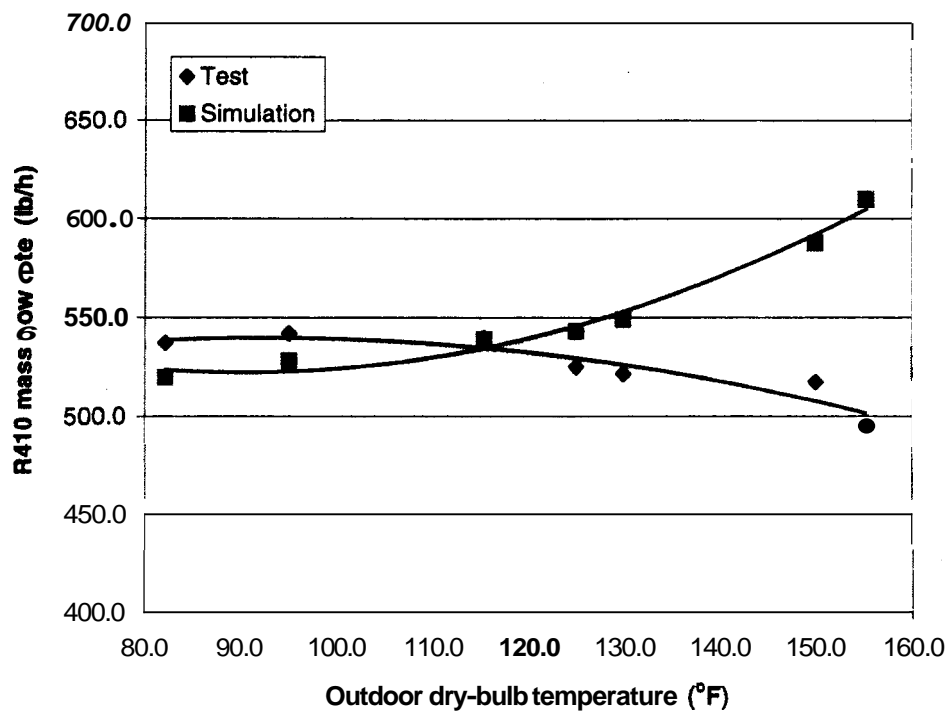


Figure 4.20 Tested and predicted refrigerant ~~mass~~ flow rates for R410A air conditioner

#### 4.5.3 Simulations of R22, R410A, R134a, and R404A systems.

Comparison simulations for R22, R410A, R134a, and R404A systems covered the 82.0 °F to 135.0°F (27.8 °C to 57.2 °C) outdoor temperature range. Each system employed the same heat exchangers ~~as~~ those ~~used~~ in the tested R22 and R410A systems. Refrigerant superheat at the evaporator outlet and subcooling at the condenser outlet were 9 °F (5 °C) for each simulation run. The isentropic efficiency ~~of~~ each compressor ~~was~~ the same as that of the R410A compressor for given suction and discharge saturation temperatures. R22, R404A, and R134a compressors had an adjusted volumetric capacity so each system could deliver the same capacity ~~as~~ the R410A system at the 95.0 °F (35.0 °C) test condition.

Table 4.9 and Figures 4.21 and 4.22 present absolute results of simulations, while Figures 4.23 and 4.24 present capacities and EERs relative to those for the **R22** system. For all systems, capacity displayed a nearly linear dependence on the ambient temperature with R404A having the highest capacity degradation and R22 having the lowest. Regarding efficiency, R410A showed the highest EER at all outdoor temperatures closely followed by R22. These results agree with the findings obtained in the laboratory. R134a was the least efficient fluid at 82.0 °F (27.8 °C) and 95.0 °F (35.0 °C) outdoor temperatures.

The obtained results were affected by a combination of thermophysical refrigerant properties and intangible aspects of system design that would fit these properties better for one refrigerant than the other. We may note that for typical operating conditions, theoretical calculations using thermodynamic properties alone would indicate R134a as the most efficient refrigerant, closely followed by R22, and indicating R410A and R404A as the least efficient refrigerants. However, in the studied system, R134a experienced excessive pressure drop in the heat exchangers, particularly in the evaporator, which resulted in the lowest efficiency. On the other hand it appeared that the circuitry design in the heat exchangers suited well R410A, which had the best overall performance.

Table 4.10 presents selected refrigerant parameters to help to explain the refrigerants' performance in our simulations. For a simplified analysis we may state that a low critical temperature and high molar heat capacity promote high efficiency in a vapor compression cycle. This disadvantages R404A, which has low critical temperature and high molar heat capacity. For R134a, a corollary of its high critical temperature is its low volumetric capacity. Since R134a

volumetric flow rate had to be increased to obtain the target capacity of the R410A system at the 95.0 °F (35.0 °C) rating point, excessive pressure drop occurred in the unmodified R134a heat exchangers. These results emphasize the importance of heat exchanger optimization for efficiency improvement of the system.

Simulation results for R22, R410A, R134a, and R404A systems					
Refrigerant	Outdoor dry-bulb temperature (°F)	Capacity (Btu/h)	Work (W)	EER (Btu/(Wh))	ṁ <sub>mass</sub> (lb/h)
R22	82	39295	2299	17.1	523.2
	95	37601	2661	14.1	527.4
	115	34774	3359	10.4	535.8
	125	33470	3805	8.8	540.0
	135	31978	4294	7.4	545.4
R410A	82	39627	2233	17.7	513.0
	95	37582	2595	14.5	521.4
	115	34063	3247	10.5	532.2
	125	32080	3648	8.8	538.2
	135	30040	4103	7.3	543.6
R134a	82	39590	2573	15.4	556.2
	95	37732	2922	12.9	564.0
	115	34485	3638	9.5	576.6
	125	32799	4091	8.0	581.4
	135	31039	4482	6.9	590.4
R404A	82	40486	2496	16.2	721.2
	95	37676	2855	13.2	732.0
	115	33208	3500	9.5	754.2
	125	30714	3895	7.9	768.0
	135	30714	4392	6.4	768.0

**Table 4.10 Selected thermodynamic parameters of studied refrigerants**

Refrigerant	critical temperature (°F)	Volumetric capacity* (Btu/ft <sup>3</sup> )	Molar heat capacity at const. pressure. (kJ/(kmol.K))
R22	205.1	110.2	66.7
R410A	158.3	159.7	85.5
R404A	161.9	112.7	101.1
R 134a	213.9	72.0	95.0

\*for a basic cycle at 45 °F evaporator sat. temperature and 100 °F condenser sat. temperature, 0 °F evaporator superheat and 0 °F condenser subcooling

\*\* for saturated vapor at 45 °F (280.4 K)

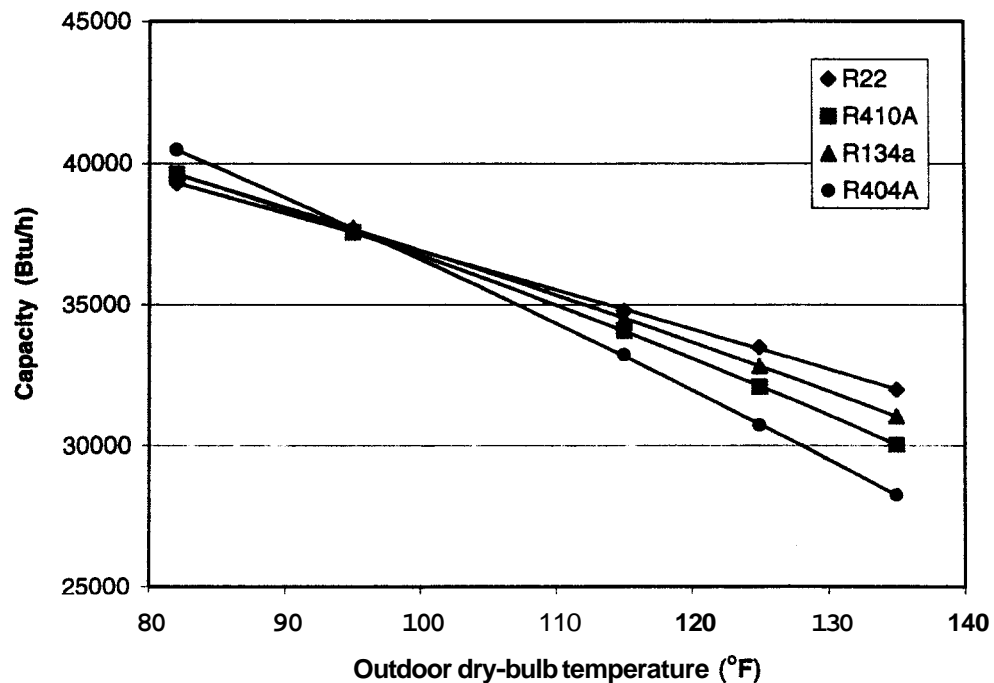


**Figure 4.21 Simulated capacities of R22, R410A, R134a, and R404A air conditioners**

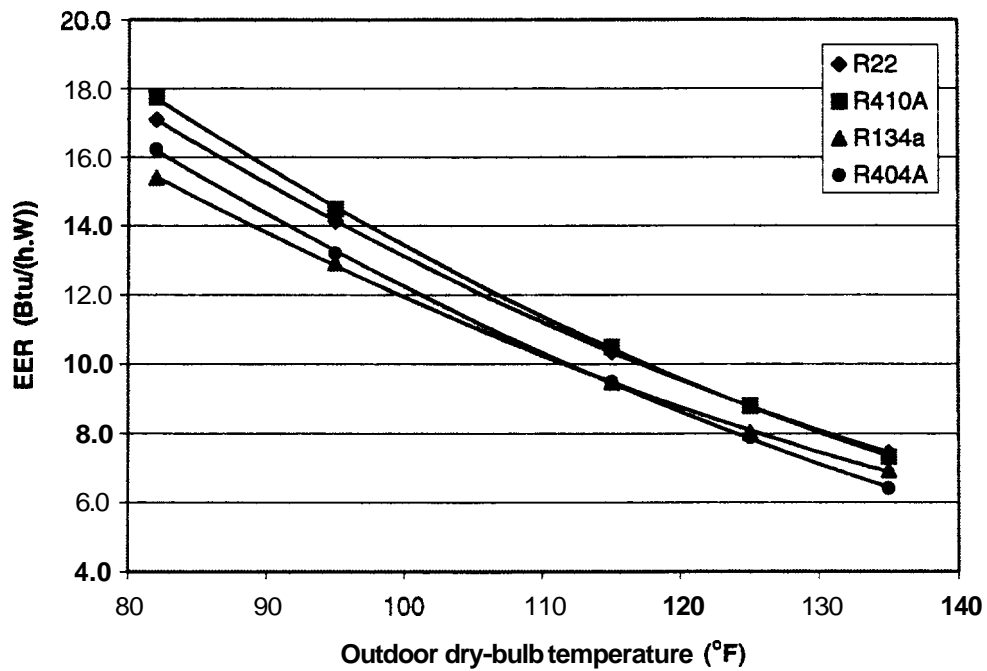


Figure 4.22 Simulated EERs for R22, R410A, R134a, and R404A air conditioners

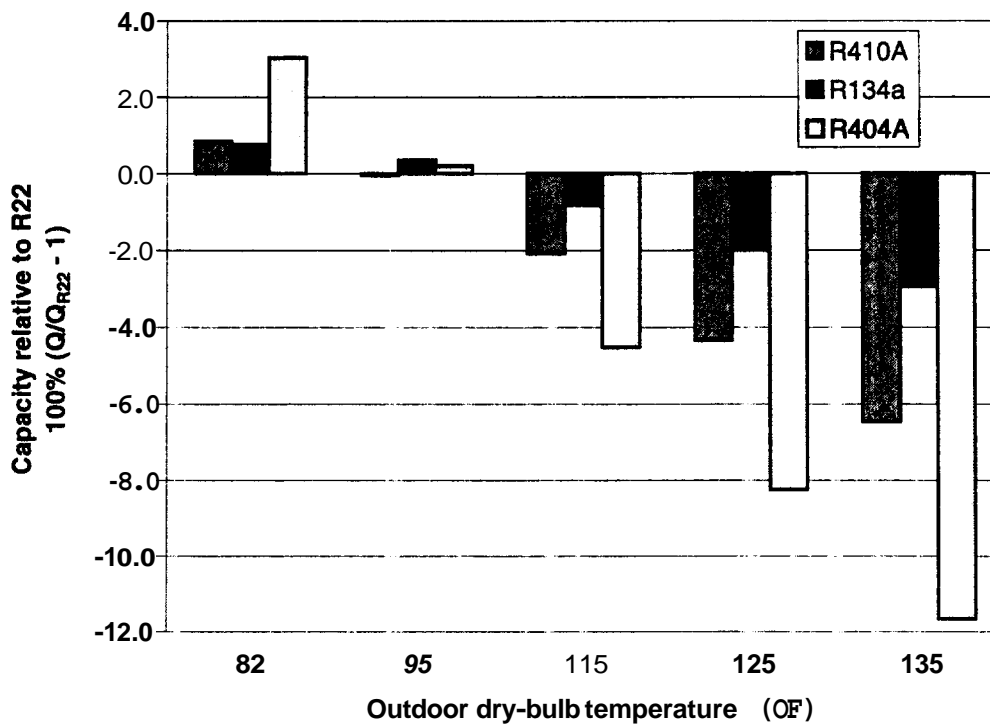
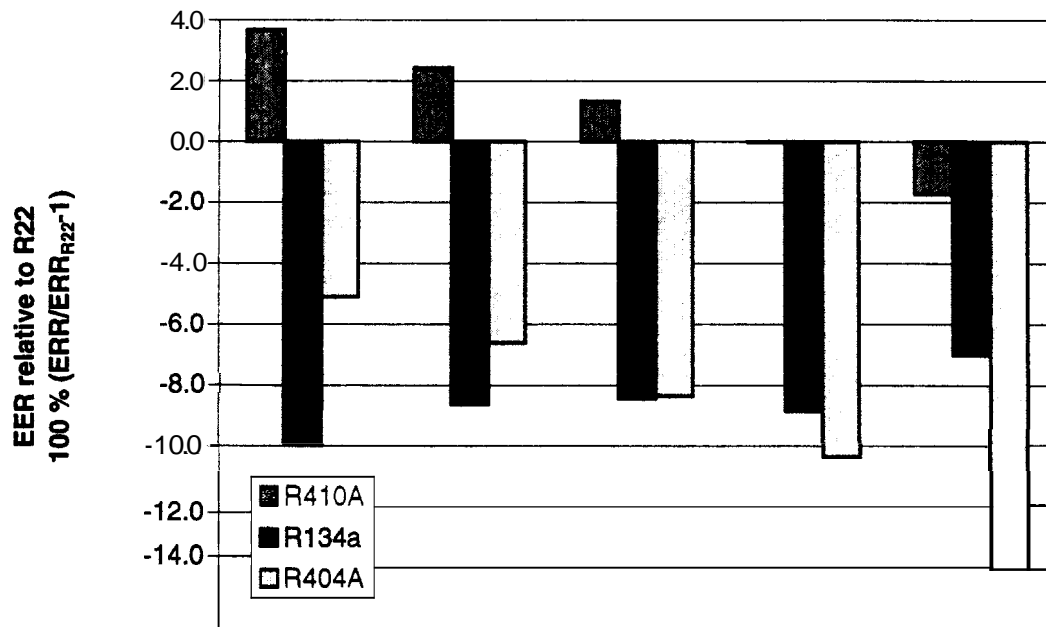


Figure 4.23 Simulated capacities of R410A, R134a, and R404A air conditioners relative to capacity of R22 air conditioner





**Figure 4.24 Simulated EERs of R410A, R134a, and R404A air conditioners relative to EER of R22 air conditioner**

## CHAPTER 5. CONCLUSIONS AND SUGGESTIONS FOR FUTURE WORK

### 5.1 Experimental Work

R22 and R410A split air-conditioning systems were tested and compared **as** outdoor temperature ranged from 82.0 °F (27.8 °C) to 130 °F (54.4 °C). The R410A system tests were extended to 155.0°F (68.3 °C) ambient temperature with a customized compressor. When outdoor temperature increased, the R410A system performance degraded more than the R22 system performance. While capacities of both systems were approximately equal at the 95.0 °F (35.0 °C) rating point, at the 130.0 °F (**54.4 °C**) outdoor temperature the R410A capacity was 9 % below that of R22. For the same test points, the R410A EER (**COP**) was **4 %** and 15 % lower than the R22 EER (**COP**), respectively. The degradation trend was linear. Since both systems employed identical heat exchangers and similar design (scroll) compressors, the refrigerant and lubricant used in each system had the dominant effect on the measured results. Operation of the R410A system **was** stable **during all** tests, including those with the customized compressors extending up to the 155.0 °F (68.3 °C) outdoor temperature and resulting in a supercritical condition at the condenser inlet.

It **is** evident that the **TXV** in combination with the large 13 SEER condenser in the current systems were able to maintain subcooled refrigerant at the inlet of the expansion valve. The TXV regulated refrigerant flowrate to prevent flooding the evaporator at the increased ambient temperatures, **and** the large outdoor condenser was able to subcool the refrigerant. In combination these factors prevented the rapid decline in performance reported by Wells et. al (1999) and predicted by some simulations.

The R410A system with compressor #2 completed tests where the compressor discharge pressure was above the critical point. Tests at an outdoor temperature of 150.0 °F (65.6 °C), 152.0 °F (66.7 °C), and 155.0 °F (68.3 °C) produced compressor discharge conditions above critical. No noticeable changes in noise level or operation of the system ~~was~~ noted. The condenser was able to condense the supercritical vapor and provide subcooling at the TXV inlet. The subcooled liquid at the TXV inlet was the main factor contributing to the stability of the system. A loss of subcooling, due either above critical outlet pressure or incomplete condensation, could have caused mass flow surging and "hunting" of the TXV.

As an additional task, it would be of interest to test the same R22 and R410A system with TXVs replaced by short tube restrictors. The fixed area expansion device would not prevent flooding of the evaporator. *Also*, a combination of a smaller area outdoor condensing unit would produce the worst case of two-phase flow in the liquid line. The current evaporator could be fitted with a short tube restrictor and tested with the current R410A condensing unit at the high outdoor temperatures seen during these tests (up to at least 155.0 °F (68.3 °C)). Then a smaller outdoor condensing unit could be installed while keeping the same evaporator and short tube restrictor. Modeling could be carried out in parallel to determine how well the current software could be adapted for a fixed area expansion device and near critical conditions.

## 5.2 Simulation Work

This project provided a thrust for the final stage of preparing a beta version of EVAP-COND, a windows-based simulation package for predicting performance of finned-tube evaporators and condenser. Both the evaporator and condenser models can account for one-dimensional non-

uniform air distributions and interaction between the air and refrigerant distributions. The visual interface helps with specifying tube-by-tube refrigerant circuitry and analyzing detailed simulation results on a tube-by-tube basis. Ten refrigerant and refrigerant mixtures are available in EVAP-COND. The package is compatible with REFPROP6 (McLinden et al., 1998), hence any refrigerant and refrigerant mixture covered by the REFPROP6 can be included. The condenser and evaporator models were validated with the **R22** and R410A test data showing good and consistent predictions. The validation effort showed the importance of proper representation of the air-side heat transfer and the inadequacy of the currently available correlations.

In the second phase of the modeling effort, we formulated a model for a TXV-equipped air conditioner to simulate system performance for R22, R410A, R404A, and R134a. The model uses the EVAP-COND evaporator and condenser model, and simulates the compressor using a compressor map algorithm. The same as for EVAP-COND, the air conditioner model is REFPROP6-compatible and technically can be used to simulate any refrigerant and refrigerant mixture that is covered by REFPROP6. We validated the system model and performed simulations for the four refrigerants for the 82.0 °F to 135.0 °F (27.8 °C to 57.2 °C) outdoor temperature range using the same heat exchangers as those tested with R22 and R410A. In general, the simulation results are consistent with the test results obtained for R22 and R410A and can be explained in terms of refrigerant thermophysical properties and their impact on performance in a system with non-optimized heat exchangers.

During the development stage of EVAP-COND, we received requests or suggestions for future work from persons who offered to test it. The suggested items for the future work included:

- capability to incorporate new or proprietary air-side and refrigerant side heat transfer correlations by the user of the program
- extension of the evaporator model to the frosting region to allow simulations of evaporators used in heat pumps and commercial refrigeration
- capability to accommodate "non-existing tubes" (empty spaces in the heat exchanger assembly)
- new option for condenser simulation where the outlet subcooling is specified in addition to inlet parameters (The program would iterate the refrigerant mass flow rate that would satisfy the input constraints)
- capability to perform sequential simulation runs.

Additional validations of the evaporator and condenser models would be highly desirable. The additional validations should include different designs, air volumetric flow rates, and tube diameters. We have to recognize that the condenser validation we performed might not be conclusive since the tested condenser had a low approach temperature, and in such situations all simulation models can predict capacity well because of the prediction limit imposed by a pinch point.

The developed simulation model for a TXV-equipped air conditioner can be extended to other expansion devices. Further, the EVAP-COND interface could be utilized as a starting point for a complete window-based heat pump simulation model.

## APPENDIX A. SUMMARY OF TEST RESULTS FOR R22 SYSTEM

Summary sheets were generated automatically after each test. For all tests a Coriolis meter ~~was~~ placed in the discharge line to measure mass flowrate in addition to the liquid line Coriolis meter. ~~This~~ redundant measurement ~~was~~ not used for all tests; therefore, the mass flow listed in the summary sheets for the discharge should be ignored.

Table A.1 lists the tests performed with the original R22 compressor and the corresponding outdoor dry-bulb temperatures.

Table A.1 R22 system tests

Filename	Outdoor Temperature (°F)
A001205a	81.8
A001208a	81.7
A001212a	135.0
<del>A001213x</del>	115.0
A001214a	134.8
A001218b	115.1
A010105	95.1
A010108a	115.0
AOIOI10a	125.4
AOIOI11a	81.9
AOIOI17b	130.5
AOIOI18x	134.5

# COOLING TEST SUMMARY SHEET

DATA FILENAME: a001205a.dat SUMMARY FILENAME: a001205a.sum

Air-Side Conditions		Range	Total Air-Side Capacity:	38979.04	Range
Indoor Dry-Bulb :	79.625	0.81	Sensible Cap (Btu/h):	28152.04	4568.84
Indoor Inlet Dew (F):	60.477	1.48	Latent Cap (Btu/h):	10827.00	1258.20
Indoor Exit Dry-Bulb:	59.067	0.87	EvapAir Delta T (F):	21.25	4085.69
Indoor Exit Dew (F):	55.444	0.84			0.90
Outdoor Dry-Bulb (F):	81.832	0.57	Sensible Heat Ratio:	0.723	0.0811
Indoor Airflow (CFM):	1188.35	17.70			
Indoor Airflow (SCFM):	1203.86	16.75	(0.075 lb/ft3 standard air)		
Evap Inlet Humidity Ratio (lbH2O/lbAir):		0.011224			
Evap Exit Humidity Ratio (lbH2O/lbAir):		0.009338			
Barometric Pressure (in HG):	29.95	Nozzle Temp (F)	59.74	1 21	
7 inch Nozzle Pressure Drop (in Water):	1.288	0.037			
Evaporator Coil Air Pressure Drop (in Water):	0.182	0.008			
-----					
Refrigerant Side Conditions					
Discharge Pressure (psia):	218.82	1.076	Ref-side Cap (Btu/h) :	39975.17	884.99
Suction Pressure :	94.78	0.977	Ref-side Cap (tons) :	3.33	0.07
Condenser Inlet Pressure:	218.06	0.977	Liq Line Mdot (lbm/min):	8.93	0.18
Condenser Exit Pressure:	194.08	1.167	Disch Mass Flow (lb/min):	-0.16	1.84
Liq MassMeter Inlet (psia):	194.08	1.167	Liq Line Density (lb/ft3):	79.17	0.32
LiqMeter Exit/TXV In (psia):	192.06	0.976	TXV Inlet Temperature (F):	86.87	0.35
			TXV Inlet Subcooling (F):	6.50	0.48
Evaporator Pres Drop (psid):	10.40	1.002	Misch Line Density (lb/ft3):	14.973	0.476
Evap Exit Pressure (psia):	97.21	1.090	Suction Temp (F):	64.02	1.22
Evap Exit Temperature (F):	61.69	1.649	Suction Superheat (F):	16.48	1.23
Evap Exit Superheat (F):	12.65	1.485	Discharge Temp (F):	147.35	0.68
			Discharge Superheat (F):	44.55	0.68
			Cond Inlet Temp (F):	150.16	0.61
			Cond Exit Temp (F)	88.45	0.55

0.36 Watthours Per Count  
 Counts : 4264.00  
 Test Period (seconds): 2503.78  
 Watthours: 1535.04  
 Cooling EER: 17.66 COP: 5.18

# COOLING TEST SUMMARY SHEET

DATA FILENAME: a001208a.dat SUMMARY FILENAME: a001208a.sum

Air-Side Conditions		Range	Total Air-Side Capacity:	39363.87	Range
Indoor Dry-Bulb :	79.887	0.90	Sensible Cap (Btu/h):	28891.73	1322.19
Indoor Inlet Flow (m)	58.301	0.25	Latent Cap (Btu/h):	10472.14	857.49
Indoor Exit Dry-Bulb	58.335	0.32	Evap Air Flow T (m):	21.87	742.52
Indoor Exit Flow (m)	54.333	0.44			0.60
Outdoor Dry-Bulb (F)	81.732	0.32	Sensible Heat Ratio	0.730	0.0157
Indoor Airflow (CFM):	1184.52	18.29			
Indoor Airflow (SCFM):	1201.08	18.22	(0.075 lb/f 8 st adard air)		
Evap Inlet Humidity Ratio (lbx2o/lbAir):	0.010992				
Evap Exit Humidity Ratio (lbx2o/lbAir):	0.009164				
Barometric Pressure (in HG)	29.95	Nozzle Temp (F):	53.33	0.84	
7 inch Nozzle Pressure (in Water):	1.281	0.035			
Evaporator Coil Air Pressure Drop (in Water):	0.177	0.010			
-----					
Refrigerant Side Conditions					
Discharge Pressure (psia):	217.99	1.907	Ref-side Cap (Btu/h) :	38833.88	1024.42
Suction Pressure :	94.15	0.733	Ref-side Cap (tons) :	3.32	0.03
Condenser Inlet Pressure:	217.25	1.759	Liq Line Mdot (lbm/min):	8.90	0.23
Condenser Exit Pressure:	197.52	1.823	Mass Flow (lb/min):	-0.12	0.23
Liq MassMeter Inlet (psia):	197.52	1.823	Liq Line Density (lb/ft3):	79.12	0.58
LiqMeter Exit/mV In (ia)	189.03	1.904	TXV Inlet Temperature (F):	86.65	0.88
Evaporator Pres Drop (psid):	10.50	1.072	TXV Inlet Subcooling (F):	5.59	0.61
Evap Exit Pressure (psia):	96.61	1.090	Disch Line Density (lb/ft3):	18.096	0.183
Evap Exit Temperature (F):	62.42	1.878	Suction Temp (F):	63.77	1.73
Evap Exit Superheat (F):	13.74	2.177	Suction Superheat (F):	16.61	1.85
			Discharge Temp (F):	147.04	1.17
			Discharge Superheat (F):	44.52	0.72
			Cond Inlet Temp (m)	49.96	0.92
			Cond Exit Temp (m):	88.58	0.86
-----					
0.38 Watt Hrs Per Count	---		Test Period (seconds):	2560.00	
Cooling	4396.00		Cooling EER:	17.69	COE: 3.13
Watt Hrs:	1582.56				



# COOLING TEST SUMMARY SHEET

DATA FILENAME: a001212a.dat SUMMARY FILENAME: a001212a.sum

Air-Side Conditions		Range	Total Air-Side Capacity	30269.60	Range
Indoor Dry-Bulb	:	79.960	0.24	Sensible Cap (Btu/h):	24807.80
Indoor Inlet Dew (F)	:	60.328	0.20	Latent Cap (Btu/h):	5461.80
Indoor Exit Dry-Bulb:	61.944	0.18	EvapAir Delta T (F):	18.79	0.24
Indoor Exit Dew (F):	57.869	0.21			
Outdoor Dry-Bulb (F):	134.980	1.13	sensible heat Ratio	0.820	0.0200
Indoor Airflow (CFM):	1190.48	20.04			
Indoor Airflow (SCFM):	1199.02	19.70	(0.075 lb/ft3 standard air)		
Evap Inlet Humidity Ratio (lbH2O/lbAir):	0.011163				
Evap Exit Humidity Ratio (lbH2O/lbAir):	0.010208				
Barometric Pressure (in HG):	29.95	Nozzle Temp (F):	≤2 52	0.79	
7 inch Nozzle Pressure Drop (in Water):	1.285	0.043			
Evaporator Coil Air Pressure Drop (in Water):	0.169	0.011			
-----					
Refrigerant Side Conditions					
Discharge Pressure (psia):	399.72	4.254	Ref-side Cap (Btu/h):	30587.20	1283.30
Suction Pressure:	103.37	0.635	Ref-side Cap (tons):	2.55	0.11
Condenser Inlet Pressure:	399.04	4.056	Liq Line Mdot (lbm/min):	8.56	0.33
Condenser Exit Pressure:	378.66	4.618	Disch Mass Flow (lb/min):	0.22	3.88
Liq MassMeter Inlet (psia):	378.66	4.618	Liq Line Density (lb/ft3):	105.28	0.76
LiqMeter Exit/TXV In (psia):	375.21	5.370	TXV Inlet Temperature (F):	134.18	0.56
			TXV Inlet Subcooling (F):	11.16	1.03
Evaporator Pres Drop (psid):	17.99	1.825	Disch Line Density (lb/ft3):	5.145	0.985
Evap Exit Pressure (psia):	105.35	1.187	Suction Temp (F):	77.49	2.16
Evap Exit Temperature (F):	65.48	3.368	Suction Superheat (F):	24.75	1.93
Evap Exit Superheat (F):	11.60	3.103	Discharge Temp (F):	232.32	1.44
			Discharge Superheat (F):	81.60	1.46
			Cond Inlet Temp (F):	237.17	1.25
			Cond Exit Temp (F):	141.67	0.95
-----					
0.35 WattsHours Per Count			Test Period (seconds):	2277.54	
Counts:	7255.00		Cooling EER:	7.33	COP: 2.15
WattsHours:	2611.80				

# COOLING    EST    SUMMARY    BHSEF

DATA FILENAME: a001213><Dat    SUMMARY FILENAME: a001213X.sum

Air-Side Conditions		Range	Total Air-Side Capacity:	34264.43	2651.27	Range
Indoor Dry-Bulb :	80.240	0.91	Sensible Cap (Btu/h):	27492.35	1093.68	
Indoor Inlet Dew (m)	59.336	0.84	Latent Cap (Btu/h):	6772.08	1990.76	
Indoor Exit Dry-Bulb	60.392	0.45	EvapAir Delta T (F):	20.61	0.78	
Indoor Exit Dew (F):	56.187	0.55				
Outdoor Dry-Bulb (F):	114.963	0.91	Sensible Heat Ratio	0.303	0.0459	
Indoor Airflow (CFM):	1199.64	12.12				
Indoor Airflow (SCFM)	1212.26	12.77	(0.075 lb/ft3 standard air)			
Evap Inlet Humidity Ratio (lbH2O/lbAir):		0.010768				
Evap Exit Humidity Ratio (lbH2O/lbAir):		0.009597				
Barometric Pressure (in HG):	29.95	Nozzle Temp (F):	≤ 0.97	0.90		
7 inch Nozzle Pressure Drop (in Water):	1.309	0.027				
Evaporator Coil Air Pressure Drop (in Water):	0.170	0.007				
-----						
Refrigerant Side Conditions						
Discharge Pressure (psia):	319.81	2.054	Ref-side Cap (Btu/h) :	34338.16	1632.22	
Suction Pressure :	99.41	0.635	Ref-side Cap (tons):	2.86	0.14	
Condenser Inlet Pressure:	319.09	1.955	Liq Line Mdot (lbm/min):	8.81	0.40	
Condenser Exit Pressure:	300.31	1.872	Disch Mass Flow (lb/min):	-0.07	1.27	
Liq MassMeter Inlet (psia):	300.31	1.872	Liq Line Density (lb/ft3):	90.54	1.64	
LiqMeter Exit/TXV In (psia):	291.22	2.099	TXV Inlet Temperature (F):	118.32	0.68	
			TXV Inlet Subcooling (m):	6.30	0.46	
Evaporator Pres Drop (psid):	16.87	1.959	Disch Line Density (lb/ft3):	29.904	0.000	
Evap Exit Pressure (psia):	101.74	0.605	Suction Temp (F):	72.29	1.24	
Evap Exit Temperature (F):	67.16	1.126	Suction Superheat (F):	21.91	1.45	
Evap Exit Superheat (F):	15.38	1.026	Discharge Temp (F):	193.37	0.88	
			Discharge Superheat (m):	61.25	0.81	
			Cond Inlet Temp (m):	197.24	0.69	
			Cond Exit Temp (m):	123.89	0.45	
-----						
0.36 WattHours Per Count			Test Period (seconds): 1326.62			
Counts : 3209.00			Cooling EER: 10.93    COP: 3.20			
WattHours: 1135.24						

# COOLING TEST SUMMARY SHEET

DATE: 08/01/2011 14:00:00 SMMARY FILENAME: a001214a sum

Air-Side Conditions		Range	Total Air-Side Capacity:	29711.40	Range
Indoor Dry-Bulb :		80.465	0.30	Sensible Cap (Btu/h):	25364.09
Indoor Inlet Air :		39.921	0.20	Latent Cap (Btu/h):	4347.32
Indoor Exit Dry-Bulb:		62.119	0.17	EvapAir Delta T (F):	19.14
Indoor Exit Dew (F):		57.962	0.15		
Outdoor Dry-Bulb (F):		134.830	0.5	Sensible Heat Ratio:	0.854
Indoor Airflow (CFM):		1195.23	12.84		
Indoor Airflow (SCFM):		1203.86	13.67	(0.075 lb/ft3 standard air)	
Evap Inlet Humidity Ratio (lbH2O/lbAir):				0.011000	
Evap Exit Humidity Ratio (lbH2O/lbAir):				0.010243	
Barometric Pressure (in HG):		29.95		Nozzle Temp (F):	57
7 inch Nozzle Pressure Drop (in Water):				1.295	0.027
Evaporator Coil Air Pressure Drop (in Water):				0.169	0.012
Refrigerant Side Conditions					
Discharge Pressure (psia):		396.83		Ref-side Cap (tons):	30405.03
Suction Pressure :		104.21		Ref-side Cap (lbm/min):	8.61
Condenser Inlet Pressure:		396.13		Disch Mass Flow (lb/min):	-0.01
Condenser Exit Pressure:		376.56		Liq Line Density (lb/ft3):	101.21
Liq MassMeter Inlet (psia):		376.56		TXV Inlet Temperature (F):	136.93
LiqMeter Exit/TXV In (psia):		369.77		TXV Inlet Subcooling (F):	7.18
Evaporator Pres Drop (psid):		19.30		Disch Line Density (lb/ft3):	29.904
Evap Exit Pressure (psia):		106.31		Suction Temp (F):	78.44
Evap Exit Temperature (F):		68.76		Suction Superheat (F):	25.22
Evap Exit Superheat (F):		14.33		Discharge Temp (F):	230.06
				Discharge Superheat (F):	79.96
				Cond Inlet Temp (F):	235.01
				Cond Exit Temp (F):	143.64

0.36 WattHours Per Count  
 Counts : 6011.00  
 WattHours: 2163.96  
 Test Period (seconds): 1906.41  
 Cooling EER: 7.27 COP: 2.13

# COOLING TEST S&M

DATA FILENAME: a001218b.dat SUMMARY FILENAME: a001218b.sum

Air-Side Conditions				Range
Indoor Dry-Bulb :	80.063	Range	Total Air-Side Cap	33843.68 2537.11
Indoor Inlet Dew (F) :	59.655		Sensible Cap	26957.45 2696.57
Indoor Exit Dry-Bulb :	60.444	0.20	Latent Cap	6886.23 1402.67
Indoor Exit Dew (F) :	56.457	0.73	EvapAir Delt T (F) :	20.3 2.01
Outdoor Dry-Bulb (F) :	115.057	0.69	Sensible Cap Ratio	0.797 0.0445
Indoor Airflow (CFM) :	1190.45	10.25		
Indoor Airflow (SCFM) :	1202.40	10.41	(0.075 lb/ft3 std air)	
Evap Inlet Humidity Ratio (lbH2O/lbAir) :	0.010894			
Evap Exit Humidity Ratio (lbH2O/lbAir) :	0.009693			
Barometric Pressure (in HG) :	29.95	Nozzle Temp (F) :	61.19	1.13
7 inch Nozzle Pressure Drop (in Water) :	1.289	0.022		
Evaporator Coil Air Pressure Drop (in Water) :	0.171	0.010		
-----				
Refrigerant Side Conditions				
Discharge Pressure (psia) :	321.20	1.956	Ref-side Cap (Btu/h) :	34130.11 1319.37
Suction Pressure :	99.49	1.222	Ref-side Cap (tons) :	2.84 0.11
Condenser Inlet Pressure :	320.43	1.955	Liq Line Mdot (lbm/min) :	8.76 0.32
Condenser Exit Pressure :	301.46	1.823	Disch Mass Flow (lb/min) :	-0.11 1.24
Liq MassMeter Inlet (psia) :	301.46	1.823	Liq Line Density (lb/ft3) :	89.68 1.84
LiqMeter Exit/TXV In (psia) :	291.00	2.441	TXV Inlet Temperature (F) :	118.42 0.60
			TXV Inlet Subcooling (F) :	6.14 0.68
Evaporator Pres Drop (psid) :	17.02	1.285	Disch Line Density (lb/ft3) :	29.904 0.000
Evap Exit Pressure (psia) :	101.85	1.433	Suction Temp (F) :	72.40 2.17
Evap Exit Temperature (F) :	66.82	2.387	Suction Superheat (F) :	21.97 1.53
Evap Exit Superheat (F) :	14.98	1.907	Discharge Temp (F) :	193.96 0.85
			Discharge Superheat (F) :	61.48 0.68
			Cond Inlet Temp (F) :	197.91 0.95
			Cond Exit Temp (F) :	124.02 0.68
-----				
0.36 WattsHours Per Count			Test Period (sec) :	1453.61
Counts :	3560.00		Cooling EER :	10.75 COP
WattsHours :	1281.60			5.14

# COOLING TEST SUMMARY SCREEN

DATA FILENAME: a010105.dat SUMMARY FILENAME: a010105.sum

Air-Side Conditions		Range	Total Air-Side Capacity: 38639.91	Range
Indoor Dry-Bulb	79.73	0.83	Sensible Cap (Btu/h): 28306.62	1209.01
Indoor Inlet Air (m)	53.951	0.74	Latent Cap (Btu/h): 10333.29	1010.49
Indoor Exit Dry-Bulb:	58.961	0.65	EvapAir Delta T (F): 21.57	0.80
Indoor Exit Dew (m)	55.028	0.80		
Outdoor Dry-Bulb (m)	95.051	1.73	Sensible Heat Ratio	0.733
Indoor Airflow (CFM):	1177.33	14.49		0.018
Indoor Airflow (SCFM)	1192.64	14.91	(0.075 lb/ft3 standard air)	
Evap Inlet Humidity Ratio (lbH2O/lbAir):	0.011012			
Evap Exit Humidity Ratio (lbH2O/lbAir):	0.009195			
Barometric Pressure (in HG):	29.95	Nozzle Temp (F): 59.81	0.92	
7 inch Nozzle Pressure Drop (in Water):	1.264	0.031		
Coil Air Pressure Drop (in Water):	0.176	0.010		
-----				
Refrigerant Side Conditions				
Discharge Pressure (psia):	259.75	3.831	Ref-side Cap (Btu/h):	38209.50
Suction Pressure:	96.35	1.954	Ref-side Cap (tons):	3.19
Condenser Inlet Pressure:	259.09	3.746	Liq Line Mdot (lbm/min):	8.96
Condenser Exit Pressure:	240.50	4.132	Disch Mass Flow (lb/min):	-0.06
Liq MassMeter Inlet (psia):	240.50	4.132	Liq Line Density (lb/ft3):	84.68
LiqMeter Exit/TXV In (psia):	233.08	3.905	TXV Inlet Temperature (F):	97.75
			TXV Inlet Subcooling (F):	9.73
Evaporator Pres Drop (psid):	12.65	1.290	Disch Line Density (lb/ft3):	29.904
Evap Exit Pressure (psia):	98.81	2.260	Suction Temp (F):	65.65
Evap Exit Temperature (F):	61.53	3.388	Suction Superheat (F):	17.13
Evap Exit Superheat (F):	11.50	3.374	Discharge Temp (F):	165.28
			Discharge Superheat (F):	49.59
			Cond Inlet Temp (F):	168.39
			Cond Exit Temp (F):	99.97
-----				
0.38 Watt Hurs Per Count			Moist Per Tod (seconds):	3055.72
Cou hrs:	5961.00		Cooling EER:	15.28
WattH hrs:	2145.96		COP:	4.48

# COOLING TEST SUMMARY SHEET

DATA FILENAME a010108a.dat SUMMARY FILENAME a010108a sum

Air-Side Conditions	Range	Total Air-Side Capacity:	34781.93	1626.60	Range
Indoor Dry-Bulb :	79.706	Sensible Cap (Btu/h):	26783.85	1228.79	
Indoor Inlet Dew (W)	59.872	Latent Cap (Btu/h):	7998.08	1887.90	
Indoor Exit Dry-Bulb	60.082	EvapAir Delta T (F):	20.41	0 81	
Indoor Exit Dew (W)	56.121				
Outdoor Dry-Bulb (F):	115.097	Sensible Heat Ratio:	0 770	0 0430	
Indoor Airflow (CFM):	1179.84				
Indoor Airflow (SCFM):	1192.62	(0.075 lb/ft³ standard air)			
Evap Inlet Humidity Ratio (lbH2O/lbAir):	0.010981				
Evap Exit Humidity Ratio (lbH2O/lbAir):	0.009575				
Barometric Pressure (in HG):	29.95	Nozzle Temp (F):	≤0.8Z	1 ≤	
7 inch zze Pressure Drop (in Water):	1.267		0.043		
Evaporator Coil Air Pressure Drop (in Water):	0.172		0.01≤		

## Refrigerant Side Conditions

Discharge Pressure (psia):	327.01	2.038	Ref-side Cap (Btu/h):	30918.81	2703.31
Suction Pressure :	99.23	1.954	Ref-side Cap (tons):	2.91	0.23
Condenser Inlet Pressure:	326.36	2.199	Liq Line Mdot (lbm/min):	8.83	0.70
Condenser Exit Pressure:	307.44	2.066	Disch Mass Flow (lb/min):	-0.05	1.35
Liq MassMeter Inlet (psia):	307.44	2.066	Liq Line Density (lb/ft³):	94.16	0.52
LiqMeter Exit/TXV In (psia):	301.76	2.929	TXV Inlet Temperature (F):	114.47	0.72
			TXV Inlet Subcooling (F):	12.98	1.02
Evaporator Pres Drop (psid):	15.60	2.064	Disch Line Density (lb/ft³):	29.904	0.000
Evap Exit Pressure (psia):	101.42	2.583	Suction Temp (F):	70.77	2.63
Evap Exit Temperature (F):	61.85	4.308	Suctio Superheat (W):	20.50	2.22
Evap Exit Superheat (F):	10.26	3.719	Discharge Temp (F):	196.02	1.61
			Discharge Superheat (F):	62.08	1.83
			Cond Inlet Temp (F):	199.84	1.58
			Cond Exit Temp (W)	119.64	0.80

0 ≤ WattHours Per Count

Counts : 14092.00

WattHours: 5073 12

Test Period (seconds): 5670.35

Cooling EER: 10.80 COP 3.16

# COOLING TEST SUMMARY SHEET

DATA FILENAME: a010110a.dat SUMMARY FILENAME: a010110a.sum

Air-Side Conditions		Range	Total Air-Side Capacity:	33420.75	Range
Indoor Dry-Bulb :	79.728	1.13	Sensible Cap (Btu/h):	25658.78	1208.28
Indoor Inlet Dew (F):	60.495	0.30	Latent Cap (Btu/h):	7761.97	861.22
Indoor Exit Dry-Bulb:	61.086	0.36	EvapAir Delta T (F):	19.39	931.44
Indoor Exit Dry Bulb (m)	56.989	0.30			0.73
Outdoor Dry-Bulb (F):	125.412	0.18	Sensible Heat Ratio	0.758	0.0202
Indoor Airflow (CFM):	1191.16	16.86			
Indoor Airflow (SCFM)	1201.77	15.54	(0.075 lb/ft3 standard air)		
Evap Inlet Humidity Ratio (lbH2O/lbAir):		0.011231			
Evap Exit Humidity Ratio (lbH2O/lbAir):		0.009877			
Barometric Pressure (in HG):	29.95	Nozzle Temp (F):	61.72	0.98	
7 inch Nozzle Pressure Drop (in Water):		1.289	0.035		
Evaporator Coil Air Pressure Drop (in Water):		0.172	0.012		
Refrigerant Side Conditions					
Discharge Pressure (psia):	366.58	2.445	Ref-side Cap (Btu/h) :	33143.49	1851.82
Suction Pressure :	101.49	0.977	Ref-side Cap (tons):	2.76	0.15
Condenser Inlet Pressure:	365.91	1.955	Liq Line Mdot (lbm/min):	8.76	0.49
Condenser Exit Pressure:	346.87	2.552	Disch Mass Flow (lb/min):	-0.07	0.47
Liq MassMeter Inlet (psia):	346.87	2.552	Liq Line Density (lb/ft3):	99.12	0.48
LiqMeter Exit/TXV In (psia):	342.02	3.417	TXV Inlet Temperature (F):	123.26	0.54
			TXV Inlet Subcooling (F):	14.36	1.21
Evaporator Pres Drop (psid):	16.84	2.102	Disch Line Density (lb/ft3):	29.904	0.000
Evap Exit Pressure (psia):	103.42	1.453	Suction Temp (F):	74.17	2.68
Evap Exit Temperature (F):	62.52	3.843	Suction Superheat (F):	22.54	2.39
Evap Exit Superheat (F):	9.76	3.891	Discharge Temp (F):	214.21	1.48
			Discharge Superheat (F):	70.82	1.37
			Cond Inlet Temp (F):	218.59	1.06
			Cond Exit Temp (m):	129.91	0.51
-----					
0.36 WattHours Per Count	----		Test Period (seconds):	3218.75	
Counts :	9124.00		Cooling EER:	9.10	COP: 2.67
WattHours:	3284.64				

# COOL TEST SUMMARY SHEET

DATA FILENAME: a010111a.dat SUMMARY FILENAME: a010111a.sum

Air-Side Conditions		Range	Total Air-Side Capacity: 40200.67	Range
Indoor Dry-Bulb	80.311	1.04	Sensible Cap (Btu/h): 29184.32	1282.92
Indoor Wet-Bulb (F)	80.088	0.30	Latent Cap (Btu/h): 11016.35	1080.80
Indoor Exit Dry-Bulb	53.036	0.41	EvapAir Delta T (F): 22.02	818.20
Indoor Exit Dew (F)	50.488	0.26		0.78
Outdoor Dry-Bulb (F)	81.835	0.71	Sensible Cap Ratio	0.728
Outdoor Airflow (CFM)	1188.87	22.77		0.0132
Indoor Airflow (SCFM)	1204.59	23.06	(0.075 lb/fc3 start stop air)	
Evap Inlet Humidity Ratio (lbH2O/lbAir)			0.011066	
Evap Exit Humidity Ratio (lbH2O/lbAir)			0.009148	
Barometric Pressure (in HG)	29.95		Nozzle Temp (F): 39.71	0.30
7 inch Nozzle Pressure Drop (in Water)			1.289	0.049
Evaporator Coil Air Pressure Drop (in Water)			0.179	0.013

## Refrigerant Side Conditions

Discharge Pressure (psia):	220.16	1.793	Ref-side Cap (Btu/h):	40405.13	1817.44
Suction Pressure:	94.94	0.977	Ref-side Cap (tons):	3.37	0.15
Condenser Inlet Pressure:	220.46	1.629	Liq Line Mdot (lbm/min):	8.95	0.37
Condenser Exit Pressure:	203.04	1.580	Disch Mass Flow (lb/min):	0.04	0.77
Liq MassMeter Inlet (psia):	203.04	1.580	Liq Line Density (lb/ft3):	78.31	0.44
LiqMeter Exit/TXV In (psia):	193.33	2.115	Liq Inlet Temperature (F):	85.42	0.59
			TXV Inlet Subcooling (F):	8.43	0.72
Evaporator Pres Drop (psid):	10.48	1.581	Misch Line Density (lb/ft3):	29.904	0.000
Evap Exit Pressure (psia):	97.27	1.574	Suction Temp (F):	63.68	2.82
Evap Exit Temperature (F):	65.41	3.550	Suction Superheat (F):	16.04	2.84
Evap Exit Superheat (F):	16.32	3.417	Discharge Temp (F):	147.99	0.81
			Discharge Superheat (F):	44.73	1.10
			Cond Inlet Temp (F):	150.64	1.00
			Cond Exit Temp (F):	86.89	0.77

0.36 WattsHours Per Count -----

Counts : 6878.00

WattsHours: 2476.08

Test Period (seconds): 4050.54

Cooling EER: 18.29 COP: 3.36



COOP1 TEST SUMMARY SHEET

DATA FILENAME 0010117b 0at SUMMARY FILENAME 0010117b sum

Air-Side Conditions		Range	Total Air-Side Capacity	Range
Indoor Dry-Bulb	80 101	0.87	31607.10	1257.21
Indoor Inlet Dew (W)	50 882	0.30	Sensible Cap Btu/hl	25718.85
Indoor Exit Dry-Bulb	81 442	0.50	Latent Cap Btu/hl	989.60
Indoor Exit Dew (W)	57 101	0.39	EvapAir Deltaw m (W)	887.11
Outdoor Dry-Bulb (W)	130 400	0.48	Sensible Heat Ratio	0.814
Indoor Airflow (CFM)	1193.27	15.39		0.0228
Indoor Airflow (SCFM)	1202.90	16.59	(0.075 lb/ft3 standard air)	
Evap Inlet Humidity Ratio (lbH2O/lbAir)		0.010984		
Evap Exit Humidity Ratio (lbH2O/lbAir)		0.009958		
Barometric Pressure (in HG)	29.35	Nozzle Temp (F)	82.10	1.10
7 inch Nozzle Pressure Drop (in Water)		1.292	0.34	
Evaporator Coil Air Pressure Drop (in Water)		0.166	0.10	

Refrigerant Side Conditions

Discharge Pressure (psia)	385.78	1.712	Ref-sid C <sub>4</sub> (Btu/h)	31732.29	806.38
Suction Pressure	101.94	1.140	Ref-side C <sub>4</sub> (tons)	2.65	0.13
Condenser Inlet Pressure	385.14	1.547	Liq Line Mdot (lbm/min)	8.61	0.44
Condenser Exit Pressure	366.17	2.188	Disch Mass Flow (lb/min)	-0.03	1.17
Liq MassMeter Inlet (psia)	366.17	2.188	Liq Line Density (lb/ft3)	101.86	0.25
LiqMeter Exit/TXV In (psia)	362.20	2.685	TXV Inlet Temperature (F)	127.77	0.57
Evaporator Pres Drop (psid)	17.35	2.393	TXV Inlet Subcooling (F)	14.60	0.96
Evap Exit Pressure (psia)	103.99	1.574	Disch Line Density (lb/ft3)	29.904	0.000
Evap Exit Temperature (F)	62.29	3.660	Suction Temp (F)	75.61	1.80
Evap Exit Superheat (F)	9.19	3.526	Suction Superheat (F)	23.72	1.66
			Discharge Temp (F)	224.42	0.93
			Discharge Superheat (F)	76.72	1.01
			Com Inlet Temp (W)	229.39	0.93
			C 0 Exit Temp (F)	135.20	0.51

0.38 WattHours Per Count

Counts : 3921.00

WattHours: 1411.58

Test Period (seconds): 1254.50

Cooling : 7.80 COP: 2.29

# COOLING MEAST SUMMARY SCREEN

DATA FILENAME: a010118x.dat SUMMARY FILENAME: a010118x.sum			
Air-Side Conditions		Range	Range
Indoor Dry-Bulb :	79.793	0.85	Total Air-Side Capacity: 30668.59
Indoor Inlet Dew (F) :	59.886	0.05	Sensible Cap (Btu/h) : 25169.33
Indoor Exit Dry-Bulb :	61.618	0.35	Latent Cap (Btu/h) : 5499.26
Indoor Exit Dew (F) :	57.382	0.29	EvapAir Delta T (F) : 19.00
Outdoor Dry-Bulb (F) :	134.487	0.73	Sensible heat Ratio: 0.82
Indoor Airflow (CFM) :	1194.35	10.50	0.014
Indoor Airflow (SCFM) :	1203.42	9.93	(0.075 lb/ft3 standard air)
Evap Inlet Humidity Ratio (lbH2O/lbAir) :	0.010986		
Evap Exit Humidity Ratio (lbH2O/lbAir) :	0.010028		
Barometric Pressure (in HG) :	29.95	Nozzle Temp (F) :	62.35
7 inch Nozzle Pressure Drop (in Water) :	1.294	0.022	0.022
Evaporator Coil Air Pressure Drop (in Water) :	0.169	0.006	0.006
-----			
Refrigerant Side Conditions			
Discharge Pressure (psia) :	401.94	2.771	Ref-side Cap (Btu/h) : 31071.02
Suction Pressure :	102.82	0.977	Ref-side Cap (tons) : 2.59
Condenser Inlet Pressure :	401.22	2.932	Liq Line Mdot (lbm/min) : 8.54
Condenser Exit Pressure :	382.05	3.119	Disch Mass Flow (lb/min) : -0.02
Liq MassMeter Inlet (psia) :	382.05	3.119	Liq Line Density (lb/ft3) : 103.77
LiqMeter Exit/TXV In (psia) :	378.55	4.393	TXV Inlet Temperature (F) : 131.13
Evaporator Pres Drop (psid) :	17.66	1.961	TXV Inlet Subcooling (F) : 14.96
Evap Exit Pressure (psia) :	104.61	1.574	Disch Line Density (lb/ft3) : 29.904
Evap Exit Temperature (F) :	65.54	2.734	Suction Temp (F) : 76.59
Evap Exit Superheat (F) :	12.08	2.785	Suction Superheat (F) : 24.18
			Discharge Temp (F) : 232.52
			Discharge Superheat (F) : 81.32
			Cond Inlet Temp (F) : 237.62
			Cond Exit Temp (F) : 138.51
			186.35
			0.16
			0.49
			0.99
			0.28
			0.42
			0.76
			0.00
			2.34
			1.91
			1.46
			1.22
			1.30
			0.90
-----			
0.36 WattsHours Per Count	Test Period (seconds) : 1467.89		
Counts : 4679.00	Cooling EER: 7.42 COP: 2.18		
WattsHours: 1684.44			

## APPENDIX B. SUMMARY OF TEST RESULTS FOR R410A SYSTEM

**Summary** sheets were generated automatically after each test. For all tests a Coriolis meter ~~was~~ placed in the discharge line to measure mass flowrate in addition to the liquid line Coriolis meter. This redundant measurement was not used for all tests; therefore, the mass flow listed in the summary sheets for the discharge should be ignored.

### B.1 R410A System With Original Compressor

Table B.1 lists the tests performed with the original R410A compressor and the corresponding outdoor dry-bulb temperatures.

Table B.1 R410A tests with compressor #1

Filename	Outdoor Temperature (°F)
B010320a	95.1
B010328a	95.0
B010329x	125.5
B010329b	125.4
B010330k	82.1
B010331x	115.4
B010402a	129.8
B010403a	125.0
B010410a	114.9
B010425x	129.9

# COOLING SUMMARY

DATA FILENAME b010320a.dat

FILENAME 0010320a sum

Range

Air-Side Conditions Range Total Air-Side Capacity: 37254.43 856.57  
 Indoor Dry-Bulb : 79.748 1.04 Sensible Cap (Btu/h): 28509.43 1074.69  
 Indoor Inlet Dew (F): 59.725 0.10 Latent Cap (Btu/h): 8745.00 662.27  
 Indoor Exit Dry-Bulb: 58.831 0.33 EvapAir Delta T (F): 21.67 0.76  
 Indoor Exit Dew (m 55.583 0.30

Outdoor Dry-Bulb (m) 95.141 1.03 Sensible Heat Ratio: 0.55 0.0165

Indoor Airflow (CFM) 1173 62 12.00

Indoor Airflow (SCFM) 1155 68 11.52 (0.075 lb/ft3 standard air)

Evap Inlet Humidity Ratio (lbx2o/lbAir): 0.010922

Evap Exit Humidity Ratio (lbx2o/lbAir): 0.009388

Barometric Pressure (in HG): 29.55 Nozzle Temp (F): 59.48 0.66

7 inch Nozzle Pressure Drop (in Water): 1.270 0.025

Evaporator Coil Air Pressure Drop (in Water): 0.148 0.009

## Refrigerant Side Condition:

Discharge Pressure (psia):	398.98	4.159	Ref-side Cap (Btu/h)	37765.34	527.16
Suction Pressure:	159.48	0.629	Ref-side Cap (tons):	3.15	0.04
Condenser Inlet Pressure:	398.25	3.964	Liq Line Mdot (lbm/min):	8.97	0.12
Condenser Exit Pressure:	386.87	4.055	Disch Mass Flow (lb/min):	-0.10	0.00
Liq MassMeter Inlet (psia):	386.87	4.055	Liq Line Density (lb/ft3):	76.57	0.23
LiqMeter Exit/TXV In (psia):	373.89	4.260	TXV Inlet Temperature (F):	99.54	0.51
			TXV Inlet Subcooling (m):	9.27	1.28
Evaporator Pres Drop (psid):	4.68	0.359	Disch Line Density (lb/ft3):	19.377	0.377
Evap Exit Pressure (psia):	161.11	1.095	Suction Temp (F):	56.91	2.30
Evap Exit Temperature (F):	55.37	4.708	Suction Subcooling (F):	5.94	2.15
Evap Exit Superheat (F):	3.77	4.940	Disch Inlet Temp (F):	158.87	1.11
			Disch Inlet Subcooling (m):	44.94	1.32

0.36 WattsPer Count

Counts : 3512.00

WattHours: 1264.32

Test Period (seconds): 1836.43

Cooling SEER: 13.03 COP: 4.41

Condenser DP (psid)	11.50	0.46	Evap Inlet Pressure after TXV (psia):	147.89	0.98
			Evap Inlet Temp after TXV (F):	52.11	0.62
			Evap Inlet Temp2 (F):	51.98	0.45
			Evap Inlet Temp3 (F):	52.53	0.76
			Cond Inlet Temp (F):	158.76	1.11
			Cond Exit Temp (F):	101.99	1.17

COOLING MESEN BMMARY

DATA FILENAME: b010328a.dat SUMMARY FILENAME: b010328a.sum

Air-Side Conditions Range Total Air-Side Capacity: 38144.46 Range  
 Indoor Dry-Bulb : 79.966 0.62 Sensible Cap (Btu/h): 28009.22 868.97  
 Indoor Inlet Air (W): 80.303 0.15 Latent Cap (Btu/h): 10135.24 873.38  
 Indoor Exit Dry-Bulb: 59.548 0.22 EvapAir Delta T (F): 21.18 486.89  
 Indoor Exit Air (W): 56.277 0.21  
 Outdoor Dry-Bulb (W): 95.018 0.48 SCo=indl x=ent Rratio: 0.730 0.0105  
 Indoor Airflow (CFM): 1186.88 18.28  
 Indoor Airflow (SCFM): 1201.33 17.87 (0.075 lb/ft3 standard air)  
 Evap Inlet Humidity Ratio (lbx20/lbAir): 0.011398  
 Evap Exit Humidity Ratio (lbH2O/lbAir): 0.009629  
 Barometric Pressure (in HG): 29.95 Nozzle Temp (F): 60.12 0.83  
 7 inch Nozzle Pressure Drop (in Water): 1.284 0.03  
 Evaporator Coil Air Pressure Drop (in Water): 0.150 0.033

Refrigerant Side Conditions

Discharge Pressure (psia): 400.48 Z.446 R=side CA (Btu/h) 38301.44 520.78  
 Suction Pressure : 160.79 0.504 Ref-side Cap (tons): 3.19 0.04  
 Condenser Inlet Pressure: 399.81 Z.594 Liq Line Mdot (lbm/min): 9.03 0.11  
 Condenser Exit Pressure: 388.75 Z.443 Disch Mass (lb/min) -0.10 0.00  
 Liq MassMeter Inlet (psia): 388.75 Z.443 Liq Line Density (lb/ft3): 76.07 0.42  
 LiqMeter Exit/TXV In (psia): 373.70 Z.203 TXV Inlet Temperature (W): 98.40 0.56  
 Evaporator Pres Drop (psid): 4.70 0.367 TXV Inlet Subcooling (F): 10.37 0.67  
 Evap Exit Pressure (psia): 162.39 0.487 Disch Line Density (lb/ft3): 21.510 0.408  
 Evap Exit Temperature (F): 55.92 3.910 Suction Temp (F): 57.64 1.43  
 Evap Exit Superheat (F): 3.83 3.864 Suction Superheat (F): 6.17 1.45  
 Discharge Temp (F): 159.24 0.94  
 Discharge Superheat (F): 45.03 0.92

0.36 WattHours per Count -----  
 Counts : 5320.00  
 WattHours: 1315.20

Compressor HP (psid) 11.20 0.40 Inlet Pressure after TXV (psia): 149.20 0.68  
 Evap Inlet Temp after TXV (F): 52.60 0.54  
 Evap Inlet Temp2 (F): 52.39 0.47  
 Evap Inlet Temp3 (F): 53.01 0.41  
 Cond Inlet Temp (F): 159.16 0.65  
 Cond Exit Temp (F): 100.68 0.57

COOLING TEST SUMMARY SHEET

DATA FILENAME: b010329x.dat SUMMARY FILENAME: b010329x.sum

Air-Side Conditions		Range	Total Air-Side Capacity: 29985.34	Range
Indoor Dry-Bulb :	80.111	0.80	Sensible Cap (Btu/h): 25280.38	919.90
Indoor Inlet Dew (F):	60.507	0.20	Latent Cap (Btu/h): 4704.96	781.12
Indoor Exit Dry-Bulb:	61.768	0.32	EvapAir Delta T (F): 19.14	548.71
Indoor Exit Dew (F):	58.414	0.40		0.51
Outdoor Dry-Bulb (F):	125.460	1.58	Sensible Heat Ratio: 0.843	0 0174
Indoor Airflow (CFM):	1189.81	12.10		
Indoor Airflow (SCFM):	1198.98	11.80	(0.075 lb/ft3 standard air)	
Evap Inlet Humidity Ratio (lbH2O/lbAir):		0.011236		
Evap Exit Humidity Ratio (lbH2O/lbAir):		0.010413		
Barometric Pressure (in HG):	29.95	Nozzle Temp (F): 20	0 57	
7 inch Nozzle Pressure Drop (in Water):	1.284	0.026		
Evaporator Coil Air Pressure Drop (in Water):	0.147	0.006		
-----				
Refrigerant Side Conditions				
Discharge Pressure (psia):	567.66	5.039	Ref-side Cap (Btu/h) :	30216.06
Suction Pressure :	171.04	1.007	Ref-side Cap (tons):	2.52
Condenser Inlet Pressure:	567.13	5.089	Liq Line Mdot (lbm/min):	8.71
Condenser Exit Pressure:	557.96	5.032	Disch Mass Flow (lb/min):	-0.10
Liq MassMeter Inlet (psia):	557.96	5.032	Liq Line Density (lb/ft3):	89.06
LiqMeter Exit/TXV In (psia):	541.65	4.848	TXV Inlet Temperature (F):	126.60
			TXV Inlet Subcooling (F):	11.27
Evaporator Pres Drop (psid):	5.64	0.413	Disch Line Density (lb/ft3):	5.257
Evap Exit Pressure (psia):	172.32	1.071	Suction Temp (F):	62.61
Evap Exit Temperature (F):	59.75	2.733	Suction Superheat (F):	7.31
Evap Exit Superheat (F):	3.98	2.746	Discharge Temp (F):	213.01
			Discharge Superheat (F):	71.15
-----				
0 36 WattHours Per Count			Test Period (seconds):	1909.54
Counts : 5864.00			Cooling EER:	7.53
WattHours: 2111.04			CO <sub>2</sub> :	2.21
-----				
Condenser ΔP (psid):	9 31	0 20	Evap Inlet Pressure after TXV (psia):	160.12
			Evap Inlet Temp after TXV (F):	56.64
			Evap Inlet Temp2 (F):	56.14
			Evap Inlet Temp3 (F):	56.72
			Cond Inlet Temp (F):	212.99
			Cond Exit Temp (F):	131.13
				1.08

# COOLING TEST SUMMARY SHEET

DATA FILENAME: b010329b.dat SUMMARY FILENAME: b010329b.sum

Air-Side Conditions		Range	Total Air-Side Capacity: 29930.40	Range
Indoor Dry-Bulb :	80.084	0.78	Sensible Cap (Btu/h): 25446.25	1199.84
Indoor Wet Bulb (W):	80.222	0.05	Latent Cap (Btu/h): 4484.14	891.42
Indoor Exit Dry-Bulb	61.812	0.28	EvapAir Delta T (F): 19.25	665.62
Indoor Exit Wet (F)	58.212	0.31		0.63
Outdoor Dry-Bulb (W)	125.409	0.98	Sensible Heat Ratio	0.850
Indoor Airflow (COP)	1190.45	16.59		0.0208
Indoor Airflow (SCOP)	1199.97	18.54	(0.075 lb/ft3 standard air)	
Evap Inlet Density Ratio (lbx20/lbAir):	0.011120			
Evap Exit Density Ratio (lbx20/lbAir):	0.010336			
Barometric Pressure (in HG):	28.95	Nozzle Temp (F):	82.12	0.82
7 inch Nozzle Pressure Drop (in Water):	1.286			
Evaporator Coil Air Pressure Drop (in Water):	0.147			

## Refrigerant Side Conditions

Discharge Pressure (psia):	566.16	4.208	Ref-sid Cap (Btu/h):	80187.70	610.41
Suction Pressure:	170.61	0.629	Ref-sid Cap (ton):	2.51	0.05
Condenser Inlet Pressure:	565.75	4.404	Liq Line Mdot (lbm/min):	8.69	0.13
Condenser Exit Pressure:	556.59	4.396	Disch Mass Flow (lb/min):	-0.10	0.00
Liq MassMeter Inlet (psia):	556.59	4.396	Liq Line Density (lb/ft3):	89.04	0.34
LiqMeter Exit/TXV In (psia):	540.36	4.897	TXV Inlet Temperature (F):	126.45	0.92
Evaporator Pres Drop (psid):	5.62	0.438	TXV Inlet Subcooling (F):	11.22	0.74
Evap Exit Pressure (psia):	171.91	0.706	Disch Line Density (lb/ft3):	5.234	0.172
Evap Exit Temperature (F):	59.35	3.874	Suction Temp (F):	62.40	2.66
Evap Exit Superheat (F):	3.73	3.963	Suction Superheat (W):	7.25	2.61
			Discharge Temp (W):	213.19	1.88
			Discharge Superheat (F):	71.55	1.65

0.36 WattHours Per Count

Counts: 10243.00

WattHours: 3687.48

Test Period (seconds): 3295.59

Cooling EER: 7.43 COP: 2.18

C	Denmer WP (WmiW)	9.29	0.27	Evap Inlet Pressure after TXV (psia):	159.66	0.98
				Evap Inlet Temp after TXV (F):	56.49	0.59
				Evap Inlet Temp2 (F):	56.13	0.57
				Evap Inlet Temp3 (F):	56.48	0.54
				Cond Inlet Temp (F):	213.15	1.82
				Cond Exit Temp (F):	131.02	0.93

# COOLING TEST SUMMARY SHEET

DATA FILENAME: b010330k.dat SUMMARY FILENAME: b010330k.sum

Air-Side Conditions		Range
Indoor Dry-Bulb	79.888	0.90
Indoor Inlet Dew (m)	60.130	0.15
Indoor Exit Dry-Bulb	58.385	0.33
Indoor Exit Wet (m)	54.970	0.31
Outdoor Dry-Bulb (F)	82.122	0.40
Indoor Airflow (CFM)	1183.95	11.10
Indoor Airflow (ECFM)	1201.27	11.97
Evap Inlet Humidity Ratio (lbH2O/lbAir)	0.011085	(0.075 lb/ft3 standard air)
Vap Exit Humidity Ratio (lbH2O/lbAir)	0.009176	
Barometric Pressure (in HG)	29.95	Nozzle Temp (F): 59.02
7 inch Nozzle Pressure Drop (in Water)	1.280	0.025
Evaporator Coil Air Pressure Drop (in Water)	0.150	0.007
Refrigerant Side Conditions		
Discharge Pressure (psia)	342.35	1.174
Suction Pressure	156.49	0.655
Condenser Inlet Pressure	341.55	1.077
Condenser Exit Pressure	329.10	1.221
Liq MassMeter Inlet (psia)	329.10	1.221
LiqMeter Exit/TXV In (psia)	314.55	1.714
Evaporator Pres Drop (psid)	4.08	0.338
Evap Exit Pressure (psia)	158.13	0.973
Evap Exit Temperature (F)	54.95	5.669
Evap Exit Superheat (F)	4.50	5.730
0.36 WattHours Per Count		
Counts	4618.00	
WattHours	1662.48	
Condenser DP (psid)	127.0	0.85
Evap Inlet Pressure after TXV (psia)	144.43	1.17
Evap Inlet Temp after TXV (F)	50.75	0.39
Evap Inlet Temp2 (F)	50.57	0.35
Evap Inlet Temp3 (F)	51.28	0.52
Cond Inlet Temp (F)	141.35	1.47
Cond Exit Temp (F)	89.53	0.69
Test Period (seconds): 2718.65		
Cooling EER: 18.33 COP: 5.37		
Ref-side Cap (Btu/h): 40281.21		
Ref-side Cap (tons): 3.36		
Liq Line Mdot (lbm/min): 8.95		
Disch Mass Flow (lb/min): -0.10		
Liq Line Density (lb/ft3): 71.13		
TXV Inlet Temperature (F): 88.02		
TXV Inlet Subcooling (F): 8.05		
Misch Line Density (lb/ft3): 11.076		
Sucti Mdot (m): 55.86		
Suction Superheat (F): 6.04		
Discharge Temp (F): 141.54		
Discharge Superheat (F): 39.07		
807.46		



COOLING TEST SUMMARY SHEET

DATA FILENAME b010333x.dat SUMMARY FILENAME: b010333x.sum

Air-Side Conditions Range

Indoor Dry-Bulb : 80.051 0.88 Total Air-Side Capacity: 33304.65 722.43

Indoor Inlet Dew (p) 60.293 0.84 Sensible Cap (Btu/h): 26674.30 607.93

Indoor Exit Dry-Bulb 60.636 0.52 Latent Cap (Btu/h): 6630.35 527.84

Indoor Exit Dew (F): 57.276 0.48 EvapAir Delta T (F): 20.22 0.28

Outdoor Dry-Bulb (F): 115.386 1.80 Sensible Heat Ratio 0.801 0.0141

Indoor Airflow (CFM): 1186 38

Indoor Airflow (SCFM): 1198 18 13 45 (0.075 lb/ft3 standard air)

Evap Inlet Humidity Ratio (lbH2O/lbAir): 0.011149

Evap Exit Humidity Ratio (lbH2O/lbAir): 0.009989

Barometric Pressure (in Hg) 29.95 Nozzle Temp (F): 61.17 0.75

7 inch Nozzle Pressure Drop (in Water): 1.280 0.029

Evaporator Coil Air Pressure Drop (in Water): 0.149 0.008

Refrigerant Side Conditions

Discharge Pressure (psia): 507.82 8.024 Ref-side Cap (wtu/h) : 481.22

Suction Pressure : 166.96 1.662 Ref-side Cap (tons) : 2.78

Condenser Inlet Pressure: 507.14 7.879 Liq Line Mdot (lbm/min): 8.99

Condenser Exit Pressure: 496.95 7.669 Misch Mass Flow (lb/min) -0.10

Liq MassMeter Inlet (psia): 496.95 7.669 Liq Line Density (lb/ft3) 88.39

LiqMeter Exit/TXV In (psia): 480.19 7.149 TXV Inlet Temperature (F) 113.45

Evaporator Pres Drop (psid): 5.70 0.397 TXV Inlet Subcooling (in) 9.71

Evap Exit Pressure (psia): 168.55 1.582 Disch Line Density (lb/ft3): 7.576

Evap Exit Temperature (F): 57.88 1.545 Suction Temp (F): 60.51

Evap Exit Superheat (F): 3.49 1.363 Suction Superheat (F): 6.71

Discharge Temp (F): 191.07 1.99

Mischwgt Sup Heat (F) 58.27 0.88

0.36 WattHours Per Count

Counts : 4685.00

WattHours: 1686.60

Test Period (seconds) 1801.60

Cooling EER: 10.05 COP 2.94

Condenser pP (psia) 10.84 0.80 Inlet Pressure after TXV (psia): 156.32 2.34

Evap Inlet Temp after TXV (F): 55.26 0.64

Evap Inlet Temp2 (F): 54.89 1.09

Evap Inlet Temp3 (F): 55.25 0.64

Cond Inlet Temp (F): 190.90 1.80

Cond Exit Temp (F): 122.30 1.52

# COOLING TEST SUMMARY SHEET

DATA FILENAME: b010402a.dat SUMMARY FILENAME: b010402a.sum

Air-Side Conditions		Range	Total Air-Side Capacity:	29006.80	Range
Indoor Dry-Bulb :	79.721	0.89	Sensible Cap (Btu/h):	24642.10	1097.52
Indoor Inlet Dew (F):	60.323	1.28	Latent Cap (Btu/h):	4364.70	443.95
Indoor Exit Dry-Bulb:	61.806	0.94	EvapAir Delta T (F):	18.69	975.40
Indoor Exit Dew (F) :	58.373	1.04			0.21
Outdoor Dry-Bulb (F):	129.817	1.74	sensible heat Ratio	0.850	0.0280
Indoor Airflow (CFM):	1188.17	22.42			
Indoor Airflow (SCFM):	1197.11	20.25	(0.075 lb/f standard air)		
Evap Inlet Humidity Ratio (lbH2O/lbAir):		0.011163			
Evap Exit Humidity Ratio (lbH2O/lbAir):		0.010398			
Bar static Pressure (in HG):	29.05	Nozzle Temp (F):	32.30	1.27	
7 inch zlp Pressure Drop (in Water):		1.280	0.046		
Evaporator Coil Air Pressure Drop (in Water):		0.143	0.009		
-----					
Refrigerant Side Conditions					
Discharge Pressure (psia):	592.22	5.920	Ref-side Cap (Btu/h) :	28870.76	1054.86
Suction Pressure :	171.66	2.367	Ref-side Cap (tons):	2.41	0.09
Condenser Inlet Pressure:	591.66	5.921	Liq Line Mdot (lbm/min):	8.58	0.27
Condenser Exit Pressure:	582.79	6.106	Disch Mass Flow (lb/min):	-0.10	0.10
Liq MassMeter Inlet (psia):	582.79	6.106	Liq Line Density (lb/ft3):	90.54	0.26
LiqMeter Exit/TXV In (psia):	566.38	7.051	TXV Inlet Temperature (F):	130.01	0.64
			TXV Inlet Subcooling (F):	11.52	0.84
Evaporator Pres Drop (psid):	5.73	0.528	Disch Line Density (lb/ft3):	7.023	0.271
Evap Exit Pressure (psia):	172.90	2.628	Suction Temp (F):	63.20	1.25
Evap Exit Temperature (F):	30.09	2.739	Suction Superheat (F):	7.67	1.21
Evap Exit Superheat (F):	4.11	2.483	Discharge Temp (F)	221.46	3.18
			Discharge Superheat (F)	76.11	2.43
-----					
0.35 Wa	Hours Per Count		Test Period (seconds):	1985.78	
Cnts :	6474.00		Cooling EER:	6.87	COP:
Wat cws:	2330.64				
-----					
Condenser DP (psid):	9.03	0.54	Evap Inlet Pressure after TXV (psia):	160.73	2.93
			Evap Inlet Temp after TXV (F):	57.01	1.03
			Evap Inlet Temp2 (F):	56.51	1.20
			Evap Inlet Temp3 (F):	56.93	0.94
			Cond Inlet Temp (F):	221.42	3.46
			Cond Exit Temp (F):	134.94	1.11

# COOLING TEST SUMMARY SHEET

DATA FILENAME: b010403a Wet SUMMARY FILENAME: b010403a.s

Air-Side Conditions	WetBulb	Total Air-Side Capacity:	3058±.00	WetBulb	47± 09
Indoor Dry-Bulb	79 701	Sensible CA (Btu/h	25370 10		406 16
Indoor Inlet Dew (F)	60.259	Latent Cap (Btu/h):	5215 ±9		300 4±
Indoor Exit Dry-Bulb:	61.294	Evap Air Delta (F)	19 19		0 ±1
Indoor Exit Dew (F):	57.913				
Outdoor Dry-Bulb (m)	124.991	Sensible Heat Ratio:	0 829		0 0096
Indoor Airflow (CFM)	1190.29				
Indoor Airflow (SCFM)	1200 34	(0 075 lb/ft3 standard air)			
Evap Inlet Humidity Ratio (lbH2O/lbAir)	0 011135				
Evap Exit Humidity Ratio (lbH2O/lbAir):	0 010±24				
Barometric Pressure (in HG):	29.95	Nozzle Temp (m):	±1 ±±		0 ±6
7 inch Nozzle Pressure Drop (in Water)	1 ±8±		0 03±		
Evaporator Coil Air Pressure Drop (in Water)	0 14±		0 011		

## Refrigerant Side Conditions

Discharge Pressure (psia):	559.45	2 838	Ref-side CA (Btu/h):	30±24.20	47±.78
Suction Pressure:	169.38	0 4±8	Ref-side CA (tons):	±.55	0.04
Compressor Inlet Pressure:	55± 06	2 ±92	Liq Line Mdot (lbm/min)	8.75	0.10
Compressor Exit Pressure:	549 ±3	± 078	Mass Flow (lb/min):	-0.10	0.00
Liq MassMeter Inlet (psia):	549.63	3.078	Liq Line Density (lb/ft3):	88.58	0.52
LiqMeter Exit/TXV In (psia):	532.52	3.085	TXV Inlet Temperature (F):	125.55	0.68
Evaporator Pres Drop (psid):	5.72	0 523	TXV Inlet Subcooling (F):	10.93	0.52
Evap Exit Pressure (psia):	170.70	0 608	Disch Line Density (lb/ft3):	7 102	0.161
Evap Exit Temperature (F):	59.05	1.715	Suction Temp (m)	6±.06	0.79
Evap Exit Superheat (F):	3.87	1 8 8	Suction Superheat (m)	7.36	0.81
			Discharge Temp (F)	208.77	0.94
			Discharge Superheat (F)	±8.11	0.70

0 36 WattHours Per Count

Count: ±01 00

WattHours 2016 3±

Test Period (seconds): 1915.92

Cooling ±ER: ± 0± COP: 2.37

Compressor DP (psid)	9 49	0 18	±±± Inlet Pressure after TXV (psia):	158.61	0.49
			Evap Inlet Temp after TXV (F):	56.14	0.29
			Evap Inlet Temp2 (F):	55.64	0.46
			Evap Inlet Temp3 (F):	56.±3	0.46
			Cond Inlet Temp (F):	208.±1	1.14
			Cond Exit Temp (F):	130.15	0.47

# COOLING TEST SUMMARY SHEET

DATA FILENAME: b010410a.dat SUMMARY FILENAME: b010410a.sum

Air-Side Conditions		Range	Total Air-Side Capacity:	33800.92	Range	
Indoor Dry-Bulb	80 125	0 15	Sensible Cap (Btu/h):	27386.28	394.19	
Indoor Wet-Bulb	66 806	0 30	Latent Cap (Btu/h):	6414.64	422.26	
Indoor Exit Dry-Bulb	80 282	0 21	EvapAir Delta T (F):	20.67	280.87	
Indoor Exit Dew (F)	56 637	0 6			0.20	
Outdoor Dry-Bulb (F):	114.850	1.07	Sensible X Ratio	0 810	0 0076	
Outdoor Airfl (CFM)	1141 05	15 76				
Indoor Airflow (SCFM)	1203 83	15 54	(0 075 lb/ft3 standard air)			
Evap Inlet Humidity Ratio (lbH2O/lbAir):		0.010874				
Evap Exit Humidity Ratio (lbH2O/lbAir):		0.009757				
Barometric Pressure (in HG):	29.55	Nozzle Temp (F):	60 83	0 42		
7 inch Nozzle Pressure Drop (in Water):	1.291		0.034			
Evaporator Coil Air Pressure Drop (in Water):	0.148		0.006			
-----						
Refrigerant Side Conditions						
Discharge Pressure (psia):	502.47	.468	Ref-side Cap (Btu/h):	33558.49	471.88	
Suction Pressure:	165.43	.655	Ref-side Cap (ton):	2.80	0.04	
Condenser Inlet Pressure:	501.88	.272	Liq Line Mdot (lbm/min):	8.94	0.12	
Condenser Exit Pressure:	491.82	.514	Disch Mass Flow (lb/min):	-0.10	0.00	
Liq MassMeter Inlet (psia):	491.82	.514	Liq Line Density (lb/ft3):	84.78	0.30	
LiqMeter Exit/TXV In (psia):	474.50	.469	TXV Inlet Temp (F)	116.76	0.21	
			TXV Inlet Subcooling (F):	10.46	0.28	
Evaporator Pres Drop (psid):	5.59	0.400	Misch Line Density (lb/ft3):	6.804	0.161	
Evap Exit Pressure (psia):	166.97	0.657	Suction Temp (F):	59.99	0.49	
Evap Exit Temperature (F):	57.13	1.711	Suction Superheat (F):	6.75	0.52	
Evap Exit Superheat (F):	3.32	1.702	Discharge Temp (F):	189.29	0.67	
			Discharge Superheat (F):	57.34	0.65	
0.36 Watthours Per Count						
Counts:	5336.00		Test Period (seconds):	2122.22		
Watthours:	1920.96		Cooling EER:	10.37	COP	3.04
-----						
C Condenser P (psid)	10 20	0 27	Evap Inlet Pressure after TXV (psia):	154.68	0.78	
			Evap Inlet Temp after TXV (F):	54.77	0.20	
			Evap Inlet Temp2 (F):	54.50	0.20	
			Evap Inlet Temp3 (F):	54.70	0.31	
			Cond Inlet Temp (F):	189.13	0.86	
			Cond Exit Temp (F):	120.55	0.41	

# COOLING TEST SUMMARY SCREEN

DATA FILENAME: b0100755<0>ac SUMMARY FILENAME: 0010425x.sum

Air-Side Conditions	Range	Total Air-Side Capacity:	29413.68	Range
Indoor Dry-Bulb :	79.885	Sensible Cap (Btu/h):	24882.60	486.91
Indoor Inlet Enthalpy (h)	80.480	Latent Cap (Btu/h):	4531.09	392.79
Indoor Exit Dry-Bulb:	61.877	EvapAir Delta T (F):	18.80	346.74
Indoor Exit Enthalpy (h)	58.480			0.15
Outdoor Dry-Bulb (F):	129.905	Heat Ratio	0.848	0.0103
Indoor Airflow (CFM):	1192.68			
Indoor Airflow (SCFM):	1201.51	(0.075 lb/ft3 standard air)		
Evap Inlet Humidity Ratio (lbX2o/lbAir):	0.011229			
Evap Exit Humidity Ratio (lbX2o/lbAir):	0.010438			
Barometric Pressure (in HG):	29.95	Nozzle Temp (F):	62.35	0.72
7 inch Nozzle Pressure Drop (in Water):	1.290			
Evaporator Coil Air Pressure Drop (in Water):	0.147			0.007

## Refrigerant Side Conditions

Discharge Pressure (psia):	587.90	1.957	Ref-side Cap (tons):	2.44	396.70
Suction Pressure :	171.68	0.378	Liq Line Mdot (lbm/min):	8.69	0.03
Condenser Inlet Pressure:	587.44	1.957	Disch Mass Flow (lb/min):	-0.10	0.12
Condenser Exit Pressure:	577.98	2.003	Liq Line Density (lb/ft3):	90.42	0.00
Liq MassMeter Inlet (psia):	577.98	2.003	TXV Inlet Temperature (F):	129.95	0.27
LiqMeter Exit/TXV In (psia):	560.32	2.203	TXV Inlet Subcooling (p):	10.70	0.10
Evaporator Pres Drop (psid):	5.87	0.438	Misch Line Density (lb/ft3):	6.819	0.39
Evap Exit Pressure (psia):	173.02	0.487	Suction Temp (F):	63.81	0.139
Evap Exit Temperature (F):	60.26	1.101	Suction Superheat (p):	8.27	0.57
Evap Exit Superheat (F):	4.23	1.171	Discharge Temp (F):	218.61	0.68
			Discharge Superheat (F)	73.86	0.89
					0.88

0.36 WattHours Per Count  
 Counts : 12278.00  
 WattHours: 4420.08

Test Period (seconds): 4021.98  
 Cooling EER: 7.43 COP 2.18

Condenser DP (psid):	9.30	0.21	Evap Inlet Pressure after TXV (psia):	160.95	0.59
			Evap Inlet Temp after TXV (F):	57.32	0.55
			Evap Inlet Temp2 (F):	56.63	0.39
			Evap Inlet Temp3 (F):	57.83	0.11
			Cond Inlet Temp (F):	218.55	0.98
			Cond Exit Temp (F):	234.74	0.61

## B.2 R410A System With Custom-Fabricated Compressor

Table B.2 lists the tests performed with the custom-fabricated R410A compressor and the corresponding outdoor dry-bulb temperatures.

**Table B.2 R410A tests with compressor #2**

<b>Filename</b>	<b>Outdoor Temperature (°F)</b>
<b>CO10712C</b>	<b>129.8</b>
<b>C010713B</b>	<b>94.6</b>
<b>C010717A</b>	<b>139.4</b>
<b>CO10718A</b>	<b>115.2</b>
<b>C010719A *</b>	<b>150.0</b>
<b>C010723A</b>	<b>95.1</b>
<b>C010723C *</b>	<b>152.2</b>
<b>C010723D *</b>	<b>155.4</b>

\*Compressor operated above the critical point at its discharge

# COOLING TEST SUMMARY SHEET

DATA FILENAME		c010712c dat		BMMARY MISENAME		c010712c.sum	
Air-Side Conditions		Range		Total Air-Side Capacity:		30478.18	
Indoor Dry-Bulb :		79.912		Sensible Cap (Btu/h):		25584.23	
Indoor Inlet Dew (F):		59.922		Latent Cap (Btu/h):		4893.94	
Indoor Exit Dry-Bulb:		61.278		EvapAir Delta T (F):		19.38	
Indoor Exit Dew (F):		57.500		Sensible Heat Ratio:		0.833	
Outdoor Dry-Bulb (m):		125.843		Sensible Heat Ratio:		0.833	
Indoor Airflow (CFM)		1188.44		(0.075 lb/ft3 sea level air)		0.011000	
Evap Inlet Humidity Ratio (lbH2O/lbAir):		0.011000		Nozzle Temp (F):		51.71	
Evap Exit Humidity Ratio (lbH2O/lbAir):		0.010144		Nozzle Temp (F):		51.71	
Barometric Pressure (in HG):		29.95		Evaporator Coil Air Pressure Drop (in Water):		0.135	
7 inch Nozzle Pressure Drop (in Water):		1.283		Evaporator Coil Air Pressure Drop (in Water):		0.135	

## Refrigerant Side Conditions

Discharge Pressure (psia):	582.76	2.495	Ref-side Cap (Btu ) :	20078.45	320.41
Suction Pressure :	169.28	0.378	Ref-side Cap (tons):	2.50	0.03
Condenser Inlet Pressure:	582.34	2.496	Liq Line Flow (lbm/min):	8.97	0.09
Condenser Exit Pressure:	571.83	2.491	Disch Mass Flow (lb/min):	-0.10	0.00
Liq MassMeter Inlet (psia):	571.83	2.491	Liq Line Density (lb/ft3):	90.29	0.18
LiqMeter Exit/TXV In (psia):	551.69	2.840	mXV Inlet Temperature (m):	130.74	0.30
Evaporator Pres Drop (psid):	6.44	0.528	mXV Inlet Subcooling (m):	8.63	0.41
Evap Exit Pressure (psia):	170.81	0.268	Disch Line Density (lb/ft3):	7.806	0.275
Evap Exit Temperature (F):	59.88	1.598	Suction Temp (m):	62.92	0.86
Evap Exit Superheat (F):	4.66	1.652	Suction Superheat (F):	8.26	0.84
			Discharge Temp (F):	208.68	0.83
			Discharge Superheat (F):	44.67	0.58

## 0.36 WattHours Per Count

Counts :	6764.00	Test Period (seconds):	2212.34
WattHours:	2435.04	Cooling EER:	7.69
		COP:	2.25

C sensor DP (psid):	10.33	0.23	Evap Inlet Pressure after TXV (psia):	177.56	0.98
			Evap Inlet Temp after TXV (F):	56.66	0.28
			Evap Inlet Temp2 (F):	55.90	0.33
			Evap Inlet Temp3 (F):	56.19	0.63
			Cond Inlet Temp (F):	208.67	0.74
			Cond Exit Temp (F):	135.57	0.59

COOLING TEST SUMMARY SHEET

DATA FILENAME: c010713b.dat SUMMARY FILENAME: c010713b.sum

Air-Side Conditions		Range	Total Air-Side Capacity: 38337.24	Range
Indoor Dry-Bulb :	80.100	0.27	Sensible Cap (Btu/h): 28684.57	521.04
Indoor Latent Dew (W) :	50.093	0.38	Latent Cap (Btu/h): 9652.66	572.14
Indoor Exit Dry-Bulb:	59.174	0.22	EvapAir Delta T (F): 21.68	655.05
Indoor Exit Dew (F)	55.579	0.25		0.37
Outdoor Dry-Bulb (W)	54.550	0.81	Sensible Heat Ratio 0.748	0.0153
Indoor Airflow (CFM)	1188	26		
Indoor Airflow (SCFM):	1202.13	11.95	(0.075 lb/ft3 standard air)	
Evap Inlet Humidity Ratio (lbH2O/lbAir):			0.011068	
Evap Exit Humidity Ratio (lbH2O/lbAir):			0.009385	
Barometric Pressure (in HG):	29.95		Nozzle Temp (F): 59.61	0.26
7 inch Nozzle Pressure Drop (in Water):	1.284		0.026	
Evaporator Coil Air Pressure Drop (in Water):	0.139		0.008	
-----				
Refrigerant Side Conditions				
Discharge Pressure (psia):	397.24	1.027	Re -side Cap (Btu/h)	38002.41
Suction Pressure:	159.73	0.629	Ref-side Cap (tons):	3.17
Compressor Inlet Pressure:	396.61	1.223	Liq Line Mdot (lbm/min):	9.03
Condenser Exit Pressure:	384.38	1.075	Disch Mass Flow (lb/min):	-0.10
Liq MassMeter Inlet (psia):	384.38	1.075	Liq Line Density (lb/ft3):	76.57
LiqMeter Exit/TXV In (psia):	366.83	1.469	TXV Inlet Temperature (F):	99.59
Evaporator Pres Drop (psid):	4.71	0.428	TXV Inlet Subcooling (F):	7.79
Evap Exit Pressure (psia):	161.20	0.584	Misch Line Density (lb/ft3):	8.470
Evap Exit Temperature (F):	56.25	1.714	Suction Temp (F):	57.49
Evap Exit Superheat (F):	4.62	1.668	Suction Superheat (F):	6.42
			Discharge Temp (F):	156.47
			Discharge Superheat (F):	42.87
-----				
0.36 WattsPer Count			Test Period (seconds):	1705.32
Counts :	3522.00		Cooling EER:	14.32
WattsPer Count	1267.92		COP:	4.20
-----				
Compressor DP (psid)	12.34	0.36	Evap Inlet Pressure after TXV (psia):	166.59
			Evap Inlet Temp after TXV (F):	52.36
			Evap Inlet Temp2 (F):	52.03
			Evap Inlet Temp3 (F):	52.36
			Cond Inlet Temp (F):	156.37
			Cond Exit Temp (F):	102.28
				0.49
				0.07
				0.35
				0.56
				0.73
				0.23



# COOLING TEST SUMMARY SHEET

DATA FILENAME: c010717a.dat SUMMARY FILENAME: c010717a.sum

Air-Side Conditions		Range	Total Air-Side Capacity:	Range
Indoor Dry-Bulb :	80.018	0.22	Sensible Cap (Btu/h):	28057.91
Indoor Inlet Dew (p)	80.180	0.17	Latent Cap (Btu/h):	3356.68
Indoor Exit Dry-Bulb	62.141	0.22	EvapAir Delta T (F):	18.68
Indoor Exit Dew (p)	58.887	0.15		0.20
Outdoor Dry-Bulb (F):	139.377	1.11	Sensible Heat Ratio:	0.880
Indoor Airflow (CFM):	1191.96	17.60		0.0102
Indoor Airflow (SCFM)	1200.21	18.62	(0.075 lb/ft <sup>3</sup> standard air)	
Evap Inlet Humidity Ratio (lbH2O/lbAir):	0.011103			
Evap Exit Humidity Ratio (lbH2O/lbAir):	0.010517			
Barometric Pressure (in HG):	29.95	Nozzle Temp (F):	62.60	0.59
7 inch Nozzle Pressure Drop (in Water):	1.288			
Evaporator Coil Air Pressure Drop (in Water):	0.131			
-----				
Refrigerant Side Conditions				
Discharge Pressure (psia):	646.17	4.990	Ref-side C <sub>4</sub> (Btu/h)	27604.98
Suction Pressure:	173.80	0.504	Ref-side Cap (tons):	2.30
Condenser Inlet Pressure:	645.82	4.894	Liq Line Mdot (lbm/min):	8.86
Condenser Exit Pressure:	635.82	4.641	Disch Mass Flow (lb/min):	-0.12
Liq MassMeter Inlet (psia):	635.82	4.641	Liq Line Density (lb/ft <sup>3</sup> ):	93.36
LiqMeter Exit/TXV In (psia):	615.34	4.995	TXV Inlet Temperature (F):	137.64
Evaporator Pres Drop (psid):	6.61	0.474	TXV Inlet Subcooling (F):	10.78
Evap Exit Pressure (psia):	175.08	0.608	Disch Line Density (lb/ft <sup>3</sup> ):	7.162
Evap Exit Temperature (F):	61.16	1.320	Suction Temp (F):	64.59
Evap Exit Superheat (F):	4.40	1.302	Suction Superheat (p)	8.29
			Discharge Temp (F)	226.98
			Discharge Superheat (p)	74.33
-----				
0.36 Watts/Hours Per Count			Test Period (seconds):	1841.32
Counts :	6678.00		Cooling EER:	5.94
WattHours:	2404.08		COP	1.75
-----				
Condenser D <sub>s</sub> (p <sub>in</sub> )	88	0.22	Evap Inlet Pressure after TXV (psia):	181.95
			Evap Inlet Temp after TXV (F):	57.96
			Evap Inlet Temp2 (F):	57.53
			Evap Inlet Temp3 (F):	57.92
			Cond Inlet Temp (F):	227.00
			Cond Exit Temp (F):	142.96
				0.57

COOLING TOWER SUMMARY SHEET

DATA FILENAME: c010718a.dat SUMMARY FILENAME: c010718a.sum

Air-Side Conditions		Range	Total Air-Side Capacity: 34813.10	Range
Indoor Dry-Bulb	≤ 0 119	0 34	Sensible Cap (Btu/h): 26912.99	525.62
Indoor Wet-Bulb	≤ 0 704	0 20	Latent Cap (Btu/h): 7900.11	419.80
Indoor Exit Dry-Bulb	60 501	0 17	EvapAir Delta T (m): 20.35	445.84
Indoor Exit Wet-Bulb	m : 57 134	0 19		0.17
Outdoor Dry-Bulb	m 115 240	0 52	Sensible Heat Ratio	0 773
Indoor Airflow (CFM):	1188.91	14.05		0 0110
Indoor Airflow (SCFM):	1201 19	14 ≤ 9	(0 075 lb/ft3 standard air)	
Evap Inlet Humidity Ratio (lbH2O/lbAir):			0.011316	
Evap Exit Humidity Ratio (lbH2O/lbAir):			0.009937	
Barometric Pressure (in HG):	29.95	Nozzle Temp (F): 6 01	0 ≤ 0	
7 inch Nozzle Pressure Drop (in Water):	1.286	0.031		
Evaporator Coil Air Pressure Drop (in Water):	0.137	0.010		
-----				
Refrigerant Side Conditions				
Discharge Pressure (psia):	505.64	1.223	Ref-side C <sub>1</sub> (Btu/h) :	34327.65
Suction Pressure :	166.62	0.478	Ref-side Cap (tons):	2.86
Condenser Inlet Pressure:	505.08	1.223	Liq Line Mdot (lbm/min):	9.16
Condenser Exit Pressure:	494.14	1.221	Disch Mass Flow (lb/min):	-0.10
Liq MassMeter Inlet (psia):	494.14	1.221	Liq Line Density (lb/ft3):	84.78
LiqMeter Exit/TXV In (psia):	474.50	1.224	TXV Inlet Temperature (F):	117.05
Evaporator Pres Drop (psid):	5.79	0.379	TXV Inlet Abcooling (m):	10.16
Evap Exit Pressure (psia):	168.17	0.608	Disch Line Density (lb/ft3):	8.510
Evap Exit Temperature (F):	57.87	1.122	Suction Temp (F):	60.05
Evap Exit Superheat (F):	3.62	1.202	Suction Superheat (F):	6.37
			Discharge Temp (F):	185.31
			Discharge Superheat (F):	52.86
-----				
0.36 WatHours Per Count				
Counts :	4941.00		Inst Period (seconds):	1846.38
WatHours:	1778.76		Cooling EER:	10.04 COP
-----				
Condenser DP (psid) :	10 95	0 29	Evap Inlet Pressure after TXV (psia):	174.41
			Evap Inlet Temp after TXV (F):	55.23
			Evap Inlet Temp2 (F):	55.02
			Evap Inlet Temp3 (F):	55.31
			Cond Inlet Temp (F):	185.25
			Cond Exit Temp (F):	120.72
				0.49
				0.22
				0.31
				0.64
				0.40
				0.60

# <COOLING MESM BMMARY EXXEM

DATA FILENAME c010719a.dac BMMARY FILE NME c010719a.sum

Air-Side Conditions	Range	Total Air-Side Capacity:	24801.22	Range
Indoor Dry-Bulb : 79.806	0.64	Sensible Cap (Btu/h):	22519.36	511.30
Indoor Inlet Dew (F): 60.939	0.60	Latent Cap (Btu/h):	2281.86	832.95
Indoor Exit Dry-Bulb: 63.561	0.37	EvapAir Delta T (F):	17.03	825.06
Indoor Exit Dew (W): 59.956	0.44			0.47
Outdoor Dry-Bulb (F): 150.003	0.81	Sensible Xent Ratio	0.903	0.0318
Indoor Airfl (CTT) 11B4 03	15.33			
Indoor Airflow (S4TT) 1199 20	17.20	(0.075 lb/ft3 sta ward air)		
Vap Inlet Humidity Ratio (lbX2O/lbAir)	0.011413			
Evap Exit Humidity Ratio (lbH2O/lbAir)	0.011014			
Barometric Pressure (in HG):	29.95	Nozzle Temp (F):	≤3.8Z	0.77
7 inch Nozzle Pressure Drop (in water):	1.289			0.05
Evaporator Coil Air Pressure Drop (in Water):	0.129			0.039

## Refrigerant Side Conditions

Discharge Pressure (psia):	709.29	3.180	Ref-side Cap (Btu/h):	24159.09	407.24
Suction Pressure:	178.49	0.982	Ref-side Cap (tons):	2.01	0.04
Condenser Inlet Pressure:	709.12	3.328	Liq Line Mdot (lbm/min):	8.62	0.17
Condenser Exit Pressure:	699.44	3.761	Disch Mass Flow (lb/min):	0.58	0.95
Liq MassMeter Inlet (psia):	699.44	3.761	Liq Line Density (lb/ft3):	96.36	0.51
LiqMeter Exit/TXV In (psia):	678.65	3.477	TXV Inlet Temperature (F):	146.27	0.63
Evaporator Pres Drop (psid):	6.84	0.397	TXV Inlet Subcooling (m):	10.46	0.57
Evap Exit Pressure (psia):	179.29	1.095	Disch Line Density (lb/ft3):	7.851	0.650
Evap Exit Temperature (F):	63.78	1.317	Suction Temp (F):	67.29	0.86
Evap Exit Superheat (F):	5.52	1.180	Suction Superheat (F):	9.31	0.80
			Discharge Temp (F):	248.42	0.97
			Discharge Superheat (m):	87.82	0.90

0.36 WattHours Per Count

Counts : 8533.00

WattHours: 3071.88

Condenser DP (W3idW)	9.59	0.31	Evap Inlet Pressure after TXV (psia):	186.75	1.86
			Evap Inlet Temp after TXV (F):	59.46	0.55
			Evap Inlet Temp2 (F):	58.97	0.59
			Evap Inlet Temp3 (F):	59.46	0.52
			Cond Inlet Temp (F):	248.60	0.91
			Cond Exit Temp (F):	152.29	0.31

Test Period (seconds): 2084.54

Cooling EER: 4.63 COP 1.36

COOLING TEST SUMMARY SHEET

DATA FILENAME: c010723a.dat SUMMARY FILENAME: c010723a.sum

Air-Side Conditions		Coop	Total Air-Side Capacity:	38722.13	Range
Indoor Dry-Bulb :	79.847	0.97	Sensible Cap (Btu/h):	28608.94	604.35
Indoor Wet Bulb (F)	60.283	0.47	Latent Cap (Btu/h):	10113.19	564.08
Indoor Exit Dry-Bulb	53.085	0.61	EvapAir Delta T (F):	21.56	518.69
Indoor Exit Dew (F):	55.590	0.50			0.39
Outdoor Dry-Bulb (F):	95.064	0.58	Sensible Heat Ratio:	0.733	0.0121
Outdoor Airflow (CFM)	1183.62	1.82			
Indoor Airflow (SCFM)	1205.53	17.88	(0.075 lb/ft <sup>3</sup> standard air)		
Evap Inlet Humidity Ratio (lbH <sub>2</sub> O/lbAir):	0.011147				
Evap Exit Humidity Ratio (lbH <sub>2</sub> O/lbAir):	0.009389				
Barometric Pressure (in HG)	23.95		Nozzle Temp (F):	53.62	0.68
7 inch Nozzle Pressure Drop (in Water):	1.291			0.037	
Evaporator Coil Air Pressure Drop (in Water):	0.135			0.008	
-----					
Refrigerant Side Conditions					
Discharge Pressure (psia):	401.76	1.272	Ref-side Cap (Btu/h)	38381.29	664.91
Suction Pressure:	160.18	1.334	Ref-side Cap (tons):	3.19	0.06
Condenser Inlet Pressure:	401.05	1.223	Liq Line Mdot (lbm/min):	9.04	0.15
Condenser Exit Pressure:	389.35	1.465	Disch Mass Flow (lb/min):	-0.10	0.00
Liq MassMeter Inlet (psia):	389.35	1.465	Liq Line Density (lb/ft <sup>3</sup> ):	76.21	0.21
LiqMeter Exit/TXV In (psia):	371.37	1.861	TXV Inlet Temperature (m):	98.71	0.56
Evaporator Pres Drop (psid):	4.68	0.495	TXV 1st Subcooling (m)	9.59	0.56
Evap Exit Pressure (psia):	161.72	1.339	Disch Line Density (lb/ft <sup>3</sup> ):	9.559	1.107
Evap Exit Temperature (F):	55.73	2.067	Suction Temp (F):	57.39	0.96
Evap Exit Superheat (F):	3.89	1.974	Suction Superheat (F):	6.15	0.59
			Discharge Temp (F):	157.86	0.87
			Discharge Superheat (F):	43.40	0.80
0.36 Watts Per Count					
Counts : 4089.00					
WattHours: 1472.04					
Test Period (seconds): 1835.33					
Cooling EER: 13.41 COP					
-----					
Condenser DP (psid)	11.33	0.37	Evap Inlet Pressure after TXV (psia):	166.79	1.56
			Evap Inlet Temp after TXV (F):	52.37	0.50
			Evap Inlet Temp2 (F):	52.41	0.82
			Evap Inlet Temp3 (F):	52.82	0.50
			Cond Inlet Temp (F):	157.75	0.74
			Cond Exit Temp (F):	101.04	0.59

# COOLING TEST SUMMARY SHEET

DATA TESTNAME C010723C MAC 3 TESTNAME C010723C HUM

Air-Side Conditions Range Total Air-Side Capacity: 24171.86 1666.44  
 Indoor Dry-Bulb 80 424 1.53 Sensible Cap (Btu/h): 22986.59 838.14  
 Indoor Inlet Dew (F) 80 582 1.03 Latent Cap (Btu/h): 1185.27 1485.20  
 Indoor Exit Dry-Bulb 80 811 1.53 EvapAir Delta T (m): 17.44 0.59  
 Indoor Exit Dew (F) 80 088 1.23 Sensible Heat Ratio 0.51 0.0304  
 Outdoor Dry-Bulb (F) 152 130 1.78  
 Indoor Airflow (CFM): 1191.11 18.41  
 Indoor Airflow (SCFM) 1135 18.56 (0.075 lb/ft3 standard air)  
 Inlet Humidity Ratio (lbH2O/lbAir): 0.011267  
 Exit Humidity Ratio (lbH2O/lbAir): 0.011059  
 Barometric Pressure (in HG): 29.95 Nozzle Temp (F): 64.17 1.34  
 7 inch Nozzle Pressure Drop (in Water): 1.282 0.040  
 Evaporator Coil Air Pressure Drop (in Water): 0.125 0.011

## Refrigerant Side Conditions

Discharge Pressure (psia): 722.06 29.697 Ref-side Cap (Btu/h) 2383.93  
 Suction Pressure: 179.68 4.683 Ref-side Cap (tons): 1.94 0.20  
 Condenser Inlet Pressure: 721.73 29.949 Lig Line Mdot (lbm/min): 8.55 0.48  
 Condenser Exit Pressure: 712.14 29.847 Disch Mass Flow (lb/min): 0.14 1.43  
 Lig MassMeter Inlet (psia): 712.14 29.847 Lig Line Density (lb/ft3): 96.63 1.90  
 LigMeter Exit/TXV In (psia): 691.36 30.555 TXV Inlet Temperature (F): 148.27 4.14  
 TXV Inlet Subcooling (F): 10.04 0.83  
 Evaporator Pres Drop (psid): 6.75 0.684 Disch Line Density (lb/ft3): 7.349 1.513  
 Evap Exit Pressure (psia): 180.80 4.551 Suction Temp (F): 68.17 1.38  
 Evap Exit Temperature (F): 64.03 2.100 Suction Superheat (F): 9.77 0.86  
 Evap Exit Superheat (F): 5.23 1.305 Discharge Temp (F): 252.27 9.84  
 Discharge Superheat (F): 90.14 6.67

0.56 Watts/Hours Per Count

Counts: 17372.00

WattHours: 6253.92

Test Period (seconds): 4004.58

Cooling EER: 4.30 COP: 1.28

Condenser DP (psid) 41 0.31 vap Inlet Pressure after TXV (psia): 188.03 4.59  
 Evap Inlet Temp after TXV (F): 60.03 1.82  
 Evap Inlet Temp2 (F): 59.54 1.67  
 Evap Inlet Temp3 (F): 59.73 1.56  
 Cond Inlet Temp (F): 252.46 9.92  
 Cond Exit Temp (F): 154.07 4.12

# COOLING MASS BALANCE SUMMARY SHEET

DATA FILENAME: c010723d.dat SUMMARY FILENAME: c010723d.sum

Air-Side Conditions		Range	Total Air-Side Capacity:	22698.83	Range
Indoor Dry-Bulb :	80.359	0.24	Sensible Cap (Btu/h):	22644.59	880.31
Indoor Inlet Dew (F):	80.114	0.34	Latent Cap (Btu/h):	54.24	674.44
Indoor Exit Dry-Bulb :	83.874	0.38	EvapAir Delta T (F):	17.19	349.79
Indoor Exit Wet Bulb (F):	80.091	0.00			0.34
Outdoor Dry-Bulb (F)	155.3	0.99	Sensible Cap Ratio:	.998	0.0152
Indoor Airflow (CFM)	1191.22	1.15			
Indoor Airflow (SCFM)	1195.2	1.24	(0.075 lb/ft3 standard air)		
Evap Inlet Humidity Ratio (lbH2O/lbAir)		0.011077			
Evap Exit Humidity Ratio (lbH2O/lbAir)		0.011067			
Barometric Pressure (in HG):	29.95	Nozzle Temp (F):	64.28	0.5	
Evaporator Coil Air Pressure Drop (inches wgl Pressure Drop (in Water):	1.282	0.0			
Evaporator Coil Air Pressure Drop (in Water):	0.122	0.036			
Refrigerant Side Conditions					
Discharge Pressure (psia):	743.08	5.773	Ref-side Cap (Btu/h):	21530.12	2833.20
Suction Pressure:	181.22	1.385	Ref-side Cap (tons):	1.79	0.24
Condenser Inlet Pressure:	742.85	5.726	Liq Line Mdot (lbm/min):	8.26	1.12
Condenser Exit Pressure:	733.54	5.715	Disch Mass Flow (lb/min):	-0.07	0.50
Liq MassMeter Inlet (psia):	733.54	5.715	Liq Line Density (lb/ft3):	96.25	15.30
LiqMeter Exit/TXV In (psia):	713.21	5.680	TXV Inlet Temperature (F):	151.06	1.06
Evaporator Pres Drop (psid):	6.54	0.485	TXV Inlet Subcooling (F):	9.94	0.63
Evap Exit Pressure (psia):	182.23	1.460	Disch Line Density (lb/ft3):	7.099	0.917
Evap Exit Temperature (F):	64.43	1.205	Suction Temp (F):	68.83	0.62
Evap Exit Superheat (F):	5.13	1.348	Suction Superheat (F):	9.89	0.86
			Discharge Temp (F):	261.45	4.12
			Discharge Superheat (F):	96.83	3.62
0.36 WattHours Per Count					
Counts :	8917.00		Test Period (seconds):	1838.14	
WattHours:	3210.12		Cooling EER:	3.61	COP
Compressor DP (psid) 10 0.28					
			Evap Inlet Pressure after TXV (psia):	189.29	1.37
			Evap Inlet Temp after TXV (F):	60.53	0.51
			Evap Inlet Temp2 (F):	60.01	0.62
			Evap Inlet Temp3 (F):	60.19	0.51
			Cond Inlet Temp (F):	261.61	4.12
			Cond Exit Temp (F):	156.95	1.06

## APPENDIX C. CAPACITY AND EER UNCERTAINTY

Table C.1 gives an example of the error associated with EER and air-side capacity for several tests. A high capacity and a low capacity test were selected. Uncertainty values for capacity and EER for all tests are bounded by these values. A complete examination of error propagation for systems tested according to ASHRAE Standard 37-1988 may be found in Payne and Domanski (2001).

Table C.1: Measurement uncertainty

Filename		Value	Percent Uncertainty at a 95 % Confidence Limit on the Mean
R22 A010111a.dat	EER	$18.29 \pm 0.65 \text{ Btu/Wh}$	3.5
	Capacity	$40200 \pm 1171 \text{ Btu/h}$	2.9
R410A C010723d.dat	EER	$3.61 \pm 0.20 \text{ Btu/Wh}$	5.4
	Capacity	$22699 \pm 1142 \text{ Btu/h}$	5.0

## **APPENDIX D. EVAP-COND INSTRUCTION PAGES**

The attached pages contain **EVAP-COND** instructions prepared to facilitate the use of the EVAP-COND package.



# EVAP- COND INSTRUCTIONS

**EVAP-COND** is a software package that contains NIST's simulation models for a finned-tube evaporator (**EVAP5**) and condenser (**COND5**). The following pages provide basic instructions on how to use this package. The instructions include preparation of input data, execution of the program, and examination of simulation results.

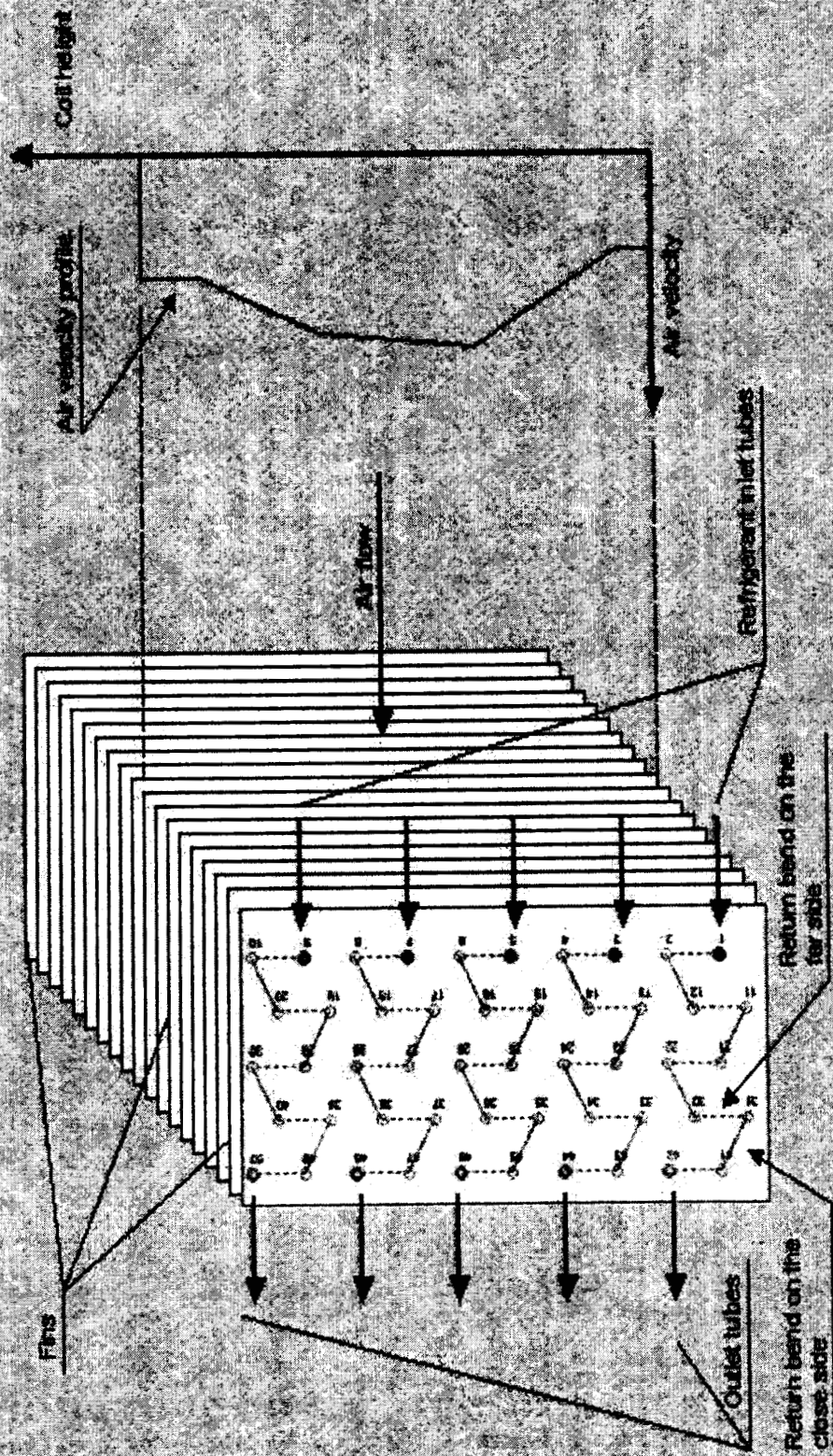
**Capabilities include:**

- tube-by-tube simulation
- non-uniform air distribution
- simulation of refrigerant distribution
- condenser model capable to simulate above the critical point
- 10 refrigerants and refrigerant mixtures
- REFPROP6 refrigerant properties



Piotr A. Domanski  
National Institute of Standards and Technology  
Building and Fire Research Laboratory  
Gaithersburg, MD, USA

# EVAPORATOR REPRESENTATION

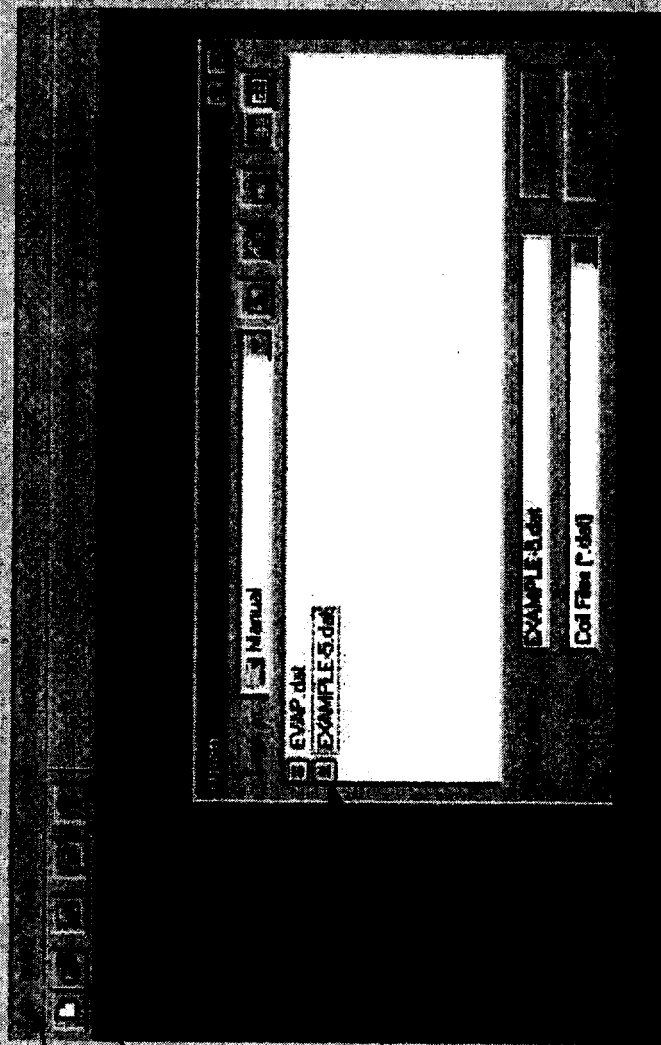




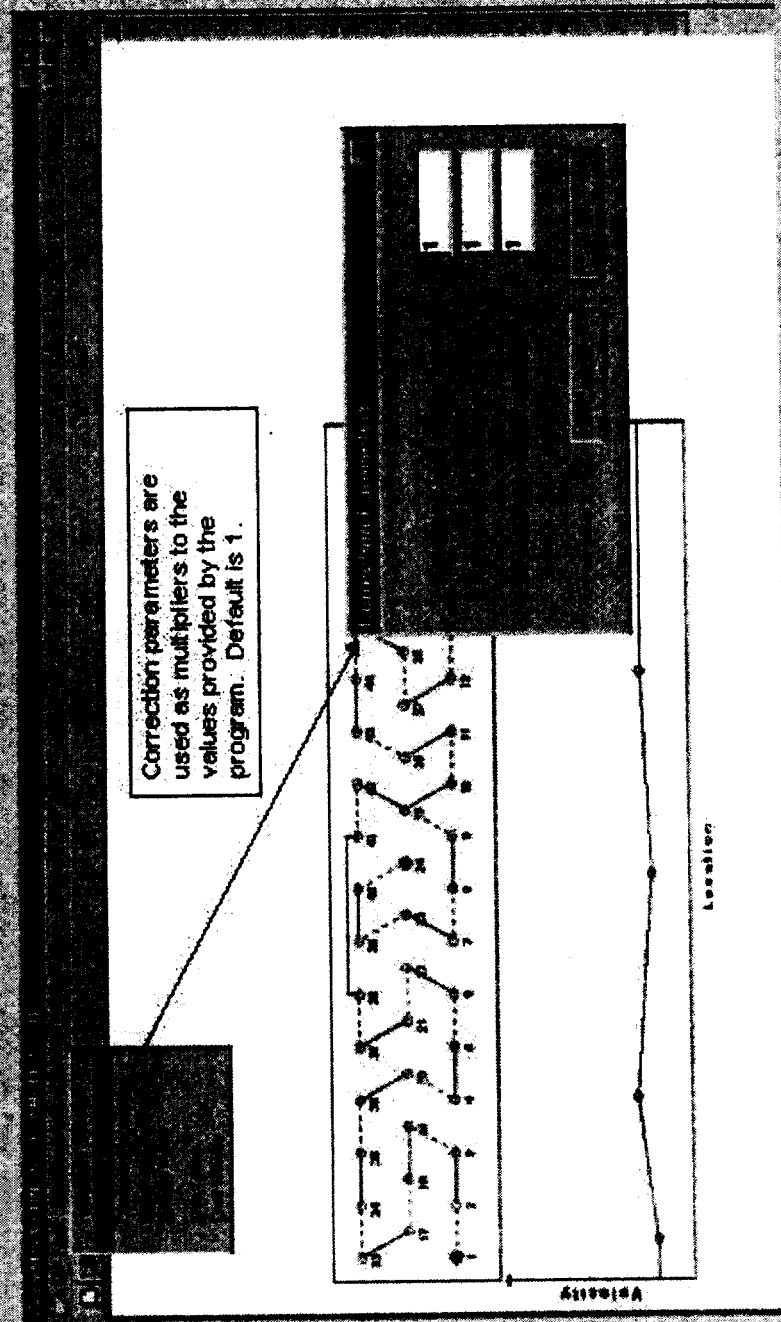
# LOADING A FILE

After starting the program, click on the "open file" button on the power bar or select "Open" on the pull down menu

Open file EXAMPLE-5 to continue this tutorial.



# PREPARING A SIMULATION RUN

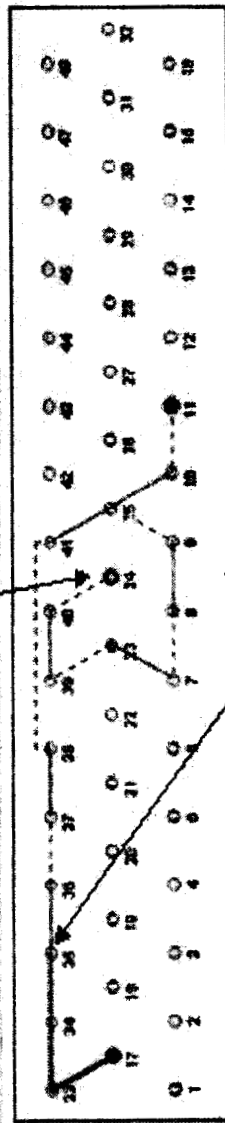


# REFRIGERANT CIRCUIT DESIGN

Follow the steps below to design a circuit:

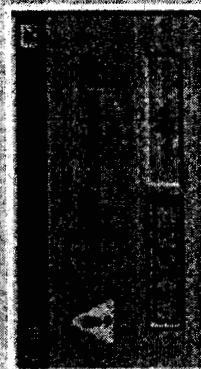
1. place the pointer on the tube
2. press the left mouse button
3. drag the pointer to the next tube
4. release the left button

Evaporator inlet tube



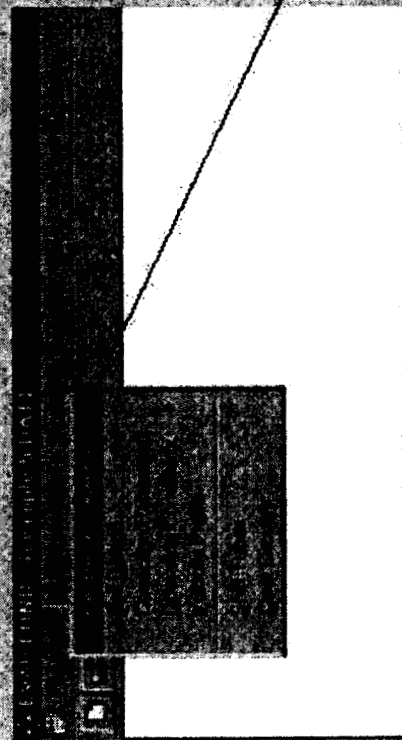
Option:

You may remove a part of the circuit by positioning the pointer on a given tube and clicking twice with the left button.

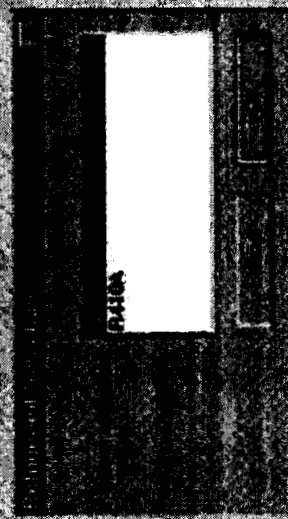




# REFRIGERANT SELECTION



EXAMPLE 5 was set up to use refrigerant inlet pressure and quality as input data (see Operating Conditions). Since the specified inlet pressure is for R22, use the pull-down menu to select R22.



# COIL DESIGN DATA

Value 1 must  
be used for  
this version of  
EVAP-COND.

EXAMPLE 5

1

16

16

16

10

10

484.023

9.2202

10.0076

25.4

72.225

Smooth

0.355013

0.2032

2.00406

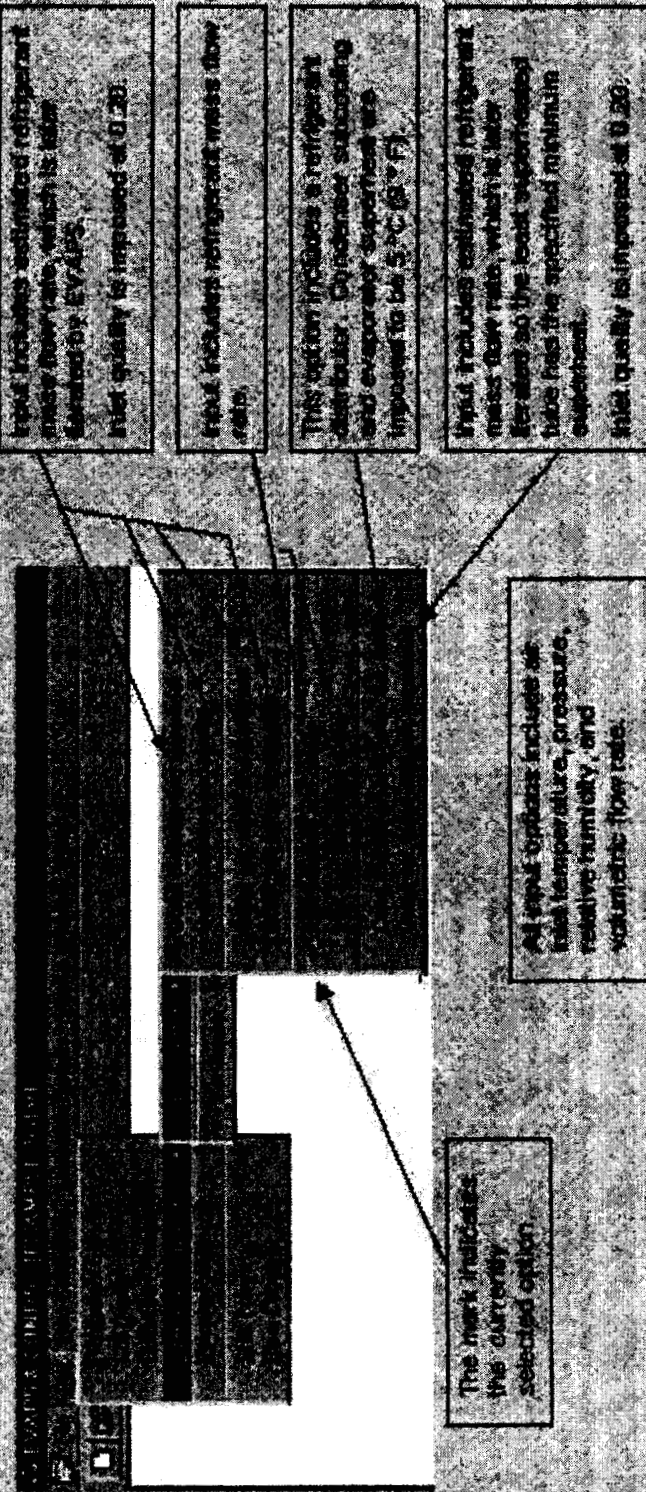
Wing

0.7271558



# EVAPORATOR OPERATING CONDITIONS

(Eight options)





# AIR VELOCITY PROFILE

Recall that the operating conditions input data included the volumetric flow rate of air. Before you leave this window you must decide between the two options:

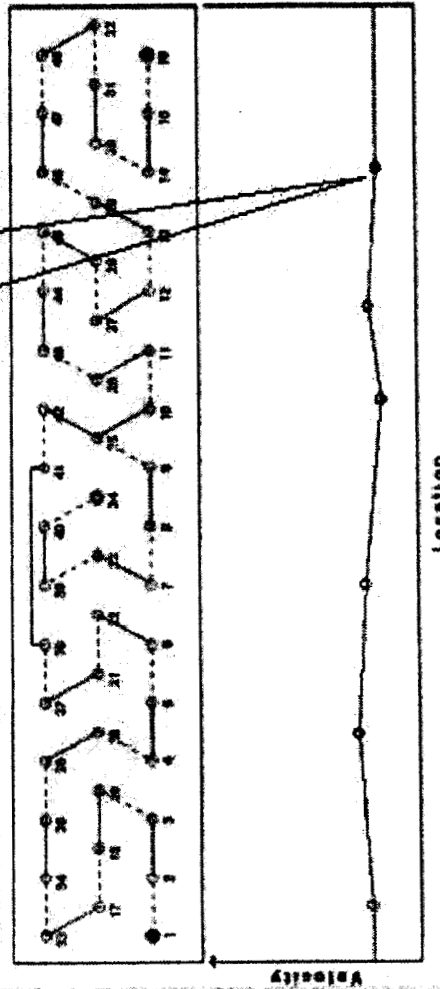
- to use the previously specified vol. flow rate and have the velocity profile scaled to match that value (recommended)

or

- to disregard the previously specified vol. flow rate and calculate a new volumetric flow rate from the velocity profile

To specify velocity at a given point, place the pointer at that point and click with the left button. The window above shows the coordinates. Up to sixteen velocity points may be specified.

Click on a given point to remove it. The Velocity Profile window must be open to make air velocity profile changes.



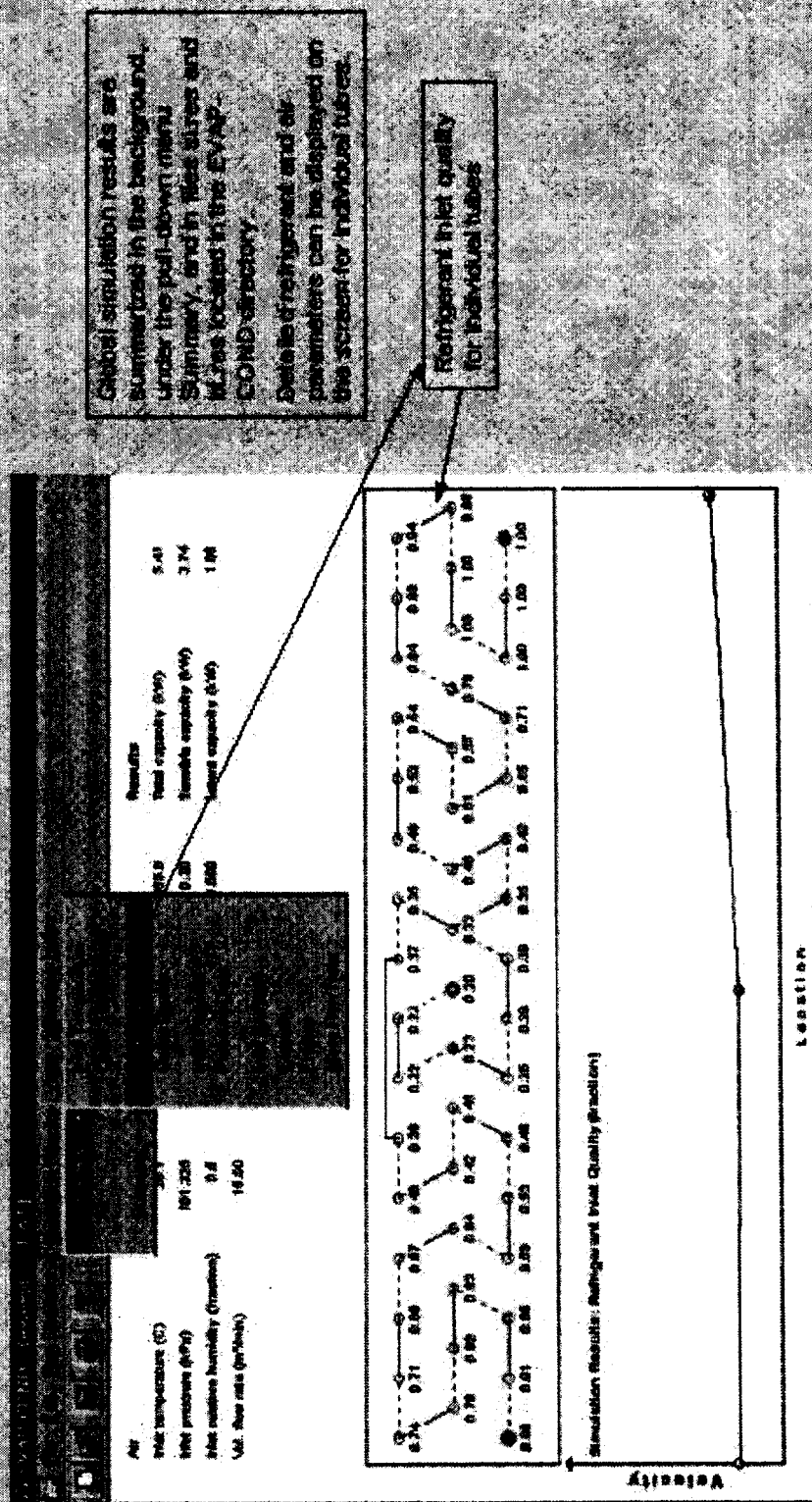
## EXECUTION OF EVAP5



Use the pull-down lever to activate EVAP5.



# SIMULATION RESULTS



# SIMULATION SUMMARY

Simulation Results Summary

## -----HVAPS SIMULATION SUMMARY-----

Cell ID: EXAMPLE-3

REFRIGERANT: R22

### REFRIGERANT SIDE

Refrigerant mass flow rate: 120.6 [kg/hr]  
 Total capacity: 5.735 [kW]  
 Latent capacity: 1.677 [kW]  
 Total capacity: 5.413 [kW]  
 Outlet saturated temp. and superheat: 7.0 6.2 [C]  
 Inlet and outlet temperatures: 9.7 19.3 [C]  
 Inlet and outlet pressures: 655.0 622.5 [kPa]  
 Inlet and outlet qualities: 0.200 1.000

### AIR SIDE

Air volumetric flow rate: 15.0 [m³/min]  
 Air temperature distribution [C]: 25.7 21.0 17.9 19.7  
 Air humidity distribution [%]: 5000 6630 7411 8877

### CONDITION OF REFRIGERANT LEAVING OUTLET TUBES

Tube #	Quality (-)	Temperature (C)	Superheat (C)	Ref. R. Fract. (-)
1				
2				
3				
4				

The Simulation Results Summary Worksheet displays results in the units selected for the input data. Flow rates and values have been converted to the SI and Imperial units, respectively.

# SIMULATION SUMMARY (cont.)

(Complete printout of file sires)

## EVAP SIMULATION SUMMARY

Coil ID: EXAMPLE-5

REFRIGERANT: R22

### REFRIGERANT SIDE

Refrigerant mass flow rate:

Sensible capacity:

Latent capacity:

Total capacity:

Outlet saturated temp and superheat:

Inlet and outlet temperatures:

Inlet and outlet pressures:

Inlet and outlet qualities:

120.0 [kg/h]  
3.735 [kg]  
1.677 [kW]  
5.413 [kW]  
7.0 [C]  
8.7 [C]  
655.0 [kPa]  
0.200 [kPa]  
1.000

### AIR SIDE

Air volumetric flow rate:

Air temperature distribution [C]:

Air humidity distribution [%]:

15.0 [m<sup>3</sup>/min]  
26.7 [C]  
5000 [kPa]  
5638 [kPa]  
7411 [kPa]  
8877

### CONDITION OF REFRIGERANT LEAVING OUTLET TUBES

Tube # Quality (-) Temperature (C) Superheat Ref M. Fract.

1 0.989 7.6 0.0 0.522  
16 1.000 23.0 16.0 0.478

Multiplier for refig. heat transfer coeff.: 1.00

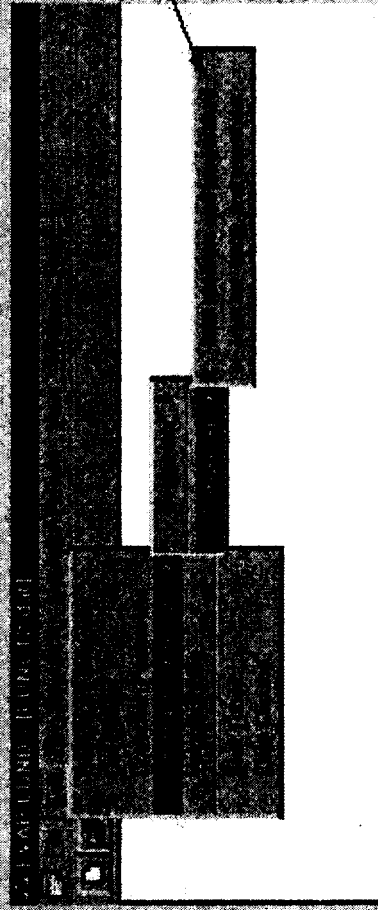
Multiplier for refrigerant pressure drop: 1.00

Multiplier for air-side heat trans. coeff.: 1.00



# CONDENSER OPERATING CONDITIONS

(Two options)



Execution of COND5 and data analysis is the same as for EVAP5

# HOW TO SIMULATE EVAPORATOR ?

(An example using the existing file EXAMPLE-5.dat)

Run Windows Explorer and go to the directory containing EVAP-COND.exe.

Double-click on EVAP-COND.exe to start the program.

Open file EXAMPLE-5.dat to simulate the evaporator. After the file is loaded, you will see a schematic representing a side view of the evaporator. The red circle(s) indicates the inlet tube to the evaporator. The blue circles indicate the outlet tubes. The horizontal line at the bottom of the screen indicates the air velocity profile at the evaporator inlet.

Review Input Data. Click on the *Edit/Coil Design* menu item to review the evaporator design information. You may select either the SI or British system of units for your input data and simulation results.

Click on the *Edit/Operating Conditions/Evaporator/Inlet pressure and quality* menu item to review operation conditions. Note, that the loaded option has a mark on the left-hand side. Since EVAP5 simulates performance tube-by-tube from the inlet to outlet, the options that specify any outlet refrigerant parameter involve iterative calls to the option that specifies refrigerant inlet pressure and quality until the target outlet parameters are obtained (e.g., saturation temperature and superheat).

Click on the *Edit/Velocity Profile* menu item to review the air velocity profile. You may use the air mass flow rate specified before or integrate the air velocity profile. In general, the first option is recommended unless very detailed and accurate local measurements of the velocity profile were taken. You may change the air velocity profile using a mouse by clicking the left button.

Run a simulation. Click on the *Run Simulation* menu item and select EVAP5. An MS-DOS window will appear and will give you a message when a simulation run is successfully completed.

Examine local and global simulation results. EVAP5 writes global simulation results to file SI.res (SI system of units) and BT.res (British system of units). The same information is provided in the pull-down menu in the units selected for data input.

# HOW TO PREPARE YOUR DATA FILE ?

Start with *Edit/Coil Design* menu item. Input all information.

Select *Edit/Operating Conditions* menu item to input operating conditions data.

Select *Edit/Velocity Profile* to change the velocity profile using a mouse (left button).

Specify refrigerant circuitry.

- For the heat exchanger working as the evaporator and condenser, start with one of the inlet tubes for the evaporator. The same data file will be used for evaporator and condenser simulations. To draw a return bend, point the mouse on a tube, press the left button, drag the mouse to the next tube, and release. If you want to modify a circuitry, you may delete a part of it from a given tube to the exit tube by pointing the mouse on the given tube and double-clicking the left button.

- For the heat exchanger working exclusively as the condenser, start with one of the outlet tubes and proceed upstream.



## **CURRENT LIMITATIONS OF EVAP-COND**

---

- Maximum number of tubes in the heat exchanger: 130
- Maximum number of tubes in a depth row: 50
- Maximum number of tube depth rows: 5
- Maximum difference between the number of tubes in different depth rows: 1
- No empty tube locations (no missing tubes in a depth row)
- No merging refrigerant points in the evaporator circuitry; no split circuitry points in the condenser
- Minimum refrigerant temperature in the evaporator: 0 °C

**COMMENTS**  
**SUGGESTIONS**  
**QUESTIONS**  
**?**

**Piotr A. Demanski**  
**National Institute of Standards and Technology**  
**Building and Fire Research Laboratory**  
**Gaithersburg, MD, USA**  
**Piotr.Demanski@NIST.gov**

## REFERENCES

ANSUAMCA Standard 210 or ANSUASHRAE Standard 51-1985. *Laboratory methods of testing fans for rating*. American Society of Heating, Refrigerating and Air-conditioning Engineers. 1791 Tullie Circle NE, Atlanta, GA, USA.

ANSI/ASHRAE Standard 37-1988. *Methods of testing for rating unitary air conditioning and heat pump equipment*. American Society of Heating, Refrigerating and Air-Conditioning Engineers. 1791 Tullie Circle **NE**, Atlanta, GA, USA.

ARI, 1999. "Positive Displacement Refrigerant Compressor and Compressor Units", Standard 540-1999, Air-conditioning and Refrigeration Institute, Arlington, VA.

ASHRAE, 2001. *ASHRAE Handbook*, Fundamentals Volume, p. 3.14, American Society of Heating, Refrigerating and Air Conditioning Engineers, Inc., Atlanta, GA.

Bergles, A.E., Collier, J.G., Delhay, J.M., Hewitt, G.F., and Mayinger, F., 1981. *Two-Phase Flow and Heat Transfer in the Power and Process Industries*, p. 146-147, Hemisphere Publishing Corp., New York, NY.

Bullock, C., 1999. The Performance Of Unitary Air Conditioners Utilizing R410A At High Outdoor Ambient Temperatures, presentation at seminar on Alternative Refrigerants for Unitary Heat Pumps and Air Conditioners, ASHRAE Annual Meeting, Seattle, WA.

Chi, J., 1979. "A Computer Model HTPUMP for Simulation of Heat Pump Steady-State Performance", National Bureau of Standards, Internal Report, Washington, D.C.

Chin, L. and Spatz, M.W., 1999. Issues Relating to the Adoption of R410A in ~~Air~~ Conditioning Systems, 20<sup>th</sup> International Congress of Refrigeration, **IIR/IIF**, Sidney, Australia.

Domanski, P.A., and Didion, D.A., 1983. "Computer Modeling of the Vapor Compression Cycle with Constant Flow Area Expansion Device", *Building Science Series 155*, National Bureau of Standards, Gaithersburg, MD.

Domanski, P.A., 1990. "Rating Procedure for Mixed Air-Source Unitary Heat Pumps Operating in the Heating Mode", NISTIR 90-4298, National Institute of Standards and Technology, Gaithersburg, MD.

Domanski, P.A., 1991. "Simulation of ~~an~~ Evaporator with Nonuniform One Dimensional Air Distribution", *ASHRAE Transactions*, Paper No. **NY-91-13-1**, Vol. 97, ~~Part~~ 1.

Domanski, P.A. and McLinden, M.O., 1992. A Simplified Cycle Simulation Model for the Performance Rating of Refrigerants and Refrigerant Mixtures, *Int. Journal of Refrigeration*, Vol. 15, No 2, pp. 81-88.

Domanski, P.A., 1999a. Evolution of Refrigerant Application, Proc. International Congress on Refrigeration, Milan, Italy.

Domanski, P.A., 1999b, "Finned-Tube Evaporator Model With a Visual Interface", 20<sup>th</sup> Int. Congress of Refrigeration, Sydney, Australia, September 19-24, 1999, International Institute of Refrigeration, Paris.

Farzad, M. and O'Neal, D.L., 1991, "System performance of an air conditioner over a range of charging conditions," *Int. Journal of Refrigeration*, 14(6).

Gallagher, J., McLinden, M.O., Morrison, G., Huber, M., 1996. *NIST Standard Reference Database 23*, Version 5.0 (REFPROP), National Institute of Standards and Technology, Gaithersburg, MD.

Gates, R.R., Sepsy, C.F., and Huffman, G.D., 1967, "Heat transfer and pressure loss in extended surface heat exchangers operating under frosting conditions," Parts I and II, *ASHRAE Transactions*, 73(2).

Gray, D.L., and Webb, R.L., 1986. "Heat transfer and friction correlations for plate fin-tube heat exchangers having plain fins", Proceedings of the 9<sup>th</sup> International Heat Transfer Conference, San Francisco, 2745-2750.

Jung, D.S., Didion, D.A., 1989, *Horizontal Flow Boiling Heat Transfer using Refrigerant Mixtures*, ER-6364, EPRI Project 8006-2.

Kays, W.M., London, A.L., 1984, *Compact Heat Exchangers*, McGraw-Hill.

Kim, N.H., Yun, J.H., and Webb, R.L., 1997. "Heat transfer and friction correlations for wavy plate fin-and-tube heat exchangers", *Journal of Heat Transfer* 119, 560-567.

Lee, J., Domanski, P. A., 1997. *Impact of Air and Refrigerant Maldistributions on the Performance of Finned-Tube Evaporators with R22 and R-407C*, Report DOE/CE/238 10-81 for ARI, National Institute of Standards and Technology, Gaithersburg, MD.

LeRoy J T., Groll E A., and Braun J E., 1998. Computer model predictions of dehumidification performance of unitary air conditioners and heat pumps under extreme operating conditions, *ASHRAE Transactions*, Paper No. TO-98-9-3, Vol. 104, Part 2, 773-788,

Lockhart, R.W. and Martinelli, R.C., 1949, *Chemical Engineering Progress*, Vol. 45, p. 39.

McLinden, M., 1987. Thermodynamic evaluation of Refrigerants in the Vapor Compression Cycle Using Reduced Properties, *International Journal of Refrigeration*, Vol. 11, pp. 134-143.

McLinden, M.O., Klein, S.A., Lemmon, E.W., and Peskin, A.P., 1998. *NIST Standard Reference Database 23*, Version 6.01 (REFPROP), National Institute of Standards and Technology, Gaithersburg, MD.

Meurer, C., Buyle, O., and Paulus-Lanckriet, M., 1999. Comparison of R22 and R410A at elevated condensing temperatures, 20<sup>th</sup> International Congress of Refrigeration, **IIR/IIF**, Sydney, Australia.

McQuiston, **F.C.**, and Parker, J.D., 1982. *Heating, Ventilating, and Air Conditioning*, J. Wiley & Sons.

Nakayama, **W.**, and Xu, L.P., 1983. Enhanced fins for air-cooled heat exchangers -heat transfer and friction correlations, Proceedings of the 1st ASME/JSME Thermal Engineering Joint Conference, 495-502.

Olson, D., 1999. Heat Transfer in Supercritical Carbon Dioxide with Convective Boundary Conditions, 20<sup>th</sup> International Congress of Refrigeration, **IIR/IIF**, Sydney, Australia.

Payne, **W. V.** and Domanski, P. A., 2001. *A Comparison of Rating Water-Source Heat Pumps Using ARI Standard 320 and ISO Standard 13256-1*, **NISTIR 6803**, National Institute of Standards and Technology, Gaithersburg, Maryland, **USA**.

Petukhov, B.S., 1970. "Heat transfer and friction in turbulent pipe flow with variable physical properties", *Advances in Heat Transfer*, Vol. 6., p. 503-564, Academic Press, New York.

Pierre, **B.**, 1964. "Flow Resistance with Boiling Refrigerants", *ASHRAE Journal*, September issue.

Rieberer, R. and H. Halozan. 1998. CO<sub>2</sub> Heat Pumps in Controlled Ventilation Systems. *Proc. IIR - Gustav Lorentzen Conference on Natural Working Fluids*, pp. 212-222, Oslo, Norway.

Sheffield, **J.W.**, Wood, R.A., and Sauer, H.J., 1988. "Experimental Investigation of Thermal Conductance of Finned Tube Contacts", *Experimental Thermal and Fluid Science*, Elsevier Science Publishing Co., Inc., New York, NY.

Schlager, L.M., Pate, M.B., Bergles, A.E., 1989. "Heat Transfer and Pressure Drop during Evaporation and Condensation of R22 in Horizontal Micro-fin Tubes", *Int. J. Refrig.*, Vol. 12, No. 1.

Schlichting, H., 1968. *Boundary-Layer Theory*, Sixth Edition, p. 590, McGraw-Hill, Inc.

Shah, M.M., 1979, "A general correlation for heat transfer during film condensation inside pipes", *International Journal of Heat and Mass Transfer*, 22, pp. 547-556.

Spatz, M.W., 2000. Private communication.

Wang, C.C., Jang, J.Y., and Chiou, N.F., 1999a. "A heat transfer and friction correlation for wavy fin-and-tube heat exchangers", *International Journal of Heat Mass Transfer* 42, pp. 1919-1924.

Wang, C.C., Lee, C.J., Chang, C.T., and Lin, S.P., 1999b. "Heat transfer and friction correlation for compact louvered fin-and-tube heat exchangers", International Journal of Heat Mass Transfer 42, pp. 1945-1956.

Wang, C.C., **Chi**, K.Y., and Chang, C.J., 2000, "Heat transfer and friction characteristics of plain fin-and-tube heat exchangers", part **II**: correlation, International Journal of Heat Mass Transfer 43, pp. 2693-2700.

Wang, C.C., Lee, **W.S.** and Sheu, W.J., 2001. "**A** comparative study of compact enhanced fin-and-tube heat exchangers", International Journal of Heat ~~Mass~~ Transfer **44**, pp. 3565-3573.

Webb, R.L., 1990. "Air-side heat transfer correlations for flat and wavy plate fin-and-tube geometries", ASHRAE Transactions 96, Pt.2, pp. 445-449.

Wells, W., Bivens, D., Yokozeki, A. and Rice, C. K., 1999. Air Conditioning System Performance with **R410A** at High Ambient Temperatures, Presentation at seminar on Alternative Refrigerants for Unitary Heat Pumps and Air Conditioners, ASHRAE Annual Meeting, Seattle, **WA**.

~~Yana~~ Motta, **S.**, and Domanski, P.A., 2000. Performance of R22 and its Alternatives Working at High Outdoor Temperatures, International Refrigeration Conference, Purdue University.